VULNERABILITY AND LOSS MODELLING

GEM TECHNICAL REPORT 2014-12 V1.0.0

Guidelines for Analytical Vulnerability Assessment - Low/Mid-Rise

D'Ayala D., A. Meslem, D. Vamvatsikos,
K. Porter, T. Rossetto and V. Silva

Guidelines for Analytical Vulnerability Assessment of Low/Mid-Rise Buildings

Version: 1.0

Author(s): D. D'Ayala, A. Meslem, D. Vamvatsikos, K. Porter, T. Rossetto and V. Silva

Date: August 01, 2015

Citation: D'Ayala, D., Meslem, A., Vamvatsikos, D., Porter, K., Rossetto, T., Silva, V. (2015) Guidelines for Analytical Vulnerability Assessment of Low/Mid-Rise Buildings, Vulnerability Global Component Project. DOI 10.13117/GEM.VULN-MOD.TR2014.12

www.globalquakemodel.org

ABSTRACT

Guidelines (GEM-ASV) for developing analytical seismic vulnerability functions are offered for use within the framework of the Global Earthquake Model (GEM). Emphasis is on low/mid-rise buildings and cases where the analyst has the skills and time to perform non-linear analyses. The target is for a structural engineer with a Master's level training and the ability to create simplified non-linear structural models to be able to determine the vulnerability functions pertaining to structural response, damage, or loss for any single structure, or for a class of buildings defined by the GEM Taxonomy level 1 attributes. At the same time, sufficient flexibility is incorporated to allow full exploitation of cutting-edge methods by knowledgeable users. The basis for this effort consists of the key components of the state-of-art PEER/ATC-58 methodology for loss assessment, incorporating simplifications for reduced effort and extensions to accommodate a class of buildings rather than a single structure, and multiple damage states rather than collapse only considerations.

To inject sufficient flexibility into the guidelines and accommodate a range of different user needs and capabilities, a distinct hierarchy of complexity (and accuracy) levels has been introduced for (a) defining index buildings, (b) modelling, and (c) analysing. Sampling-wise, asset classes may be represented by random or Latin hypercube sampling in a Monte Carlo setting. For reduced-effort representations of inhomogeneous populations, simple stratified sampling is advised, where the population is partitioned into a number of appropriate subclasses, each represented by one "index" building. Homogeneous populations may be approximated using a central index building plus 2k additional high/low observations in each of k dimensions (properties) of interest. Structural representation of index buildings may be achieved via typical 2D/3D element-by-element models, simpler 2D storey-by-storey (stick) models or an equivalent SDOF system with a user-defined capacity curve. Finally, structural analysis can be based on variants of Incremental Dynamic Analysis (IDA) or Non-linear Static Procedure (NSP) methods.

A similar structure of different level of complexity and associated accuracy is carried forward from the analysis stage into the construction of fragility curves, damage to loss function definition and vulnerability function derivation.

In all cases, the goal is obtaining useful approximations of the local storey drift and absolute acceleration response to estimate structural, non-structural, and content losses. Important sources of uncertainty are identified and propagated incorporating the epistemic uncertainty associated with simplifications adopted by the user. The end result is a set of guidelines that seamlessly fits within the GEM framework to allow the generation of vulnerability functions for any class of low/mid-rise buildings with a reasonable amount of effort by an informed engineer. Two illustrative examples are presented for the assessment of reinforced-concrete moment-resisting frames with masonry infills and unreinforced masonry structures, while a third example treating ductile steel moment-resisting frames appears in a companion document.

Keywords: vulnerability; fragility; low/mid-rise buildings.

TABLE OF CONTENTS

LIST OF FIGURES

LIST OF TABLES

Page

GLOSSARY

Building or Storey Fragility Curve/Function: A probability-valued function of the intensity measure that represents the probability of violating (exceeding) a given limit-state or damage state of the building or the storey given the value of the seismic intensity measure (IM) that it has been subjected to. Essentially, it is the cumulative distribution function (CDF) of the IM-capacity value for the limit-state and it is thus often characterized by either a normal or (more often) a lognormal distribution, together with the associated central value and dispersion of IM-capacity.

Central Value of a Variable: The median value used to characterize the "central tendency" of the variable. This is not necessarily the most frequent value that it can take, which is called its mode. The three quantities, mean, median and mode, coincide for a normal distribution, but not necessarily for other types, e.g., a lognormal.

Component Fragility Curve/Function: A probability-valued function of an engineering demand parameter (EDP), that represents the probability of violating (exceeding) a given limit-state or damage-state of the component, given the value of EDP that it has been subjected to. Essentially, it is the cumulative distribution function (CDF) of the EDP-capacity value for the limit-state and it is thus often characterized by either a normal or (more often) a lognormal distribution, together with the associated central value and dispersion of EDP-capacity.

Cost Replacement (New): The cost of replacing a component/group of components/an entire building. Since this is often compared to losses, demolition/removal costs may be added to it to fully represent the actual cost of constructing a new structure in place of the (damaged or collapsed) existing one.

Dispersion of a Variable: A measure of the scatter in the random variable, as measured around its central value. A typical quantity used is the standard deviation of the variable X, especially for a normal distribution, represented by σ_X. For a lognormal distribution, one often uses the standard deviation of the logarithm of the variable instead. The latter is often symbolized as β_X or $\sigma_{\ln X}$.

Distribution of a Variable: The probabilistic characterization of a random/uncertain variable. Comprehensively, this is represented by the probability density function (PDF), or its integral, the cumulative distribution function (CDF). For example, the PDF of a normally distributed variable is the well-known Gaussian bell function, while its CDF (and actually most CDFs regardless of distribution) resembles a sigmoid function, exactly like any fragility function.

Engineering Demand Parameter (EDP): A measure of structural response that can be recorded or estimated from the results of a structural analysis. Typical choices are the peak floor acceleration (PFA) and the interstorey drift ratio (IDR).

Intensity Measure (IM): Particularly for use within this document, IM will refer to a scalar quantity that characterizes a ground motion accelerogram and linearly scales with any scale factor applied to the record.

While non-linear IMs and vector IMs have been proposed in the literature and often come with important advantages, they will be excluded from the present guidelines due to the difficulties in computing the associated hazard.

Joint Distribution of a Set of Variables: This refers to the probabilistic characterization of a group of random/uncertain variables that may or may not depend on each other. If they are independent, then their joint distribution is fully characterized by the product of their individual probability density functions (PDFs), or marginal PDFs as they are often called. If there are dependencies, though, at a minimum one needs to consider additionally the correlation among them, i.e., whether one increases/decreases as another decreases, and how strongly.

Loss: The quantifiable consequences of seismic damage. These can be (a) the actual monetary cost of repairing a component, a group of components, or an entire building, or (b) the casualties, i.e., number of fatalities or injured occupants.

Loss ratio: For monetary losses, this is the ratio of loss to the cost replacement new for a component/group of components/building. For casualties, it is the ratio of fatalities or injured over the total number of occupants

Population (of Buildings): The ensemble of all buildings that actually constitute the class examined. For example, the set of all the existing US West Coast steel moment-resisting frames.

Sample of Index Buildings: A sample of representative buildings, each called an index building, that may be either real or fictitious, yet they have been chosen to represent the overall population by capturing the joint probabilistic distribution of its most important characteristics.

Vulnerability Curve/Function: A loss or loss ratio valued function of the intensity measure (IM), that represents the distribution of seismic loss or loss ratio given the value of IM that a certain building or class of buildings has been subjected to. Since at each value of IM we actually get an entire distribution of losses, there is never a single vulnerability curve. It is therefore most appropriate to directly specify which probabilistic quantity of the distribution each vulnerability curve represents, thus resulting, for example, to the 16/50/84% curves, the mean vulnerability curve or the dispersion curve.

Uncertainty: A general term that is used within these guidelines to describe the variability in determining any EDP, cost, or loss value. The typical sources considered are the ground motion variability, the damage state capacity and associated cost variability, and the errors due to modelling assumptions or imperfect analysis methods.

1 Introduction

1.1 Scope of the Guidelines

The main goal of the GEM Analytical Structural Vulnerability (GEM-ASV) Guidelines is to propose the most advanced methods, practical for everyday use, for the derivation of robust analytical seismic and fragility curves and vulnerability functions accounting for regional differences and cultural factors for the classification of buildings typologies and characteristics.

The methodologies are subject to limitations based on the availability and quality of input data and the Analyst's skills. This being a given, their performance depends highly upon the sophistication of the structural and material modelling. For this reason the GEM-ASV Guidelines provide a thorough critical review of the different techniques, the choice of the relevant variables and their values attribution, as well as possible simplification that can be adopted to reduce computation burden. As a substantial body of work exist in literature for the derivation of Analytical Structural Vulnerability functions, the Guidelines draw largely from such literature, which has been collated and organized in the twin Compendium document Guide for Selection of existing analytical fragility curves and Compilation of the Database [D'Ayala and Meslem 2012].

1.2 Purpose of the Guidelines

This set of Guidelines for developing analytical seismic vulnerability functions is offered within the framework of the Global Earthquake Model (GEM). Emphasis is on low/mid-rise buildings, where the analyst has the skills and time to perform non-linear structural analyses to determine the seismic response of the structures. The target audience is expected to have education and training equivalent to Master's level, and the Guidelines are designed to enable users to create simplified non-linear structural models to determine the vulnerability functions pertaining to structural response, in terms of damage or loss within 20-40 man-hours for a single structure, or 80-160 man-hours for a class of buildings defined by the GEM Taxonomy level 1 attributes [Brzev et al 2012]. At the same time, sufficient flexibility is incorporated to allow full exploitation of cutting-edge methods by knowledgeable users. The resulting document draws from the key components of the state-of-art PEER/FEMA methodology for loss assessment, incorporating significant simplifications for reduced computational effort and extensions to accommodate a class of buildings rather than a single structure, and multiple building-level damage states rather than collapse only considerations.

To inject sufficient flexibility into the guidelines and accommodate a range of different user needs and capabilities, a distinct hierarchy of complexity (and accuracy) levels has been introduced for (a) sampling, (b) modelling and (c) analysing. Sampling-wise, asset classes may be represented by random or Latin Hypercube sampling in a Monte Carlo setting. For reduced-effort representations of inhomogeneous populations, simple stratified sampling is advised, where the population is partitioned into a number of appropriate subclasses, each represented by at least 3 "index" buildings representing median, low, and high quality of performance of the subclass. Homogeneous populations may be approximated using a central index building plus 2k additional high/low observations in each of k dimensions (properties) of interest. A minimum set of relevant k dimensions is set for each structural typology as defined by the GEM Taxonomy level 1 attributes [Brzev et al 2012]. Structural representation of index buildings may be achieved via typical 2D/3D element-by-element models, simpler 2D storey-by-storey (stick) models, or an equivalent SDOF system with a user-defined capacity curve. Finally, structural analysis can be based on variants of Incremental Dynamic Analysis (IDA) or Non-linear Static Procedure (NSP) methods.

A similar structure of different level of complexity and associated accuracy is carried forward from the analysis stage into the construction of fragility curves, damage to loss function definition and vulnerability function derivation, by indicating appropriate choices of engineering demand parameters, damage states, and damage thresholds.

In all cases, the goal is obtaining meaningful approximations of the local storey drift and absolute acceleration response to estimate structural, non-structural, and content losses. Important sources of uncertainty are identified and propagated incorporating the epistemic uncertainty associated with simplifications adopted by the analyst. The end result is a set of guidelines that seamlessly fits within the GEM framework to allow the generation of vulnerability functions for any class of low/mid-rise buildings with a reasonable amount of effort by an informed engineer. Two illustrative examples are presented for the assessment of reinforced-concrete moment-resisting frames with masonry infills and unreinforced masonry structures, while a third one concerning ductile steel moment-resisting frames appears in a companion document [Vamvatsikos and Kazantzi 2015].

1.3 Structure of the Guidelines

The Guidelines document is structured to take the analyst through the process of producing vulnerability functions by using analytical approaches to define the seismic performance of a variety of building typologies. The Guidelines document is divided in seven Sections besides the present:

Section 2 summarises the main steps for the different options that are available to the analyst for the calculation of vulnerability functions. These different options are presented in decreasing order of complexity, time requirement, and accuracy.

Section 3 guides the analyst to the choice of the most appropriate sampling technique to represent a class of buildings for analytical vulnerability estimation depending on the resources of the undertaking. The choice between these different methods is guided by the trade-off of the reduced calculation effort and corresponding increased uncertainty.

Section 4 discusses the basic criteria to distinguish components in structural and non-structural and reasons for inclusion in or exclusion from the structural analysis and fragility curve construction. For each component, the relevant attributes and parameters that affect the quality of the analysis and the estimation of fragility and vulnerability are also included.

Section 5 provides details concerning the choice of modelling strategy that the analyst can use to evaluate the seismic response of the structure: i.e. simulation of failure modes. Several options in terms of simplifications and reduction of calculation effort are provided (the use of 3D/2D element-by-element, the simplified MDoF model, simplified equivalent 1D model).

Section 6 discusses the different existing definitions of Engineering Demand Parameters (EDPs) damage thresholds. The Analyst is offered two distinct choices/levels for the evaluation of these EDPs: Custom-definition of capacities for each index building, and Pre-set definition of capacities for building typologies.

Section 7 presents a comprehensive overview of the variety of procedures available to compute EDPs damage state thresholds, and how they relate to different types of structural analysis. This Section provides the user with a robust set of criteria to inform the choice among such procedures, in relation to availability of input data, analyst's skills, acceptable level in terms of computational effort/cost, and declared level of acceptable uncertainty.

Finally, Section 8 leads the analyst to generate different forms of vulnerability curves (estimation of repair and reconstruction cost given a level of intensity measurement), depending on the study's requirements and objectives.

1.4 Relationship to other GEM Guidelines

At the quickly evolving state-of-the-art, the seismic vulnerability functions and fragility curves can be derived, in decreasing order of credibility, by: EMPIRICAL, ANALYTICAL, and EXPERT OPINION approaches [Porter et al. 2012a]. Within GEM Vulnerability Estimation Methods, the purpose is developing guidelines for each of these three categories. In terms of relationship, the three guidelines are complementary to each other. The strategy foreseen by the GEM Global Vulnerability Methods (GEMGVM) consortium is that, when consistent empirical vulnerability functions (see GEM Empirical Guidelines document by Rossetto et al. [2014] are lacking, gaps are filled using the results from analytical methods, and then by using expert opinion (see Jaiswal et al. [2013] if the gaps still remain. However the increasing volume of research on both groundmotion prediction equations and performance based assessment of exisiting structures, together with increasing availability of exposure data, is resuting in important improvements in the reliability of analytical vulnerability and fragility curves. It is therefore important to highglights the best procedures to use to maintain and enhance such reliability and robustness of the analytical approaches.

With this in mnd, the GEM Global Vulnerability Methods (GEMGVM) consortium has devised a framework for the comparison and calibration of different vulnerability functions from the Empirical, Analytical and Expert Opinion Guidelines, considering the framework of uncertainties treatment [Rossetto et al. 2014]. The process of vulnerability assessment involves numerous assumptions and uses many approximations. As a result, there are uncertainties at every step in the analysis that need to be identified and quantified. Different sources of uncertainties might have significant effects for different steps in deriving analytical fragility curves and vulnerability functions.

For what concerns the nomenclature of the typology and sub typology and the attributes at the various levels, reference is made to the classification recommended by GEM-Taxonomy [Brzev et al. 2012]. For what concerns the hazard and the seismic demand reference is made to the output of the Global Ground Motion Prediction Equation component [Douglas et al. 2013] and the Uniform Hazard Model [Berryman et al. 2013], while for data on typology distributions, exposure and inventory reference should be made to the Global Exposure Database [Huyck et al. 2011].

2 Methodology and Process of Analytical Vulnerability Assessment

2.1 Steps in the Methodology for Analytical Vulnerability Assessment

This section summarises the main steps in the methodology for analytical vulnerability assessment by way of a schematic roadmap for the calculation of fragility functions and vulnerability functions. For each step, multiple options are available to the analyst, as shown in Figure 2.1. *These different options are presented in decreasing order of complexity, time requirement, and accuracy.* Note that the recommended choices presented in this document are for generic low/mid-rise reinforce-concrete, steel, or masonry building structures. For other structural typologies or materials other options may be more appropriate and appropriate judgment should be exercised.

The first step in the process of analytical vulnerability assessment is to define the population of analysed buildings that a given vulnerability function will represent. In the present Guidelines, buildings are defined in terms of structural, material, and economic characteristics, according but not limited to the GEM Taxonomy first level attributes [Brzev et al 2012] (see Table 2.1), and including other attributes and parameters needed for successful sampling and modelling. Depending on the scope of the work and available resources, the Analyst will be required to choose the analysis type, model type and define a set of damage states in a consistent framework of complexity and accuracy.

Table 2.1 Definition of building class as per GEM-Taxonomy

#	GEM Taxonomy		
	Attribute	Attribute Levels	
1	Material of the Lateral Load-Resisting System	Material type (Level 1)	MAT99/CR/S/MR/W/MATO….
		Material technology (Level 2)	CIP/SL/STRUB/WHE…
		Material properties (Level 3)	WEL/MON/MOCL…
2	Lateral Load-Resisting System	Type of lateral load-resisting system (Level 1)	L99/LN/LFM/LFINF…
		System ductility (Level 2)	D99/DU/ND
3	Roof	Roof material (Level 1)	RM/RE/RC/RWO
		Roof type (Level 2)	RM1/RE1/RC99/RWO2….
4	Floor	Floor material (Level 1)	FM/FE/FC/FW…
		Floor type (Level 2)	FM1/FC1/FME1/FW1….
5	Height	Number of stories	H99/H:n – H:a,b/HE
6	Date of Construction	Date of construction	Y99/YN/YA/YP
7	Structural Irregularity	Type of irregularity (Level 1)	IR99/IRN/IRH/IRV
		Irregularity description (Level 2)	TOR/REC/CRW/CHV…
8	Occupancy	Building occupancy class - general (Level 1)	OC99/RES/COM/GOV…..
		Building occupancy class - detail (Level 2)	RES1/COM1/IND1/REL1…

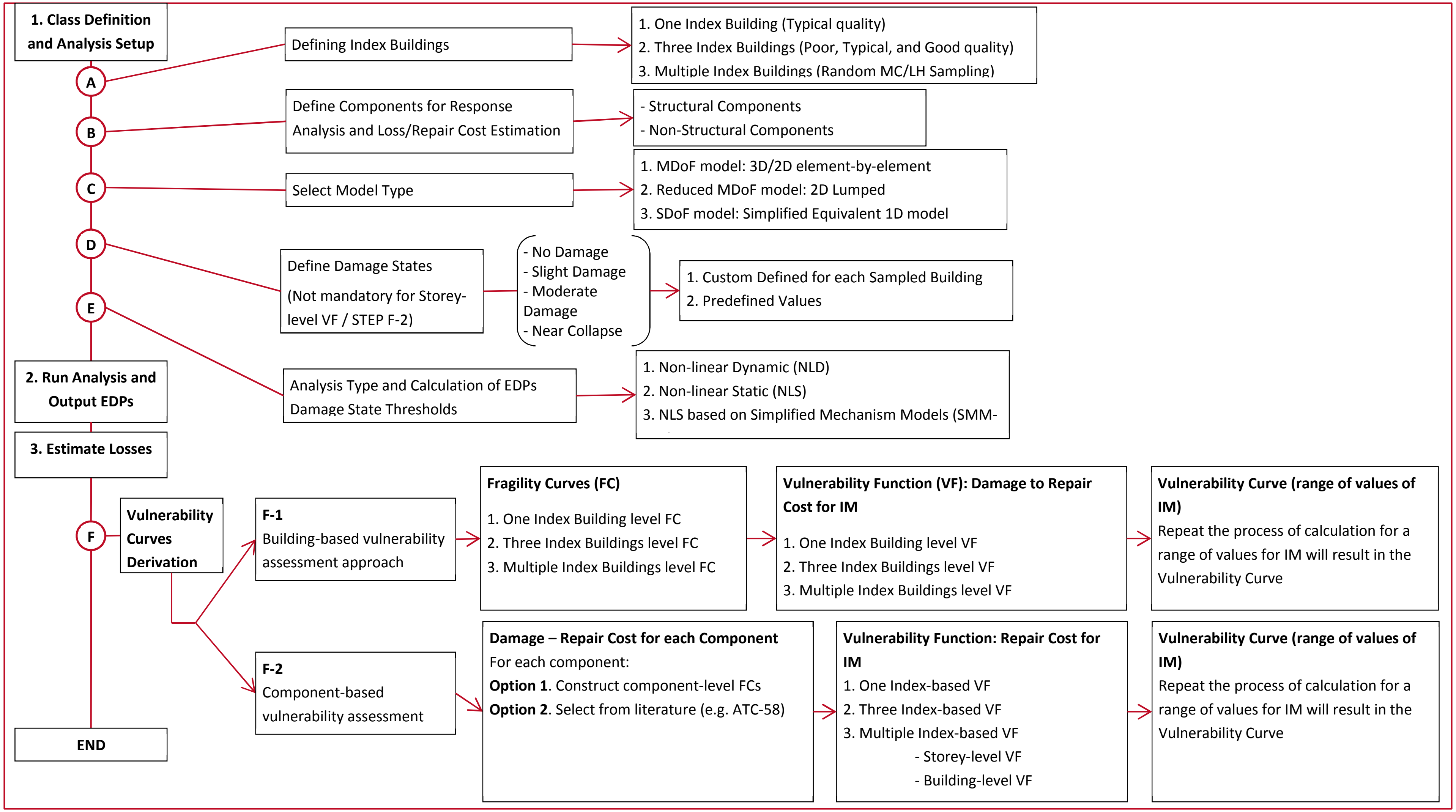

Figure 2.1 Schematics of the roadmap for the calculation of vulnerability functions with the analytical method

STEP A: Defining Index Buildings

As first step in analytical vulnerability assessment, the analyst will need to select the most appropriate sampling technique to represent a class of buildings. Three building sampling levels are offered to determine a prototype that will be used to represent each class' population. Depending on the resources of the study, the choice between these different levels is dependent on acceptable calculation effort and corresponding epistemic uncertainty:

- One Index Building: the analyst uses only a single index building that represents, for instance, a typical case in terms of capacity and seismic response (i.e., lateral load-resisting system and material type). This representation of class' population is in general selected if the analyst is constrained regarding time or if data for the population is very poor.

- Three Index Buildings: the analyst identifies the most important parameters and their variance in order to create three sub-classes of buildings, in terms of capacity and seismic response. The central index building is associated to typical building performance, while the other two are associated respectively to a Poor and Good building performance for the same nominal GEM Taxonomy building typology. In general the parameters that will influence the capacity and seismic response and are affected by the quality of material and workmanship within a real building stock, are those associated to the lateral load-resisting system and the material type, i.e. the mechanical characteristics, dimension characteristics, geometric configuration, and structural detailing (e.g. strength of the material of the lateral load-resisting system, typical dimension and lay-out of structural elements, structural connections).

- Multiple Index Buildings: this procedure will provide a good coverage of the variability within a sample, i.e. the analyst can explicitly quantify between-specimen variability using, for instance, Monte Carlo simulation or Latin Hypercube sampling. Depending on the number of properties considered, full permutations will require a large number of analyses, and hence it is advisable only in cases of simple forms of modelling, requiring a small set of parameters and short computing times. Moreover, this level of sampling may require advanced skills in statistical simulation.

STEP B: Define Components for Response Analysis and Loss Estimation

Two groups/classes of components should be considered in seismic vulnerability assessment: Structural Components and Non-structural Components (see Meslem and D'Ayala [2012]):

- Structural components: components from this class are the main elements that contribute to the seismic response behaviour of the structure. Hence, these components should be considered in developing the mathematical model to conduct the response analysis. In addition, these components should be considered for loss estimation.
- Non-structural components: should be divided into two categories:
    - Category A: are those that may contribute to the response behaviour of the structure, e.g. masonry infill walls for the case of reinforced concrete (RC) buildings. Hence, components from this class/category will be considered in both the developing of mathematical model for response analysis and the loss estimation;

- Category B: they do not contribute to the response behaviour of the structure, but they are considered to be dominant in terms of contribution to construction cost and hence should be considered in loss estimation.

The remit of the present Guidelines is the fragility assessment and vulnerability function definition of structural components and whole structure. Hence Structural Components and Category A of the Non-Structural Components, form the object of the vulnerability assessment of these Guidelines. For the vulnerability assessment of Category B Non-Structural Components the reader is referred to the relevant Guidelines (see Porter et al. [2012b]). In addition, for adding the loss of Contents, appropriate guidelines can be found in (see Porter et al. 2012c).

STEP C: Select Model Type

Three levels of model complexity are proposed (in decreasing order of complexity), offering three distinct choices of structural detail:

- Multi Degree of Freedom (MDoF) model (3D/2D elements): a detailed 3D or 2D multi-degree-of-freedom model of a structure, including elements for each identified lateral-load resisting component in the building, e.g., columns, beams, infills walls, shear walls, URM walls, etc.
- Reduced MDoF model (2D lumped): a simplified 2D lumped stiffness-mass-damping representation of a building, where each of the N floors (or diaphragms) is represented by one node having 3 degrees of freedom, two translational and one rotational to allow representation of both flexural and shear types of behaviour. This representation is not suitable for plan-irregular buildings, buildings where torsional effects are anticipated, or very slender structures.
- Single Degree of Freedom (SDoF) model: a simple SDoF representation by a one-dimensional non-linear element, for which stiffness, mass damping, and ductility of the structure as a whole are defined. This representation is in general very simplistic and assumes that higher vibration modes are not relevant to the seismic response of the structure.

It should be noted that although modelling level 3 is not recommended as a choice of structural modelling, the simplification to an equivalent degree of freedom system is called upon when computing the performance point and damage state of a structure in a number of procedures illustrated in Chapter 7 for the determination of fragility curves. The rationale for following this approach is further discussed in that context.

All model levels incorporate the following interface variables: (a) seismic input via a scalar seismic intensity measure (IM) to connect with probabilistic seismic hazard analysis results (e.g. hazard curves), (b) response output via the Engineering Demand Parameters (EDPs) of individual storey drifts for allowing structural/non-structural loss estimation.

STEP D: Define Damage States at Element and Global Level

Five levels structural damage states are suggested: No Damage, Slight, Moderate, Near Collapse and Collapse. Thus four EDPs (i.e. Peak Storey Drift) thresholds are needed to differentiate among the five damage states. These are inherently random quantities that are generally assumed to be log-normally distributed and need a median and a dispersion value to be fully defined.

The Analyst is offered two distinct choices/levels for the evaluation of these EDPs:

- Custom-definition of EDPs damage thresholds for each index building

  The non-linear modelling of structural elements or storeys (depending on the model type used) usually implicitly defines the damage threshold information for each element by assigning specific parameters' values which describe changes in structural behaviour. It is hence common practice to use the model definition or some combination of model defining parameters to also define the threshold for each damage state at elemental or global level. This approach provides the flexibility of tailoring the damage threshold values to a given index building or sub-class of building typologies and introduces capacity-demand correlations that may have a major influence in the fragility analysis results and

- Pre-set definition of capacities for building typologies

  A single definition of damage state (or performance level) capacities are used for all index buildings within a typology, regardless of their inherent properties (e.g. quality of construction, ductility…etc.). This is a less accurate option that may be preferable due to simplicity, as typical values are taken from performance based design standards or other seismic assessment codes.

NOTE:

When implementing the component-based vulnerability assessment approach (see STEP F-2):

- if the analyst wishes to generate *Storey-Level Vulnerability Functions*, then STEP D for the definition of the different damage states at building level is not mandatory.
- if the analyst wishes to generate *Building-Level Vulnerability Functions*, only the identification of Collapse (median and dispersion values at Collapse) in STEP D is mandatory.

STEP E: Analysis Type and Calculation of EDPs Damage State Thresholds

This step provides criteria for choosing a method for analysing a given structural model to evaluate the median and dispersion of its structural response, i.e. an Engineering Demand Parameter (EDP), for a given level of the seismic intensity measure (IM). The following analysis options (three levels in decreasing order of complexity) are provided:

- Non-linear Dynamic (NLD) analysis: requires a set of ground motion records to perform dynamic response history analysis of a mathematical model (3D or 2D model).
- Non-linear Static (NLS) analysis: it is based on the use of a first-mode load pattern to perform a pushover analysis of a 3D/2D structure, and then fit the resulting capacity curve with an elastic-plastic, elastic-plastic with residual strength or a quadrilinear backbone curve response model. The evaluation of seismic performance is then conducted using one of the following options:
  - *Non-linear static analysis with dispersion information*: the procedure uses a set of ground motion records to estimate both the median and the record-to-record dispersion of the lognormally distributed responses.
  - *Non-linear static analysis without dispersion information*: the procedure uses smoothed design response spectrum that only provide the median responses.

- Non-linear Static analysis based on Simplified Mechanical Models (SMM-NLS): non-numerically based methods. The capacity curve is obtained through simplified analytical or numerical methods (e.g. a limit-state analysis) which do not require finite elements modelling. Note that this approach uses smoothed design response spectrum only, hence, the results are exploited without record-to-record dispersion information.

STEP F: Construction of Vulnerability Curves

Depending on the needs of the study and the availability of data/information, alternatives are offered for the generation of different types of vulnerability curves:

- vulnerability curve at the level of one index building,
- vulnerability curve at the level of three index buildings, and
- vulnerability curve at the level of multiple index buildings.

In order to generate these curves, two approaches can be used, depending on the level of available information/data and a specific knowledge, as well as the analyst's requirements:

- **STEP F-1*: Building-based vulnerability assessment approach***:

The implementation of this approach is suited to studies of large population of buildings. As recommended in HAZUS-MH [FEMA 2003], the approach consists of generating vulnerability curves by convolving of fragility curves with the cumulative cost of given damage state ds_i (damage-to-loss functions). Hence, the analysts will first need to derive the fragility curves at global building level, or, alternatively, select existing ones from literature (if available) as long as they can be considered representative of the considered structural typology performance.

The Guidelines document also provides details regarding the translation of these fragility curves to loss/repair and replacement cost of new. The analyst might use existing average values of loss/cost, such as those provided in HAZUS-MH [FEMA 2003], or other references.

- **STEP F-2*: Component-based vulnerability assessment approach***:

In this approach, recommended in ATC-58 [FEMA P-58 2012], the vulnerability functions are obtained by correlating the components level-based drifts directly to loss. In general, this approach is mostly suitable for the vulnerability analysis of single buildings, and where the majority of the economic losses are associated to non-structural components. The analyst will need to ensure that specific knowledge is available and time and monetary resources are at hand to perform such detailed analysis.

Within this approach, the analyst will have two alternatives in order to estimate loss/cost associated to damage for each component (i.e., component-level fragility curves and the translation to loss/cost):

  - The first alternative requires the availability of necessary data/information to provide a definition of the performance criteria (e.g. plastic rotation values...etc.) for each structural and non-structural component and then run analyses to derived component-level fragility curves, which can then be cumulated to determine overall vulnerability.
  - The use of existing average component-level fragility curves, and their associated loss/cost, from literature. As default source of data, ATC-58 PACT (FEMA P-58 2012), is suggested. The Analysts

may also adopt, if available, other sources for the selection of component-level fragility curves if they are more suited to the real characteristics for the existing buildings in their regions.

In the component-based vulnerability assessment approach, the vulnerability function can be generated at STOREY LEVEL, and at the ENTIRE BUILDING LEVEL. The generation of Storey-Level vulnerability functions does not require the definition of different global damage states, i.e. STEP D/Section 6 is not mandatory. The generation of Building-Level vulnerability functions requires the definition of median collapse capacity only from STEP D/Section 6.

2.2 Mixing and Matching of Mathematical Model/Analysis Type (Calculation Effort - Uncertainty)

The Guidelines document proposes several options for the choice of mathematical modelling and type of analysis. It is obvious to note that the accuracy and the level of uncertainty will directly depend on the level of complexity or simplification that the analyst will choose to pursue in conducting the vulnerability assessment as shown in Table 2.2. While it is evident that the best matching of modelling and analytical procedure is along the major diagonal of the matrix in Table 2.2, it is not uncommon for vulnerability studies to be conducted using very sophisticated analytical tool but very basic modelling. (Meslem and D'Ayala 2013, D'Ayala and Meslem 2013b) The Analyst should be aware that reducing or better quantifying the uncertainty associated with one of the components of the procedure does not necessarily means improving the overall reliability and robustness of the results.

Table 2.2 Mixing and matching for modelling/analysis type.

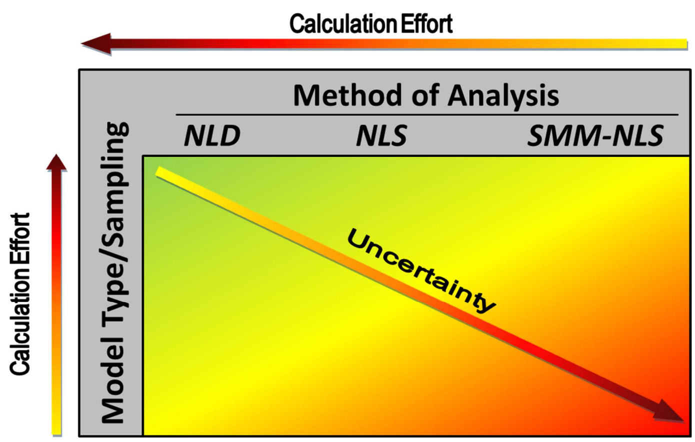

2.3 Efficiency and Sufficiency for IM Selection

The analytical estimation of seismic losses is based on combining the results of seismology, i.e., probabilistic seismic hazard analysis, with structural engineering, i.e., the analytical derivation of fragility curves. The latter is the focus of this document but it is essential to the robustness of the process that the hazard is correctly represented and correlated in a commensurate way to the analytical derivation of the fragility curves. The single point of contact is the variable that links seismic hazard with structural response, usually referred to as intensity measure (IM). The IM can be chosen in different ways; however, for the analysis to be robust, it needs to accurately represent the relevant seismological properties of ground motion to make any assessment (a) practical (b) efficient and (c) sufficient with respect to the underlying issues related to site and source [Luco and Cornell 2007]. Given the spatial distribution of the building stock and the relevance of its exposure, it is practical and advisable to use IMs for which ground motion prediction equations (GMPEs, also known as attenuation relationships) are available. At the current state of the art, these cover peak ground acceleration, peak ground velocity, peak ground displacement, and (pseudo) spectral acceleration values. Efficiency means that EDP response at any given level of the IM should show a reduced record-to-record variability, thus enabling its evaluation with a small number of time-history analyses without incurring considerable estimation errors. Finally, the sufficiency requirement stipulates that the IM can “cover” the effect of any important seismological parameter, thus removing any bias from considering, e.g. ground motions of different magnitude, distance, fault rupture mechanism, or epsilon. Epsilon represents the number of standard deviation that a certain ground motion is away from the average for the site and source parameters that characterize it. It is a measure of how extreme a response a record can cause at a period of interest. An IM that still leaves the EDP response sensitive to any of these parameters can cause unwanted bias to creep into vulnerability estimates wherever the ground motion characteristics do not match the source and site requirements for the building and IM level that is being considered.

Since vulnerability curves are needed for low to high IM levels, a structure needs to be subjected to a wide range of IM values that will force it to show its full range of response (and losses), from elasticity to global collapse. Due to limitations in the catalogue of ground motion recordings at a given site or for a given source, it is often desirable to be able to modify (i.e. scale) a record to display the desired IM level. A sufficient IM theoretically allows unrestricted scaling of ground motions to match any IM levels. In reality, though, no single IM is perfect. Therefore, exercising at least a minimum of care in selecting ground motions is advised. Since vulnerability curves are usually developed to be applicable to wide geographic regions, it is often not possible to do ground motion selection according to the most recent research findings, using the conditional mean spectrum proposed by Baker and Cornell, (2008a), or incorporating near source directivity. In general, is best to use an IM that will allow a wide range of scaling, plus a suite of relatively strong ground motion records recorded on firm soil. For most applications, the far field suite recommended by FEMA P695 (FEMA, 2009) is a safe choice. Whenever sufficient information exists about the dominant seismic mechanism, range of magnitudes or soil site in the region for which the vulnerability curve is developed (e.g. crustal earthquakes in California, low magnitude events in central Europe or soft soil in Mexico City), it may help an experienced analyst to choose records compatible with the source’s characteristics. More details can be found in NIST GCR 11-917-15 (NIST, 2011)

The most commonly used IM is spectral acceleration $S_a(T)$, i.e. the 5% damped spectral acceleration at the period of interest (usually a structure’s first mode period). It is relatively efficient, yet it has often been criticized for lack in sufficiency wherever large scale factors (higher than, say 3.0) are employed (Luco and Cornell 2007, Luco and Bazzurro, 2007). This is mainly the case for modern structures that need considerably intense ground motions to experience collapse. On the other hand, this is rarely the case for older and deficient buildings. Better efficiency and sufficiency are obtained using the average spectral response acceleration $S_{agm}(T_i)$, i.e., the sum of the natural logarithm of spectral acceleration values computed over a range of T_i values, when compared to Sa(T). It also remains practical as a GMPE for $S_{agm}(T_i)$ although not readily available, can be estimated from existing $S_a(T)$ GMPEs. Since $S_{agm}(T_i)$ offers considerable extension to the applicability of scaling [Vamvatsikos and Cornell 2005, Bianchini et al. 2010], it is the recommended approach when undertaking non-linear dynamic analysis (e.g., IDA). For non-linear static procedure methods, the reduction of the structural response to an equivalent SDoF means that $S_a(T_1)$ is used by default.

3 STEP A: Defining Index Buildings

This section guides the analyst to the choice of the most appropriate sampling technique to represent a class of buildings for analytical vulnerability estimation depending on the resources of the study. The choice between these different methods is dependent on the calculation effort available and the level of acceptable epistemic uncertainty.

Three levels/methods for building sampling are offered to identify and create a set of classes within a building population: ***One Index Building***, ***Three Index Buildings***, and ***Multiple Index Buildings***. For the implementation of either of these different sampling methods, it is important to identify the most important parameters, more specifically, those accounting for the lateral load-resisting system (structural elements) and its material, as they highly influence building capacity and seismic response, and maybe subject to considerable scatter due to the quality of workmanship and original materials.

In more details, the parameters that should be considered are those associated to the mechanical characteristics, dimension characteristics, geometric configuration, and structural detailing as categorised in Table 3.1.

It is important to ensure that each index building is defined in such a way to be comprehensively representative of the building stock population; which can be achieved by defining a ***Central Value*** with ***Lower Bound*** and ***Upper Bound*** values for each or many of the parameters in Table 3.1, as to reach a realistic distribution of characteristics membership, even though this might not be normalised, as shown in Figure 3.1. This requires some statistical information for the structural characteristics-based parameters, i.e. such as a mean or median value for each parameter and a most probable range of existence, if not a standard deviation.

Table 3.1 Example of parameters characterizing building capacity and seismic response

Type of Parameter	Examples
Mechanical Characteristics	Strength of the material of the lateral load-resisting system
Dimension Characteristics	Total height / Storey height Number of storeys Plan dimensions - Bay length
Structural Detailing	Tie spacing at the column Reinforcement ratio at the column Hardening ratio of steel
Geometric Configuration	Perimeter Frame Building - Space Frame Building (PFB/SFB) Rigid Roof / Deformable Roof (RR/DR) Column orientation (OR)

Table 3.2 Asset definition of One Index Building considering building-to-building variability: Typical Quality (see also Table 3.1)

	Typical Quality			
	Lower Bound	Central Value	Upper Bound	Standard Deviation
Mechanical Characteristics				
Dimension Characteristics				
Structural Detailing				
Geometry Characteristics				

Table 3.3 Asset definition of Three Index Buildings considering building-to-building variability: Poor, Typical, and Good Quality (see also Table 3.1)

	Poor Quality				Typical Quality				Good Quality			
	Lower Bound	Central Value	Upper Bound	Standard Deviation	Lower Bound	Central Value	Upper Bound	Standard Deviation	Lower Bound	Central Value	Upper Bound	Standard Deviation
Mechanical Characteristics												
Dimension Characteristics												
Structural Detailing												
Geometry Characteristics												

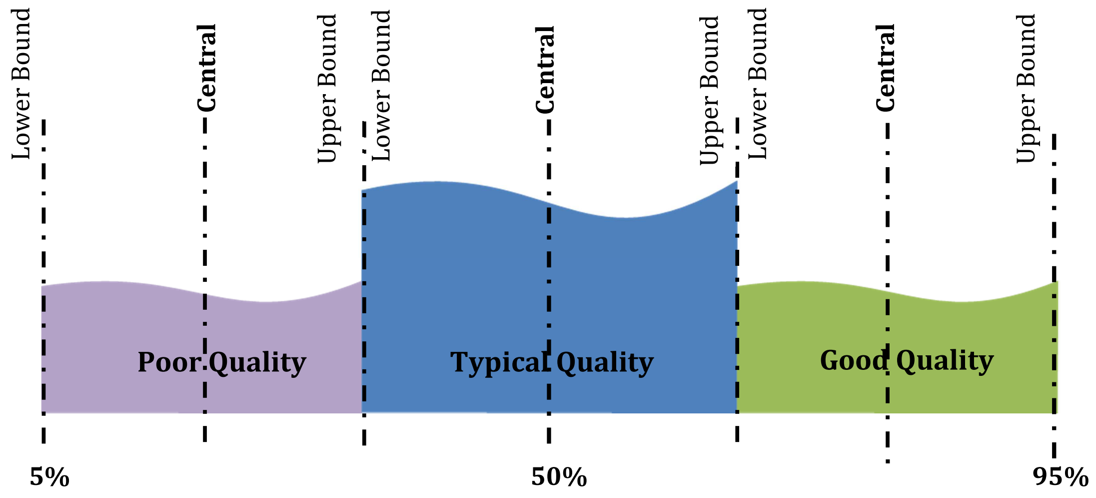

Figure 3.1 Defining index buildings.

3.1 One Index Building

This can be considered the simplest approach to represent a class' population of buildings, and is in general selected if the analyst is constrained regarding time. The approach consists on assigning for the parameters associated to the capacity and seismic response, i.e. lateral load-resisting system and material type (See Table 3.1), values representing a median or ***Typical Quality*** case of the buildings class, i.e. medium design base shear and components' fragility.

By selecting this approach and in order to account for building-to-building variability, the analyst should identify the ***Central Value***, plus the ***Lower Bound*** and ***Upper Bound*** values (which should be obtained as result from structural characteristics assessment) for each parameter, as shown in Figure 3.1 and Table 3.2. This identification should be done for structural and non-structural components; depending on the type of the selected approach for generating the vulnerability curves (See Section 8).

3.2 Three Index Buildings

With more time or need to explicitly propagate uncertainty, the analyst can generate this level of index building sampling, which is considered as quite sufficient to ensure the accuracy and reliability in terms of representation of the classes of buildings/population. The procedure may be implemented using the following three index buildings (See in Figure 3.1 and Table 3.3): ***Poor Quality***, which characterizes group of buildings with lower design shear base and fragile components, a ***Typical Quality*** case which characterises building with the expected performance, and a superior or ***Good Quality*** case, which characterizes group of buildings with higher design shear base and better post elastic performance. For each index building, the analyst should identify the ***Central Value*** of relevant parameters, plus the ***Lower Bound*** and ***Upper Bound*** values, as shown in Figure 3.1 and Table 3.3, so as to ensure collectively exhaustive and mutually exclusive subclasses.

The Poor, Typical, and Good-quality index buildings can represent in the analyst's mind cases where repair cost would be exceeded respectively by 10%, 50%, and 90% of buildings of same classification according to

GEM Taxonomy first level attributes. This assumption quantifies variability of vulnerability between specimens within an asset class. In absence of better estimates, and conservatively, the uncertainty in vulnerability within an individual specimen can be assumed to be equal to the lower-upper bound range variability set above for each index building.

3.3 Multiple Index Buildings

Using five or more index buildings significantly improves the quality of the estimated vulnerability curves at the cost of additional calculations. The main difference of this approach compared to the previous ones described is that comprehensive coverage is sought for the most uncertain characteristics that define the class, thus offering an actual sample estimate of the class variability, rather than using estimates of central values and assumed distribution as seen in the previous subsections. Thus, the analyst needs to possess a comprehensive knowledge of the probabilistic distribution of the most important structural parameters defining the population of buildings in the class of interest, which essentially means that appropriate statistical data need to be at hand. The most important characteristics that typically need to be accounted for are:

- Distribution of building height, given a number or range of stories;
- Distribution of the level of base shear used to design the building and its deformation capability, defining the reference design code basis. For buildings of a given lateral-load resisting system this can be understood to be a reflection of the prevailing detailing and capacity design requirements at the time of construction;
- Distribution of the degree of plan irregularity, defined for example for any of the two orthogonal directions of an L-shaped building as the ratio of the length of the shortest side to the longest side, parallel to that direction;
- Distribution of the degree of vertical irregularity, defined for example by the presence of a soft/weak storey and the ratio of its strength or stiffness to that of the adjacent stories. For more uniformly designed buildings, one can use the ratio of the tallest storey (usually the first) to the shortest one.

For all of the above, it is important to have at least a rough shape of the probabilistic distribution and its statistical properties (e.g., Mean and Standard Deviation). Knowledge of the existence of correlations among the different characteristics are especially important in helping select one of the following methods to properly generate a sample of index buildings. Each index building is described by a single probability value p_i that represents its probability of occurrence in the population, plus a set of values: one for each of the k characteristics. Selecting the value of k itself does not need to be done a priori, as any number of characteristics can be supplied and the highest p_i values will indicate which characteristics need to be considered. The analyst will determine the building configuration that matches each of the k characteristic values supplied for every one of the index buildings.

3.3.1 Moment-Matching

This is an algorithmic procedure for determining a set of 2k+1 index buildings that preserves the statistical characteristics of a population with k important characteristics [Ching et al. 2009, Cho and Porter 2013, Porter et al. 2014]. One index building characterizes the centre of the population while two more are needed to define the properties of each of the k features. The ensembles of these pairs of index buildings, which are used to define the deviation from the central point, are termed sigma set. Moment-matching is mainly applicable to populations that display two important characteristics:

i. They are unimodal, i.e. one cannot identify two or more distinct sub-classes that concentrate the majority of the buildings, but rather a "continuum" of buildings and their associated properties;

ii. The k important characteristics are (largely) uncorrelated. In other words, high values in one characteristic are not systematically connected to lower or higher values in a different characteristic, e.g., taller structures in the class do not necessarily have higher or lower plan irregularity.

If the above are satisfied, then moment-matching can be applied via the following steps:

i. For each of the k-characteristics, the first five moments need to be estimated: E[X], …. E[X5].

ii. Three initial weights p_i and three corresponding X_{i1}, X_{i2}, $Xi_{3,}$ values for each of the building characteristics need to be supplied. Convergence is helped by using sets of X_{ij} values close to where one expects to capture a low, typical, and high value respectively, for each of the k-characteristics.

iii. The algorithm supplied in Appendix of Non-structural Guidelines document (Porter et al. 2012b) can be applied, e.g., in Matlab to perform iterative Newton-Raphson approximation of the solution to the non-linear problem and get the suggested values of p_i and X_{i1}, X_{i2}, X_{i3}.

3.3.2 Class Partitioning

This technique constitutes an actual partitioning of the population into a set of collectively exhaustive and mutually exclusive subclasses of buildings each of which is represented by a single index building. This is highly recommended for populations that may be inhomogeneous in terms of their significant properties, e.g., the corresponding distributions may be strongly bimodal or non-continuous. Similarly to moment-matching, the overall properties of the building population are simply approximated by the joint Probability Mass Function (PMF) established by the index buildings. In simpler terms, this means that the distribution properties (e.g., mean and standard deviation of) the population are assessed by condensing the population to just the index buildings used, to each of which a certain weight is assigned, according to its actual membership (percentage of buildings it represents) in the entire population.

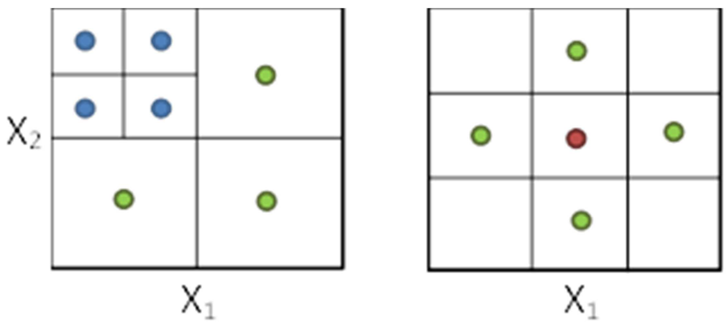

Figure 3.2 An example of class partitioning (left) versus moment matching (right) for a class with two significant properties, X1 and X2. In the former case, the two characteristics are correlated, while high values of X2 combined with low values of X1 were found to represent a significant percentage of the population, prompting a finer discretization.

For large statistical samples, formal clustering methods such as k-means clustering (see http://en.wikipedia.org/wiki/K-means_clustering) need to be used. For most simple cases, though, the intuition and knowledge of an analyst that is intimately familiar with his/her dataset will be enough to select a number of appropriate index buildings, again as characterized by k significant properties, and the appropriate probabilities of occurrence, p_i. Conceptually, this approach can be aided by loosely following these two steps:

i. Splitting: For each building characteristic, 2 or 3 subclasses are determined that partition the population to distinct parts, each of which represents at least 15% of the population's distribution for the specified characteristic

ii. Merging: The total number of possible partitions for the entire population is between 2^k or 3^k subclasses (actually 2 to the number of dimensions split in two parts times 3 to the number of dimensions split in three parts). Starting from the smaller subclasses, any adjacent subclasses whose participation to the overall population is found to be less than, say, 5% should be concatenated and the sum of their participation percentage assigned to the new wider subclass. Subclasses with participation larger than 15% should not be merged with others. This process is terminated when the desired number of subclasses is reached, typically 7-12.

3.3.3 Monte Carlo Simulation

Monte Carlo simulation involves the generation of a large sample (see

Figure **3.3**), typically far larger than the 5-7 index buildings of the previous two methods, that can accurately represent the underlying (far more numerous) population. At present it is not practical for complex model and analysis options, mainly because of the effort involved in modelling and analysing any single building, unless automated software and generous computing resources are available. Thus, Monte Carlo is only advisable for the simplest forms of modelling, i.e. the equivalent SDoF with direct capacity curve definition. In this case, its application together with improved sampling strategies to drastically reduce the computational cost, for example Latin Hypercube Sampling (LHS), rather than classic random sampling, offers unique insights into the actual population statistics and its overall seismic vulnerability, sacrificing accuracy at the level of a single building to gain resolution at the level of the entire population. We anticipate the use of such methods to be of little help for most analysts, yet their continuing evolution suggests an increased importance in the future. No detailed guidance is supplied for applying Monte Carlo, as the analyst should already have the necessary skills and expertise to follow this approach.

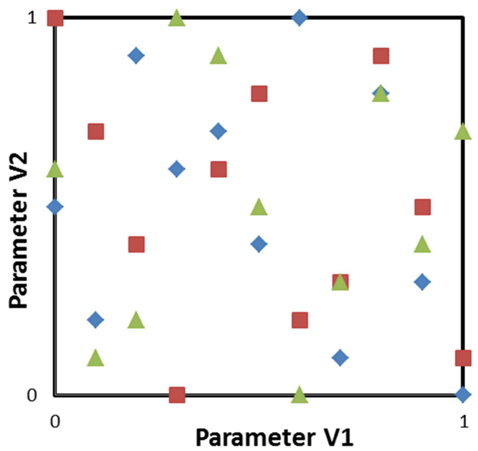

Figure 3.3 Example of Latin hypercube sampling for a building population with two significant parameters V_1, V_2.

4 STEP B: Define Components for Response Analysis and Loss Estimation

A complete seismic vulnerability assessment of an asset or a building class or building stock, typically includes the evaluation of the structural response to the expected hazards and computes the consequences of such response, in terms of monetary losses accrued by damage to structural, non-structural component and contents and, human losses, including casualties and fatalities. The remit of this Guidelines covers mainly the loss associated to structural damage of structural components, while for a more detailed treatment of the procedure used to establishes losses accruing from damage to non-structural components, content and human casualties, the analyst is directed to the specific companion Guidelines in the GEM repository.

In the following we present the basic criteria to distinguish components in structural and non-structural and reasons for inclusion in or exclusion from the structural analysis and fragility curve construction. For each component the relevant attributes and parameters that affect the quality of the analysis and the estimation of fragility and vulnerability are also included (see Meslem and D'Ayala 2012).

Within an asset construction two fundamental sets of component can be distinguished: Structural Components, and Non-structural Components:

- Structural components: components from this class are the main elements that contribute to the response behaviour of the structure. Hence, these components will be considered in developing the mathematical model to conduct the response analysis. In addition, the components will be considered for loss estimation.
- Non-structural components: they can be divided into two categories:
  - Category A: are those that may contribute to the response behaviour of the structure, e.g. masonry infill walls for the case of reinforced concrete (RC) buildings. Hence, components from this class/category will be considered in both, the development of mathematical model for response analysis and the loss estimation;
  - Category B: they do not contribute to the response behaviour of the structure, but they are considered to be dominant in terms of contribution to reconstruction cost.

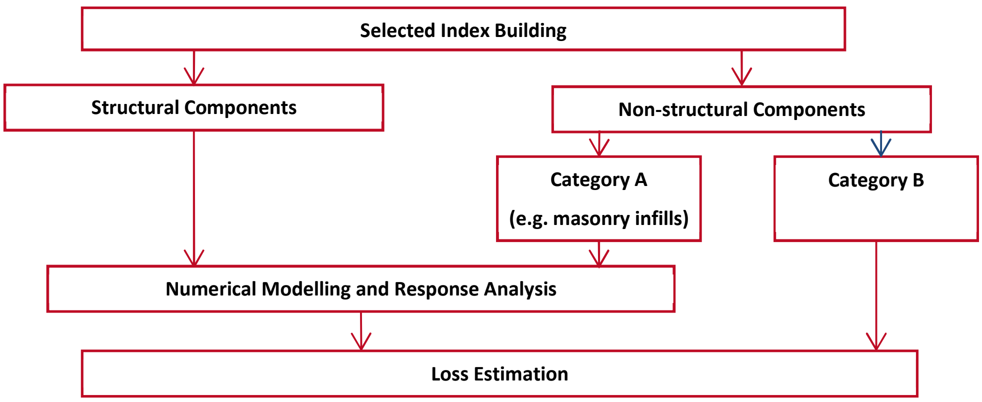

Figure 4.1 Definition of structural and non-structural components for response analysis and loss estimation

4.1 Structural Components

By structural component is intended any component that is directly modelled by an element or sets of element within the chosen model and structural analysis. The linear and non-linear behaviour of the structural component need to be defined and explicitly simulated in the analysis and directly affect the response of the overall structure. Other structural elements, such as roof and floor slabs and diaphragms, although having a structural role, they are not usually explicitly modelled, their effect on the modelled components being accounted for by means of introduction of specific constraint conditions.Table 4.1, Table 4.2, and Table 4.3 present the basic components and the corresponding parameters, respectively, for modelling and analysis requirements for the building typologies considered in GEM Taxonomy. In Table 4.1 and Table 4.2 the modelling attributes are divided into three classes of relevance: *Essential*, if no meaningful result can be obtained without it; *Qualifying*, if relevant to discriminate behaviour; and *Desirable*, for results refinement. In Table 4.3, parameters are presented in terms of buildings configuration, mechanical characteristics, geometric characteristics, and structural detailing requirements (see Meslem and D'Ayala 2012).

Table 4.1 Construction components critical for modelling and response analysis requirement for frames (RC, steel), shear walls, confined masonry

Basic Attributes		Modelling Requirement			Source of Information
		Essential	Qualifying	Desirable	
Construction component	Frame Elements (RC, Steel)	X			design documentation, on site observation, literature reference, code reference
	Shear Walls (RC, Steel)	X			
	Loadbearing Walls (conf. masonry)	X			
	Non-Loadbearing Walls (infills)		X		
	Diaphragm Elements		X		
	Roof		X		
	Claddings		X	X	
Loads	Live and Dead loads	X			
Modifications	Retrofitting		X	X	on site observation, literature reference
	Damage		X	X	

Table 4.2 Basic structural components for modelling and response analysis requirement for unreinforced masonry and adobe

Basic Attributes		Modelling Requirement			Source of Information
		Essential	Qualifying	Desirable	
Construction component	Loadbearing Walls	X			design documentation, on site observation, literature reference, code reference
	Connections		X		
	Diaphragm Elements	X			
	Roof		X		
Loads	Live and Dead loads	X			
Modifications	Retrofitting		X		on site observation, literature reference
	Damage		X	X	

Table 4.3 Parameters defining components for modelling and response analysis requirement for RC, masonry, and steel buildings

Basic Attributes			Source of Information
Building Configuration and Dimension		Number of stories	Design documentation, on site observation, literature reference, code reference
		Storey heights (floor-to-floor height for the ground floor, and for other floors)	
		Number of lines (number of bays) and spacing in x-direction	
		Number of lines (number of frames/walls) and spacing in y-direction	
Mechanical characteristics	Concrete	Compressive strength	
		Modulus of elasticity	
		Strain at peak stress	
		Specific weight	
	Reinforcing Bar	Modulus of elasticity	
		Yield stress	
		Ultimate stress	
		Strain hardening parameter	
		Specific weight	
	Masonry-infill	Compressive strength	
		Modulus of elasticity	
		Shear strength	
		Specific weight	
	Masonry-loadbearing	Compressive strength	
		Modulus of elasticity	
		Shear strength	
		Specific weight	
	Steel	Modulus of elasticity	
		Shear strength	
		Yield stress	
		Ultimate stress	
		Specific weight	
Geometry Characteristics and Structural Detailing	Reinforced concrete elements	Cross-section dimensions for columns and beams, or shear walls	
		Transversal reinforcement: type and spacing	
		Longitudinal reinforcement: type and number	
		Thickness of slabs	
	Masonry infill panel	Dimensions and thickness of walls	
		Dimension of opening: windows and doors	
	Masonry loadbearing elements	Dimensions and thickness of walls	
		Dimension of opening: windows and doors	
		Connections with other walls	
	Steel	Cross-section dimensions for columns and beams	
		Cross-section dimensions for bracing systems	
		Connection types	

4.2 Dominant Non-Structural Categories

For the loss estimation purpose, and in addition to the structural components that have been identified in Table 4.1 and Table 4.2, the analyst should also identify and consider the most dominant non-structural components contributing to construction cost. An example for the selection and classification of the most dominant non-structural components is shown in Table 4.4. As per Porter et al. [2013], the identified dominant non-structural components/losses are as follows:

- Interior partitions
- Exterior closure
- Ceilings
- Heating, ventilation, and air conditioning equipment
- Electrical equipment
- Plumbing equipment

The analyst should be aware that the above list of dominant components might vary substantially among building types (e.g. in terms of occupancy) and geographically according to living habits and standards. The analyst should refer to the appropriate sources in each region which may provide additional guidance, e.g. RS Means [2009] for US buildings.

Table 4.4 Example of ranking of non-structural components in decreasing order of contribution to construction cost.

Non-structural Components						
Rank	1	2	3	4	5	6
Component Name	Terminal & package units	Plumbing fixtures	Lighting branch wiring	Partitions	Interior doors	Exterior windows
Unit	Ea	N/A	Ea	100 lf = 30m	Each	Each (4' by 8' panel)
NISTIR 6389 class ID	D3050	D2010	D5020	C1010	C1020	B2020
FEMA P-58 class ID	D3052.011d		C3034.001	C1011.001d	C1020.001	B2022.035
Demand parameter	PFA	PFA	PTD	PTD	PTD	PTD
Ref (default PACT 1.0)	PACT 1.0	N/A	PACT 1.0	PACT 1.0	Porter judgment	PACT 1.0
Cost per m^2	$196	$143	$126	$74	$47	$42

5 STEP C: Select Model Type

Structural models can only properly represent a number of failure modes, dependent on the modelling capabilities of the structural analysis software chosen by the analyst. Thus, a careful distinction of simulated and non-simulated modes of failure is needed. Non-simulated modes of failure can only be applied a posteriori during post-processing and their effect may not be “cumulated”: The joint influence of more than one such element failures that do not occur simultaneously cannot be judged reliably unless they are included in the structural model itself. The analyst should consider that even advanced sophisticated modelling may neglect some modes of failure.

Three levels of model complexity are proposed, offering three distinct choices of structural detail:

- ***MDoF model (3D/2D element-by-element):*** a detailed 3D or 2D multi-degree-of-freedom model of a structure, including elements for each identified lateral-load resisting component in the building, e.g., columns, beams, infills, walls, shear walls, etc.
- ***MDoF model (2D lumped):*** a simplified 2D lumped (2D stick) representation of a building, where each of the N floors (or diaphragms) is represented by one node having 3 to 6 degrees of freedom, allowing at best, representation of both flexural and shear types of behaviour.
- ***SDoF model (Simplified equivalent 1D model):*** a simple SDoF representation by a 1D non-linear spring.

With regards to the choice of model type, it is clear that the performance of any selected path for vulnerability assessment will depend upon the sophistication of numerical modelling (i.e. the adopted materials behaviour, and the simplified assumptions that are made to reduce the calculation efforts…etc.). Note that any adopted model type should be consistent with the type of analysis implemented. In the following sections, some advice is provided in relation to the choices and limitation of modelling approaches (D’Ayala and Meslem 2013a, 2013b, 2013c).

5.1 MDoF Model: 3D/2D Element-by-Element

For the implementation of 3D/2D element-by-element model, the analyst should identify the primary and secondary elements or components of the building; define the non-structural elements; determine foundation flexibility, determine level of diaphragm action; define permanent gravity actions (i.e. dead loads, live loads). The level of detailed modelling of each structural component will depend on the choice of analysis type selected. If non-linear dynamic analysis is performed, components should be modelled over their full range of expected deformation response using hysteretic properties based upon test data. Similarly, when performing non-linear pushover analysis, component strength and stiffness degradation should be modelled explicitly for each structural component. For all types of analysis, the analyst should use median values of structural characteristics-related parameters when defining the component behaviour. If median values are not available, mean values should be used. The analyst should make sure to simulate all possible modes of component damage and failure (e.g., axial, flexural, flexure-axial interaction, shear, and flexure-shear interaction), P-Delta effects…etc. Further guidance on detailed component modelling for frame structures is provided in ASCE/SEI 41-06 [ASCE 2007].The analyst may also refer to the NIST GCR 10-917-5 [NEHRP 2010] and ATC-58 [FEMA P-58 2012] where additional information is provided.

For unreinforced masonry structures further guidance maybe found in Eurocode-8 [CEN 2004], D'Ayala and Speranza [2003].

Ideally, the building should be modelled as three-dimensional. In some cases the analyst may wish to use two-dimensional (planar) in order to reduce the calculation effort. However, this later may be acceptable only for buildings with regular geometries where the response in each orthogonal direction is independent and torsional response is not significant.

It is worth to mention that only engineers well versed in non-linear structural modelling should follow this approach for vulnerability analysis; it is bound to be quite time-consuming for the average analyst, depending on the level of complexity of the analysed structure.

Box 5.1: Development of MDoF model_3D/2D element-by-element

A proper 3D or 2D element-by-element model of the full-scale structure needs to be prepared by considering the following steps:

Step 1: *The choice of a 3D or 2D (planar) model depends on the plan asymmetry characteristics of the building, 3D being most appropriate wherever significant eccentricity exists, e.g. torsion effects;*

Step 2: *Identify primary and secondary elements or components; define non-structural elements, foundation flexibility, etc.*

Step 3: *Each structural element (e.g. beam, column, loadbearing wall) and non-structural element (e.g. masonry infill panel) should be represented by one or more finite elements;*

Step 4: *The level of detailed modelling of components will depend on the choice of analysis type that is selected. If non-linear dynamic analysis is performed, components should be modelled over their full range of expected deformation response using hysteretic properties based upon test data;*

Step 5: *For all type of analysis, median values of structural characteristics-related parameters should be used for models. If median values are not available, mean values should be used;*

Step 6: *Make sure to simulate all possible modes of component deformation and failure (e.g., axial, flexure, flexure-axial interaction, shear, and flexure-shear interaction), P-Delta effects…etc.;*

Step 7: *Define carefully all permanent gravity actions, i.e. dead loads, live loads.*

Frame / shear wall element modelling procedure

With regard to the choice of finite element for structural frames or flexure-critical shear walls, the analyst will have the possibility to choose between two analytical modelling procedures for non-linear analysis, fibre-based structural modelling procedure, and plastic hinge-based structural modelling procedure [D'Ayala and Meslem 2013b].

Fibre-based structural modelling technique

This technique models a structural element by dividing it into a number of two-end frame elements, and by linking each boundary to a discrete cross-section with a grid of fibres. The material stress-strain response in each fibre is integrated to get stress-resultant forces and stiffness terms, and from these, forces and stiffness over the length are obtained through finite element interpolation functions which must satisfy equilibrium and compatibility conditions. Example of implementation of fibre modelling for the case of RC member is shown in Figure 5.1.

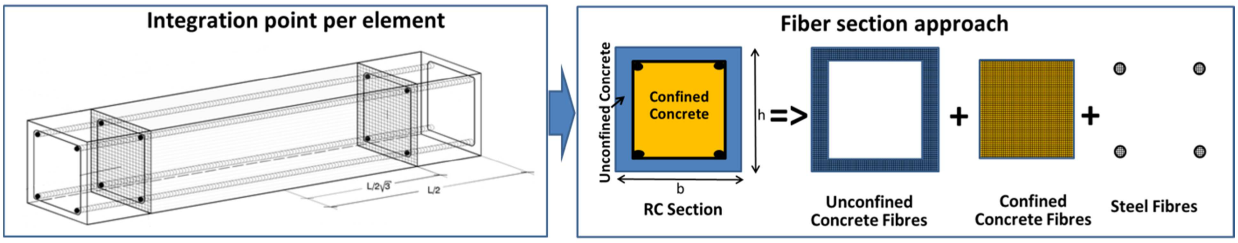

Figure 5.1 Idealisation into fibres of reinforced concrete (RC) members. This numerical technique allows characterizing in higher detail, the non-linearity distribution in RC elements by modelling separately the different behaviour of the materials constituting the RC cross-section (.i.e. cover and core concrete and longitudinal steel) and, hence, to capture more accurately response effects.

Box 5.2: Fibre-based numerical technique

Fibre-based numerical technique can be implemented by considering the following steps:

Step 1: *Define number of section fibres used in equilibrium computations. It is important to ensure that the selected number is sufficient to guarantee an adequate reproduction of the stress-strain distribution across the element's cross-section. Actually, the required number of section fibres varies with the shape and material characteristics of the cross-section, depending also on the degree of inelasticity to which the element will be forced to*;

Step 2: *Define number of integration sections. The analyst may adopt a number between 4 and 7 integration sections. Up to 7 integrations sections may be needed to accurately model hardening response, but, on the other hand, 4 or 5 integration sections may be advisable when it is foreseen that the elements will reach their softening response range*.

The analyst may refer to the literature for further guidance.

Plastic Hinge-based Structural Modelling.

This technique uses the assumption of the concentrated or distributed plasticity zones for the structural elements, with corresponding plastic hinges formation. The lumped hinge model is applied for cases where the yielding will most probably occur at the member ends, unlikely along a member. The distributed hinge model is applied for cases where the yielding may occur along a member [CSI 2009].

It should be noted that in general both approaches outlined above, while they provide a reliable simulation of flexural mode of failure (both) and combined axial and flexural mode of failure (mainly fibre models), they do not simulate the through-depth shear and the mode of failure associated with it, neither the reduction in flexural capacity due to combined shear and bending. For components which are expected to be subjected to high value of shear resultants, it is suggested to perform post analysis check as proposed in Ellul and D'Ayala [2012].

Masonry infill panel modelling procedure

For the case of masonry infilled RC load bearing frame buildings, the analyst should be aware of the critical simplification and the corresponding reduction in reliability of the results which are associated to the simulation of such structures as "bare frames", i.e. neglecting the contribution of the masonry infill to the seismic response of the system. It is highly recommended that the analyst considers the contribution of infill panels in the evaluation of seismic performance of the structure. The analyst may refer to results of comparative and sensitivity studies provided in literature (e.g. D'Ayala and Meslem 2013a, 2013b, 2013c; Meslem and D'Ayala 2013; Ellul and D'Ayala 2012).

In general practice, the infill panels are commonly made of masonry bricks or blocks, varying in specific weight, strength and brittleness depending on age and quality of construction. The simulation of a masonry infill panel in the form of diagonal equivalent strut model (see Figure 5.2) is the most frequently used simplified modelling approach for bulk analysis, and has been adopted in many documents and guidelines, such as, CSA-S304.1 [CSA 2004], ASCE/SEI 41-06 [ASCE 2007], NZSEE [2006], MSJC [2010]…etc. In the present guidelines, the diagonal strut model adopted is the one based on the early work of Mainstone and Weeks [1970], following the recommendation given by ASCE/SEI 41-06:

$$a = 0.175\left(\lambda_I h_{col}\right)^{-0.4} r_{inf} \tag{5.1}$$

where

$$\lambda_I = \left[\frac{E_m t_{\inf} \sin 2\theta}{4E_c I_{col} h_{\inf}}\right]^{\frac{1}{4}} \tag{5.2}$$

λ_I is a coefficient used to determine the equivalent width of the infill strut; h_{col} is the column height between beams' centrelines; h_{inf} is the height of the infill panel; E_c is the expected modulus of elasticity of frame material; E_m is the expected modulus of elasticity of the masonry panel (taken as $E_m = 550 f_m$; where f_m is the compressive strength of the infill material); I_{col} is the moment of inertia of the column; $r_{\inf}$ is the diagonal length of the infill panel; $t_{\inf}$ is the thickness of infill panel and equivalent strut; and θ is the angle whose tangent is the infill height-to-length aspect ratio.

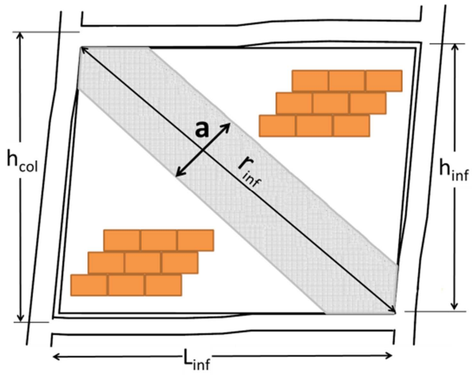

Figure 5.2 Diagonal strut model for masonry infill panel modelling

It is worth to mention that in the literature many models of infill panel have been proposed in an attempt to improve the simulation of the real behaviour of infilled frames. More details and a comparative analysis to show variance associated to these models are provided in Meslem and D'Ayala [2012], D'Ayala and Meslem [2013b] and in Asteris et al [2011].

Unreinforced Masonry modelling procedure

Modelling procedures for the structural analysis of unreinforced masonry structures can be classified following two criteria: the first defines the scale of the analysis, whether the modelling focus is on material behaviour or structural element behaviour (micro modelling or meso modelling); the second defines the type of interaction among the component materials, leading to the simulation of a continuum or discrete model.

For the computation of capacity curves for masonry structures a number of procedures are available in literature. These are based either on the equivalent frame approach or on the macro-elements' kinematics approach. Among the first, in the past decade a relatively significant number of procedures aimed at defining reliable analytical vulnerability function for masonry structures in urban context have been published [Lang and Bachmann 2004; Erberick 2008; Borzi et al. 2008; Erdik et al. 2003]. Although they share similar conceptual hypotheses, they differ by modelling complexity, numerical complexity, and treatment of uncertainties. Far fewer are the approaches based on limit state and mechanism behaviour, and among those it is worth mentioning VULNUS [Bernardini et al. 2000] and FaMIVE [D'Ayala and Speranza 2003].

Incremental dynamic analysis can in theory be used for equivalent frame procedures, however usually, given the geometric complexity of real structures, epistemic uncertainty on material constitutive laws and difficulty in representing masonry hysteretic behaviour, it is advisable to use push-over analysis or limit state kinematic approach, especially if the simulation entails the vulnerability assessment of a class of buildings, rather than single buildings, as the computational effort associated with such approaches is rather high.

In the equivalent frame approach, each loadbearing wall contributing to the lateral capacity of the structure is discretized into a set of masonry panels in which the non-linear behaviour is concentrated [Galasco et al., 2004; Roca et al. 2005]. The masonry panels are modelled as bi-linear beam elements, the shear damage being controlled by a Turnsek and Cacovic [1970] criterion, in which the ultimate shear is defined as follows:

$$V_t = \frac{lt}{b} 1.5\tau_0 \sqrt{1 + \frac{\sigma_0}{1.5\tau_0}} \tag{5.3}$$

where b is the ratio of the height over the length of the wall panel ($b = h/l$), σ_0 is the axial state of stress, τ_0 is the characteristic shear strength. In some procedures only the piers are modelled as deformable and damageable, while the spandrels are considered as infinitely rigid and strong. In other more sophisticated ones the spandrels are also modelled with finite stiffness and strength. See for instance TRE-MURI [Galasco et al. 2009]. The major limitation of these approaches is that they can only simulate the in-plane behaviour of the walls, while out of plane failures are non-simulated modes.

In the macro-element modelling approach, the entire building is subdivided in a number of blocks which are identified in geometry by assuming a predefined crack pattern. The reliability of the results depends on the sophistication of the simulation of the interaction among the blocks, the accurate simulation of connections, of material behaviour (such as finite values of tensile strength, friction and cohesion). As the kinematism approach identifies the ultimate conditions in terms of a limit state determined by a collapse load multiplier, it is essential for the reliability of the results that a large number of possible mechanisms is considered for any given geometric and structural configuration, and that this is expressed in parametric form and the layout of the crack pattern optimised to deliver the minimum possible collapse load multiplier among all possible mechanism configurations.

Combined Mechanisms			
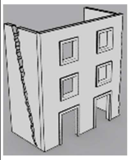 B1: façade overturning with one side wall	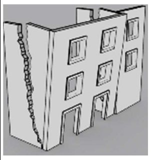 B2: façade overturning with two side walls	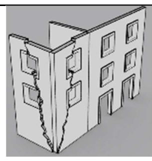 C: overturning with diagonal cracks involving corners	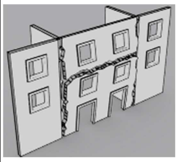 F: overturning constrained by ring beams or ties
In plane Mechanisms			
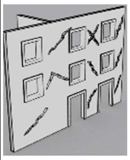 H1: diagonal cracks mainly in piers	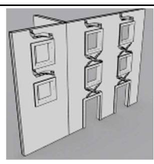 H2: diagonal cracks mainly in spandrel	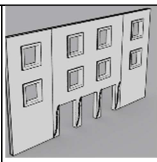 M1: soft storey due to shear	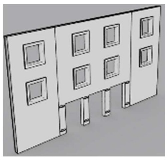 M2: soft storey due to bending
Out of Plane Mechanism			
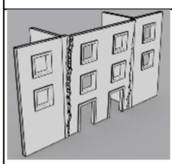 A: façade overturning with vertical cracks	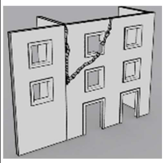 D: façade overturning with diagonal crack	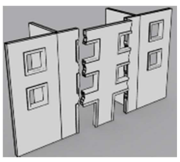 E: façade overturning with crack at spandrels	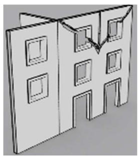 G: façade overturning with diagonal cracks

Figure 5.3 The different mechanisms considered in the FaMIVE procedure

The FaMIVE procedure is based on the macroelement modelling approach, and determines the minimum collapse load multiplier of a range of possible configurations, using a parametric approach within a linear programming optimisation technique, implemented within an Excel VBA environment. The procedure considers both in-plane and out of plane mechanisms as shown in Figure 5.3. The analyst is referred to D'Ayala and Speranza [2003], Casapulla and D'Ayala, [2006] for details of the analytical formulation of each mechanism.

The FaMIVE procedure allows to retain a high level of detail of the geometry and kinematics of the problem. At the same time, because it computes only the ultimate condition, it does not require the computing and time demands of a typical pushover analysis incremental approach. Once the ultimate conditions are defined, an idealised capacity curve is obtained considering an equivalent single degree of freedom.

5.2 Reduced MDoF Model: 2D Lumped

As seen in the previous section, appropriate component level modelling requires advanced structural skills and it is a critical aspect of the vulnerability estimation. When data is not very accurate and or resources are modest, it might be worth to adopt a reduced MDOF model employing storey-level, rather than component-level, characterization of mass, stiffness and strength. It should be noted that substantial approximations are made in adopting these models, in the determination of storey level mass stiffness and strength, which assume either an average or homogenous behaviour of single components. This may affect substantially the global failure modes. The advantage is that such models can be analysed within a few seconds using either non-linear dynamic or static methods. These simplified modelling techniques are only appropriate for structures having (a) rigid diaphragms (b) no appreciable plan asymmetries in mass/stiffness/strength (c) relatively uniform bay characteristics (length, stiffness, strength) within each floor, and (d) total building height over width ratio that is less than 3. The analyst can choose between two approaches:

Stick Models

The basic idea stems from the use of fishbone models [Luco et al 2003, Nakashima et al 2002] to represent moment-resisting frame buildings using only a single column-line with rotational restrictions for each floor owing to the presence of beams. This idea is hereby simplified and standardized to cover different structural moment resisting framed systems.

The concept is presented in Figure 5.4. It comprises N nodes for N stories, each with 3 degrees of freedom (horizontal, vertical, rotational) in 2D space. The nodes are connected by N columns in series and further restrained rotationally by N springs representing the strength and stiffness of beams at each floor. All elements are non-linear, at the very minimum having a simple elastic-perfectly-plastic force-deformation (or moment-rotation) behaviour with an ultimate (capping) ductility limit (or a dramatic loss of strength) that is explicitly modelled. Element characteristics can be derived using the aggregate stiffness of the columns/piers/walls/beams in each storey together with the corresponding yield and ultimate displacements or rotations.

Columns may be modelled using lumped-plasticity or distributed-plasticity force-based beam-column elements. Displacement-based elements are not recommended unless every single column is represented by at least four such elements, with the ones closer to the ends being considerably smaller to allow for a reliable localization of deformation. In all cases, for each storey-level column the user needs to define the moment-rotation characteristics of the element section. Thus, assuming a capped elastic-plastic model (see Figure 5.5) at the very minimum, together with a lumped plasticity column representation, each storey of a given height is characterized at minimum by the following parameters:

1. Column plastic hinge, with its nominal yield (i.e. the plastic plateau value) moment M_{yc}, yield rotation θ_{yc} and collapse rotation θ_{cc}. The yield moment can be taken to represent the total yield moment of all the columns in the storey. The yield and ultimate rotations need to represent the average values across all columns of the storey. This can result in a gross simplification if the real structure has columns of substantially diverse stiffness.
2. Column stiffness, or equivalently its moment of inertia, taken to characterize the sum of the stiffness of all columns in the storey.
3. Beam rotational spring, with its nominal yield moment M_{yb}, yield rotation θ_{yb}, and collapse θ_{cb}. Similarly to the column plastic hinge, this needs to represent the sum of all yield moments and the average of the corresponding rotational values for all beams (including any slab contributions, if thought to be significant). It is noted that since each beam contains two plastic hinges that yield at the same time, M_{yb} should contain the contribution of 2N plastic hinge yield moments, where N is the number of bays.
4. The rotational spring stiffness. This is selected to represent the ensemble stiffness of all beams flexing in double curvature. For a moment-resisting frame this can be estimated as $K = N \cdot 12 \cdot E \cdot I/L$, where I is the moment of inertia of a representative beam, N the number of bays and L the bay length.
5. The storey translational mass, to be applied at each storey node.
6. At the ground node, one can include a foundation spring to account for foundation flexibility.

P-Delta effects are taken into account by applying appropriate gravity loads and assigning the proper geometric transformation to columns. For use with perimeter (rather than space) frame systems, the use of a leaning column is not necessary as the entirety of the storey mass (and gravity load) is applied at the single storey node. Still, this means that the area of the column element, but not its moment of inertia, needs to be increased to represent the total column area of both moment-resisting and gravity framing elements.

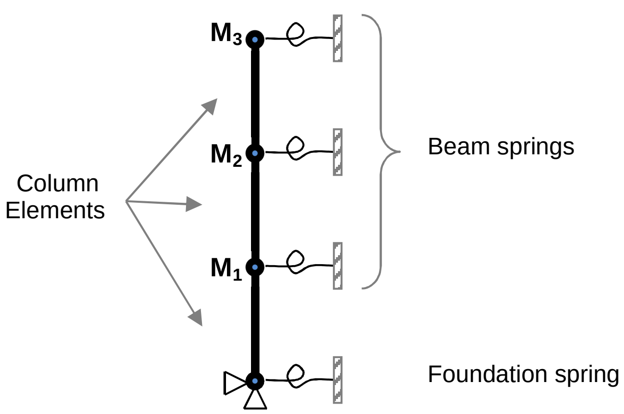

Figure 5.4 A three-storey stick model, showing rotational beam-springs, column elements and floor masses M1 – M3

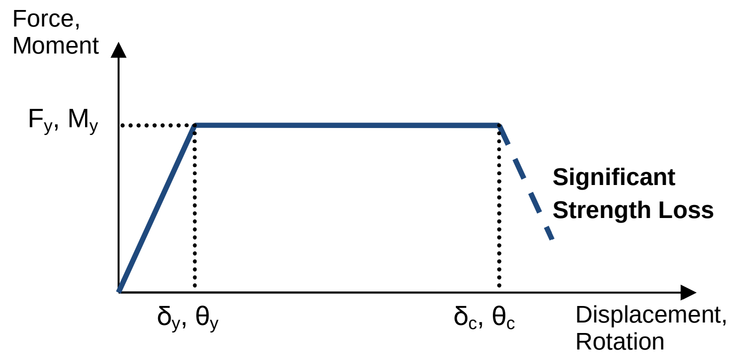

Figure 5.5 Capped elastic-plastic force-deformation (or moment-rotation) relationship

In general, stick models are not recommended for cases where the building height is larger than three times its width, as the flexural component of deformation due to column elongation may become important. Still, this is not considered an issue for most low/mid-rise buildings. When dual systems are to be modelled, e.g. systems where both structural walls or braces and moment-frames significantly contribute to lateral stiffness and strength, it is advised to employ two stick models side-by-side, connected by horizontal translation constraints to represent the rigid diaphragm.

Single-bay frame:

Whenever it is desirable to further distinguish the behaviour of the column springs to their individual constituents, a single-bay multi-storey frame may be employed instead of a simple stick. Each storey is now represented by two columns and one connecting beam plus any additional element acting at the storey level, such as, braces, infills etc. While a complex storey-level element would need to be defined for an equivalent stick model, the larger number of elements employed by the single-bay model allows an easier way for defining the behaviour of the storey. For example, braces and infills can be explicitly added by the inclusion of the proper element(s), as for a proper 2D component-by-component model. Definition of beam and column characteristics follows exactly the details laid out for the stick model. The only difference is that all strength and stiffness terms need to be divided equally between the two columns. Similarly, each storey's beam has two distinct plastic hinges. Thus each of those should represent the contribution of N beam plastic hinges, where N is the number of bays.

Such models should still be used with caution wherever the flexural component of deformation becomes important as they may overestimate its magnitude if the columns are known to have appreciable axial deformations. This is typically an issue only for high-rise buildings; therefore it is not considered to be significant within the scope of this document.

The definition of appropriate stick or single-bay models should be assisted by using a small number of detailed 2D-3D models as reference. This is particularly useful in cases where, for example, non-uniform bays or several different lateral-load resisting systems are present in each (or any) storey. Using the results of classical pushover analysis, appropriate beam and column spring properties can be calibrated to create stick or single-bay models that can help capturing the behaviour of an entire class of structures similar to the detailed model, with a reduced computational effort. However, attention should be paid to attribution of realistic values to those springs when modifying the original configuration.

5.3 SDoF Model: 1D Simplified Equivalent Model

Although a very poor approximation of the real behaviour of the structure, an SDoF equivalent model might be employed when there are very modest resources or the knowledge of the specific structural characteristic is so poor that does not warrant the effort of detailed modelling. This becomes possible by adopting experience-based mechanical models that are able to represent the dominant response characteristics of specific structural types. Thus, each such model should use analytic expressions or simple calculations to provide at least:

- the capacity curve of the structure;
- the first mode period and associated mass
- the equivalent stiffness of the system

Additionally, it is also desirable to have a normalized profile for interstorey drift ratios (IDRs) along the height (i.e., at each story) of the building that can be scaled according to the roof drift corresponding to each point of the capacity curve computed by the analysis. Having these components allows using the static pushover based methodologies described earlier. Still, it is not recommended to employ the component-fragility approach for vulnerability estimation, as the increased uncertainty associated with such simplified modelling will nullify the advantages of having a more accurate assessment methodology.

There are several methods that use the equivalent SDOF model for low/mid-rise structures. One such examples is DBELA (Procedure 4.2), described in Section 7.3.2, respectively.

6 STEP D: Define Damage States

Five structural damage states are suggested as shown in Figure 6.1: No Damage, Slight Damage, Moderate Damage, Extensive Damage, and Complete Damage (Collapse). Thus four EDP capacities are needed to differentiate among the four damage states. These are inherently random quantities that are generally assumed to be log-normally distributed and need a median and a dispersion value to be fully defined.

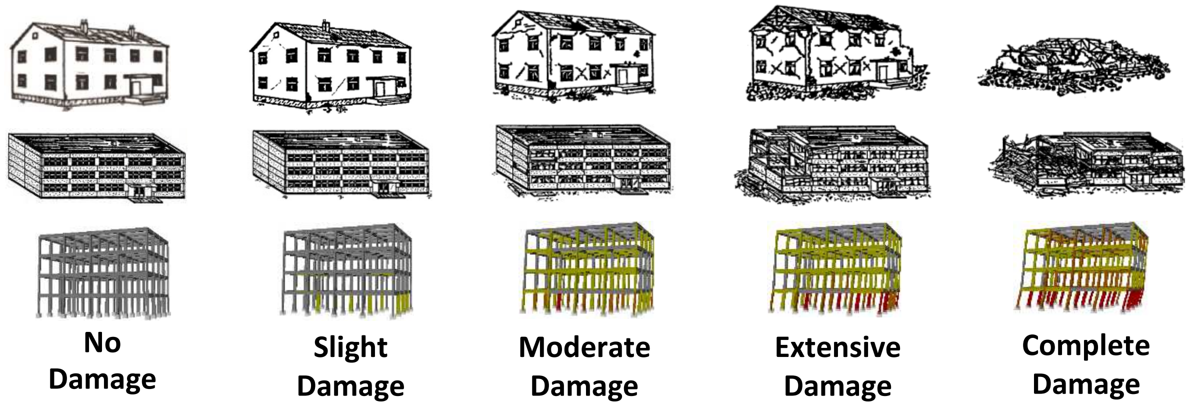

Figure 6.1 Definition of different damage states

Box 6.1: Definition of EDPs damage thresholds

Four EDP capacities are needed to differentiate. The corresponding damages are defined as follows:

ds_1 **:** *represents the attainment of Slight Damage level (SD); it usually corresponds to the limit of elastic behaviour of the components*

ds_2 **:** *represents the attainment of Moderate Damage level (MD), it usually corresponds to the peak lateral bearing capacity beyond which the structure loses some of its strength or deformation sets in at a constant rate of load*

ds_3 **:** *represents the attainment of Extensive Damage level (ED), it usually corresponds to the maximum controlled deformation level for which a determined value of ductility is set. Up to this point, the structure is able to maintain its gravity load capacity without collapsing.*

ds_4 **:** *represents the attainment of Complete Damage (Collapse) level (CD).*

The Analyst is offered two distinct choices/levels for the evaluation of these EDPs:

- ***Custom-definition of capacities for each index building:*** The non-linear modelling of structural elements or storeys (depending on the model type used) essentially incorporates the damage capacity information in each element. It makes sense to utilize the model definition to also define the threshold of each damage state. This essentially introduces capacity-demand correlation that may have a major influence in the fragility analysis results.
- ***Pre-set definition of capacities for all buildings:*** A single definition of damage state (or performance level) capacities can be used for all index buildings, regardless of their inherent properties (e.g.

quality of construction, ductility…etc.). This is a less accurate option that may be preferable due to simplicity.

NOTE:

When implementing the component-based vulnerability assessment approach (see STEP F-2):

- if the analyst wishes to generate *Storey-Level Vulnerability Functions*, then STEP D for the definition of the different damage states at building level is not mandatory.
- if the analyst wishes to generate *Building-Level Vulnerability Functions*, only the identification of Collapse (median and dispersion values at Collapse) in STEP D is mandatory.

6.1 Custom Defined for Each Sampled Building

This option for assessment/ evaluation of different damage states is recommended for analysts with a high degree of experience and knowledge of structural behaviour. The analyst is advised to refer to the definitions implemented in ATC-58-2 [ATC, 2003] and Eurocode-8 [CEN 2004], which covers No Damage, Slight, Moderate, and Extensive Damage. An example of existing definition of limit states for the case of RC building is shown in Table 6.1. For global Complete Damage (or Collapse state), ATC-58 [FEMA P-58 2012] provides different definition depending on different possibilities of mechanisms of Collapse (It is worth to mention that these definitions of Collapse mechanisms were evaluated based on the analysis of RC bare frames only). Table 6.3 shows examples, from literature, of interstorey drifts values associated to damage states for the case of RC buildings. For instance:

For the first four damage states, the analyst might refer to the following definitions provided by Dolsek and Fajfar [2008], to evaluate EDPs and the corresponding IM for the case of RC buildings: No Damage, Damage Limitation (DL), Significant Damage (SD), and Near Collapse (NC).

- No Damage: No deformation is attained either for infill panels or members;
- Damage Limitation (which may be associated to Slight Damage): for the case of infilled frames: limit state is attained at the deformation when the last infill in a storey starts to degrade. For the case of bare frames: this limit state is attained at the yield displacement of the idealized pushover curve
- Significant Damage (which may be associated to Moderate Damage): the most critical column controls the state of the structure: the limit state is attained when the rotation at one hinge of any column exceeds 75% of the ultimate rotation;
- Near Collapse (which may be associated to Extensive Damage): the most critical column controls the state of the structure: the limit state is attained when the rotation at one hinge of any column exceeds 100% of the ultimate rotation.

For the Collapse level, the analyst might refer to any of the definitions provided by ATC-58 [FEMA P-58 2012]:

- instability occurs in the analysis;
- storey drift exceed non-simulated collapse limits;
- storey drift at which the analytical model is no longer believed to be reliable (examples of values provided in Table 6.3 for the case of RC buildings).

Table 6.4 provides some definition of different Collapse mechanisms as per ATC-58 [FEMA P-58, 2012].

Table 6.1 Example of definition of damage states at global level for RC buildings, as per several existing guidelines

			Slight Damage	Moderate Damage	Extensive Damage	Complete Damage
ASCE/SEI 41-06 (ASCE 2007); ATC-58-2 (ATC 2003), FEMA-356 (ASCE 2000)	Performance Level		Immediate Occupancy (IO)	Life Safety (LS)	Collapse Prevention (CP)	
	Concrete Frames	Primary	Minor hairline cracking; limited yielding possible at a few locations; no crushing (strains below 0.003)	Extensive damage to beams; spalling of cover and shear cracking (<1/8" width) for ductile columns; minor spalling in non-ductile columns; joint cracks < 1/8" wide.	Extensive cracking and hinge formation in ductile elements; limited cracking and/or splice failure in some non-ductile columns; severe damage in short columns.	
		Secondary	Minor spalling in a few places in ductile columns and beams; flexural cracking in beams and columns; shear cracking in joints < 1/16" width.	Extensive cracking and hinge formation in ductile elements; limited cracking and/or splice failure in some non-ductile columns; severe damage in short columns.	Extensive spalling in columns (limited shortening) and beams; severe joint damage; some reinforcing buckled.	
	Unreinforced Masonry Infill Walls	Primary	Minor (<1/8" width) cracking of masonry infills and veneers; minor spalling in veneers at a few corner openings.	Extensive cracking and some crushing but wall remains in place; no falling units. Extensive crushing and spalling of veneers at corners of openings.	Extensive cracking and crushing; portions of face course shed.	
		Secondary	Same as primary.	Same as primary.	Extensive crushing and shattering; some walls dislodge.	
ATC-58-2 (ATC 2003), Vision 2000 (SEAOC 1995)	Performance Level		Operational	Life Safe	Near Collapse	Collapse
	Primary RC Elements		Minor hairline cracking (0.02”); limited yielding possible at a few locations; no crushing (strains below 0.003)	Extensive damage to beams; spalling of cover and shear cracking (<1/8”) for ductile columns; minor spalling in non-ductile columns; joints cracked < 1/8” width.	Extensive cracking and hinge formation in ductile elements; limited cracking and/or splice failure in some non-ductile columns; severe damage in short columns.	Partial or total failure/cracking of columns and beams
	Secondary RC Elements		Same as primary	Extensive cracking and hinge formation in ductile elements; limited cracking and/or splice failure in some non-ductile columns; severe damage in short columns	Extensive spalling in columns (possible shortening) and beams; severe joint damage; some reinforcing buckled	Partial or total failure/cracking of infill panels and other secondary elements
Eurocode-8 (CEN 2004)	Performance level		Damage Limitation (DL)	Significant Damage (SD)	Near Collapse (NC)	
	Observed damage		Building is considered as slightly damaged. Sustain minimal or no damage to their structural elements and only minor damage to their non-structural components.	Building is considered as significantly damaged. Extensive damage to structural and non-structural components.	Building is considered as heavily damaged. Experience a significant hazard to life safety resulting from failure of non-structural components.	

Table 6.2 Example of definition of damage states at global level for RC buildings, as per several existing guidelines (continued)

		Slight Damage	Moderate Damage	Extensive Damage	Complete Damage
Dolsek and Fajfar (2008)	Performance Level	Damage Limitation (DL)	Significant Damage (SD)	Near Collapse (NC)	
	Observed damage	For the case of infilled frames: limit state is attained at the deformation when the last infill in a storey starts to degrade. For the case of bare frames: this limit state is attained at the yield displacement of the idealized pushover curve.	The most critical column controls the state of the structure: the limit state is attained when the rotation at one hinge of any column exceeds 75% of the ultimate rotation	The most critical column controls the state of the structure: the limit state is attained when the rotation at one hinge of any column exceeds 100% of the ultimate rotation	
ATC-58 (FEMA P-58, 2012)	Performance level				Collapse
					Several definitions of collapse failure have been proposed

Table 6.3 Example of interstorey drift values (ID) associated to damage states, for RC buildings, as per several existing guidelines.

				Slight Damage	Moderate Damage	Extensive Damage	Complete Damage
Vision 2000 (SEAOC 1995); ATC-58-2 (ATC 2003)	Damage State			Light	Moderate	Severe	Complete
	Overall Building Damage	Interstorey Drift (ID)	Transient	ID < 0.5%	0.5% < ID < 1.5%	1.5% < ID < 2.5%	2.5% < ID
			Permanent	Negligible	ID < 0.5%	0.5% < ID < 2.5%	2.5% < ID
FEMA-356 (ASCE 2000); ASCE/SEI 41-06 (ASCE 2007); ATC-58-2 (ATC 2003)	Damage State			Light	Moderate	Severe	
	Concrete Frame Elements	Interstorey Drift (ID)	Transient	ID = 1%	ID = 2%	ID = 4%	
			Permanent	Negligible	ID = 1%	ID = 4%	
	Unreinforced Masonry Infill Wall Elements	Interstorey Drift (ID)	Transient	ID = 0.1%	ID = 0.5%	ID = 0.6%	
			Permanent	Negligible	ID = 0.3%	ID = 0.6%	

Table 6.4 Definition of different collapse mechanisms as per ATC-58 [FEMA P-58, 2012]

Graphic Illustation	Description of Collapse
	Undamaged structure
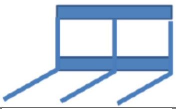	1st Storey Mechanism: 1st storey collapse, in which 100% of the first storey floor area is compressed, but none of the second.
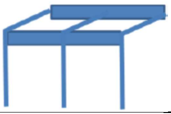	2nd Storey Mechanism: 2nd storey collapse in which 100% of the second storey floor area is compressed but none of the 1st.
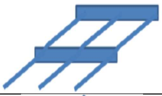	Multi-storey Mechanism: total collapse in which 100% of the building floor is involved in the collapse
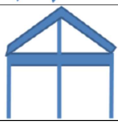	2nd Storey Column Shear Failure: is a partial collapse of the 2nd storey, in which perhaps 40% of the 2nd floor area is subject to space compression.

Box 6.2: Custom defined damage state

The evaluation of different damage states can be conducted considering the following steps:

Step.1. *Ensure the simulation of most of critical modes of failure for each structural and non-structural element. Incorporate strength capacity information (strain-stress model) in each structural and non-structural element. See Section 5;*

Step.2. *Given the modelling and structural analysis choices made, run the analysis for each index building (see Section 3) and compute the EDPs for each value of the IM in the range of interest;*

Step.3. *Damage states are evaluated as a progression of local damage through several elements (by a combination of the structural performance level and the non-structural performance level). Depending on the typology of the analysed structure, refer to ATC-58-2 [ATC 2003] and use the definitions that are provided for No Damage, Slight, Moderate, and Near Collapse. For Collapse, refer to ATC-58 [FEMA P-58 2012].*

It is quite important that the analyst considers the following:

Step.4. *Non-simulated modes of failure may need to be included in defining the transition points from one damage state to another. The shear failure of columns in brittle RC frames is one such example. In such cases, additional capacities and EDPs may have to be introduced to help in accurately defining the damage states;*

Step.5. *If a detailed component-by-component loss analysis is to be employed, as per FEMA P-58 [2012], further local element-level EDPs will have to be defined.*

6.2 Pre-Defined Values

Alternatively, the analyst might employ the proposed simplified formula and relations from literature, to estimate directly global damage states and the corresponding median capacity values. Relations commonly used are expressed as functions of yield and ultimate roof displacement. The global damage states are estimated from a simplified bilinear capacity curve representative of an index building or class.

HAZUS 99 [FEMA 1999] provide the median values of spectral displacements $\hat{S}_{d,ds_i}$ at the damage state ds_i as:

$$\hat{S}_{d,ds_i} = \delta_{roof,\, ds_i} \alpha_2 H \quad (6.1)$$

where, δ_{roof,ds_i} is the drift ratio at roof level at the damage state ds_i, α_2 is the fraction of the building height at the location of the pushover mode displacement and *H* is the typical roof level height of the building type considered. HAZUS-MH [FEMA 2003] provides α_2 and *H* values for different building types. The values of δ_{roof,ds_i} and α_2 are provided as a function of the seismic design level and damage state for different building types.

For the European building taxonomy, Kappos et al. (2006) define five damage thresholds for RC frame and dual buildings, as shown in Table 6.5.

Table 6.5 Predefined values of damage thresholds for RC frame and dual buildings (Kappos et al. 2006)

Damage State	RC buildings	
	Infilled RC frames	RC dual
Slight	$0.7 \cdot S_{dy}$	$0.7 \cdot S_{dy}$
Moderate	$S_{dy} + 0.05 \cdot (S_{du} - S_{dy})$	$S_{dy} + 0.05 \cdot (S_{du} - S_{dy})$
Substantial to Heavy	$S_{dy} + (1/3) \cdot (S_{du} - S_{dy}) \sim S_{dy} + (1/2) \cdot (S_{du} - S_{dy})$	$S_{dy} + (2/3) \cdot (S_{du} - S_{dy}) \sim 0.9 \cdot S_{du}$
Very Heavy	$S_{dy} + (2/3) \cdot (S_{du} - S_{dy})$	S_{du}
Collapse	S_{du}	$1.3 \cdot S_{du}$

S_{dy} and S_{du} are the spectral displacments at yield and ultimate, respectively, at the equivalent SDOF system level.

Lagomarsino and Giovinazzi [2006] identify the following damage states on the global capacity curve (see Equation 6.2); where $\hat{S}_{d,ds_i}$ $(\mathrm{i} = 1,2,3,4)$ identify the median value of spectral displacements at damage states ds_i. Four damage states are associated with these median values: Slight, Moderate, Extensive, and Complete (Collapse), respectively.

$$\begin{cases} \hat{S}_{d,ds_1} = S_{dy} \\ \hat{S}_{d,ds_2} = 1.5 \cdot S_{dy} \\ \hat{S}_{d,ds_3} = 0.5 \cdot \left(S_{dy} + S_{du} \right) \\ \hat{S}_{d,ds_4} = S_{du} \end{cases} \quad (6.2)$$

S_{dy} and S_{du} are the spectral displacments at yield and ultimate, respectively, at the equivalent SDOF system level.

For masonry buildings, D'Ayala et al. [2012], D'Ayala [2013] have suggested 4 damage thresholds, as shown in Table 6.6, obtained by regression from available laboratory or in-situ experimental tests reported in literature on whole houses or full size walls, distinguishing by mode of failure. The range given for each value also reflects the scatter dependent on the type of masonry considered, which includes both stone and brickwork, made with lime mortar. These values are used for reference in developing the fragility curves with the procedure FaMIVE (see Section 7.3.1).

Table 6.6 Predefined values of damage thresholds for masonry buildings

Damage threshold	Damage state	Drift range (%)	
		In-plane failure	Out-of-plane failure
S_{ds_1}	Slight: cracking limit	0.18 -0.23	0.18-0.33
S_{ds_2}	Structural damage: maximum capacity	0.65 -0.90	0.84-0.88
S_{ds_3}	Near Collapse: loss of equilibrium	1.23 – 1.92	1.13-2.3
S_{ds_4}	Collapse	2.0 – 4.0	2.32-4.

7 STEP E: Analysis Type and Calculation of EDPs Damage State Thresholds

A number of procedures based on different types of analysis can be followed to compute Engineering Demand Parameters (EDPs) damage state thresholds and hence develop building fragility and vulnerability functions. The choice between these procedures will depend on the availability of input data, the analyst's skills, and the acceptable level in terms of computational effort/cost. Note that the accuracy of these procedures will be highly dependent on the choice of modelling type, and hence the choices in Step B and Step C are highly correlated. Moreover the most appropriate choice is also a function of the lateral load resisting system and material, as reliable structural modelling is not available for all material types and structural forms at the same level of accuracy. The analyst is referred to the Sensitivity and Compendium documents (D'Ayala and Meslem 2013a, 2013b; Meslem and D'Ayala 2013) for a critical discussion of analytical and modelling approaches available in literature, their use in fragility and vulnerability curve derivation, and their associated reliability.

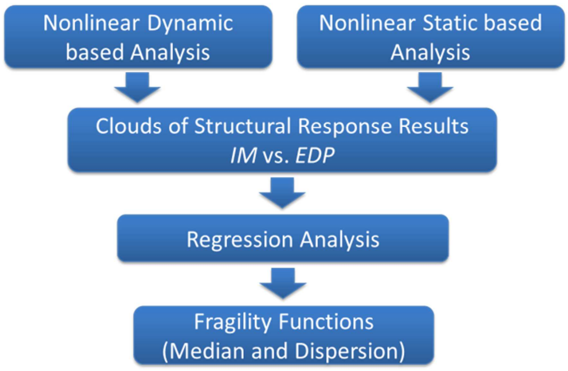

Figure 7.1 Steps for the derivation of seismic fragility functions.

Procedures are subdivided in three categories according to the type of structural analysis chosen:

- Non-linear Dynamic Analysis (NLD): Incremental Dynamic Analysis (IDA) is the most accurate in comparison to the two other procedures. IDA uses a large number of non-linear response history simulations to determine a so-called backbone or envelop capacity curve. This allows an accurate quantification of the uncertainties associated with record variability, but the accuracy of the response is a function of the appropriate level of complexity of the model.
- Non-linear Static procedures (NLS): They are based on the use of capacity curve obtained from static pushover analysis. Response history simulation is not required for the development of fragility and vulnerability functions. Note that these procedures can provide reasonable and sufficient accuracy for the estimation of fragility and vulnerability functions for many structures. Options for considering record to record variability are proposed, alongside single spectrum evaluations
- Non-linear Static Analysis based on Simplified Mechanism Models (SMM-NLS): The reliability of these procedures is highly dependent on the exhaustive identification of relevant realistic failure mechanisms and the computation of their associated capacity curves.

In relation to the structural typology analysed it is recommended to use procedures NLD and NLS for reinforced concrete (RC) and steel frames, RC shear walls, and confined or reinforced masonry, while procedures SMM-NLS are most suitable for unreinforced masonry (URM), and adobe buildings. This does not exclude the use of simplified procedures existing in literature for frame analysis such as DBELA [Silva et al. 2013], neither the use of advanced non-linear modelling for masonry structures such as TReMURI [Lagomarsino et al. 2013]. The analyst is advised that in such cases attention should be paid to failure modes that might be overlooked by the use of these procedures or to simplifying assumptions which might lead to diverse levels of uncertainty.

Table 7.1 shows a list of existing building typologies in the world, as presented by GEM-Taxonomy [Brzev et al. 2012] and PAGER-SRT Taxonomy [Jaiswal and Wald 2008] documents, and their associated analysis types that have been recommended within the present GEM-ASV Guidelines. More details are discussed in the next sub-sections.

Table 7.1 Association of GEM-ASV methods /Analysis Type with building typologies in accordance with GEM-Taxonomy and PAGER-Taxonomy.

Building Taxonomy						Method for Seismic Performance Assessment					
GEM-Taxonomy			PAGER-SRT Taxonomy			Non-linear Dynamic Procedure (NLD)	Non-linear Static Procedures (NLS)				Simplified mechanism models (SMM-NLS)
Main Attribute [ID]	Secondary Attributes [ID]		Material	ID	Description	Procedure 1.1	Procedure 2.1	Procedure 3.1	Procedure 3.2	Procedure 3.3	Procedure 4.1
Material [MA]	Material Type [MA**]	Timber [MATI]	Wood/Timber	W	Wood frames, Timber frames / walls	■		■	■	■	
		Masonry [MAMA]	Reinforced / Confined Masonry	RM	Reinforced masonry bearing walls / Confined masonry	■		■	■	■	
		Reinforced Concrete [MACO]	Reinforced Concrete	C	Reinforced concrete with masonry infills	■	■				
					Concrete moment-resisting frames/ shear walls	■		■	■	■	
			Precast Concrete	PC	Precast concrete frames / walls	■		■	■	■	
		Steel [MAST]	Steel	S	Braced steel frames	■					
					Steel moment-resisting frames and others	■		■	■	■	
		Earthen [MAEA]	Adobe/Mud Walls	M	Mud walls	■		■	■	■	■
				A	Adobe blocks walls	■		■	■	■	■
				RE	Rammed earth walls	■		■	■	■	■

Table 7.2 Association of GEM-ASV methods /Analysis Type with building typologies in accordance with GEM-Taxonomy and PAGER-Taxonomy (continued).

Building Taxonomy						Method for Seismic Performance Assessment					
GEM-Taxonomy			PAGER-SRT Taxonomy			Non-linear Dynamic Procedure (NLD)	Non-linear Static Procedures (NLS)				Simplified mechanism models (SMM-NLS)
Main Attribute [ID]	Secondary Attributes [ID]		Material	ID	Description	Procedure 1.1	Procedure 2.1	Procedure 3.1	Procedure 3.2	Procedure 3.3	Procedure 4.1
Material [MA]	Material Type [MA**]	Masonry [MAMA]	Stone/Block Masonry	RS	Rubble stone (field stone) masonry walls	■		■	■	■	■
				DS	Rectangular cut-stone masonry block	■		■	■	■	■
				MS	Massive stone masonry in lime or cement mortar	■		■	■	■	■
				UCB	Unreinforced concrete block masonry with lime or cement mortar	■		■	■	■	■
			Brick Masonry	UFB	Unreinforced fired brick masonry	■		■	■	■	■
		Other [MAOT]	Other	MH	Mobile homes						
				INF	Informal constructions						
				UNK	No specified						

7.1 Ground Motion Selection and Scaling

7.1.1 Ground Motions Selection

In order to cover the full range of structural behaviour from elastic to inelastic and finally to global collapse [Vamvatsikos and Cornell 2002], and account for record-to-record variability (variability related to the mechanism of the seismic source, path attenuation effects, local site effects), suites of ground motion records have to be selected and, if necessary, scaled to a certain level of seismic intensity.

As per EN 1998-1 [CEN 2005] the suite of records should be in accordance with the following rules:

- the duration of the records shall be consistent with the magnitude and the other relevant features of the seismic event underlying the establishment of ag;
- in the range of periods between 0.2T1 and 2T1 (T1 being the fundamental period of the structure in the direction of application of the record) the value of the mean 5% damping elastic spectrum, calculated from all time histories, should not be less than 90% of the corresponding value of the 5% damping elastic response spectrum;
- spectral matching of records to a design spectrum or site-specific spectrum may be used to represent same hazard level.

The approaches adopted for record selection and spectrum matching, have a significant effect on the resulting fragility curve, as shown by Gehl et al. [2014]. Figure 7.2 visualises the results of using different criteria for the matching of the natural spectrum to a reference elastic response spectrum.

Since the properties of the seismic response depend on the intensity, or severity, of the seismic shaking, a comprehensive assessment calls for numerous non-linear analyses at various levels of intensity to represent different possible earthquake scenarios. Attention should be paid to the extent to which is reasonable to scale a given record up or down to match a reference intensity. It is advisable to choose records that are associated to the reference magnitude considered for the scenario of interest.

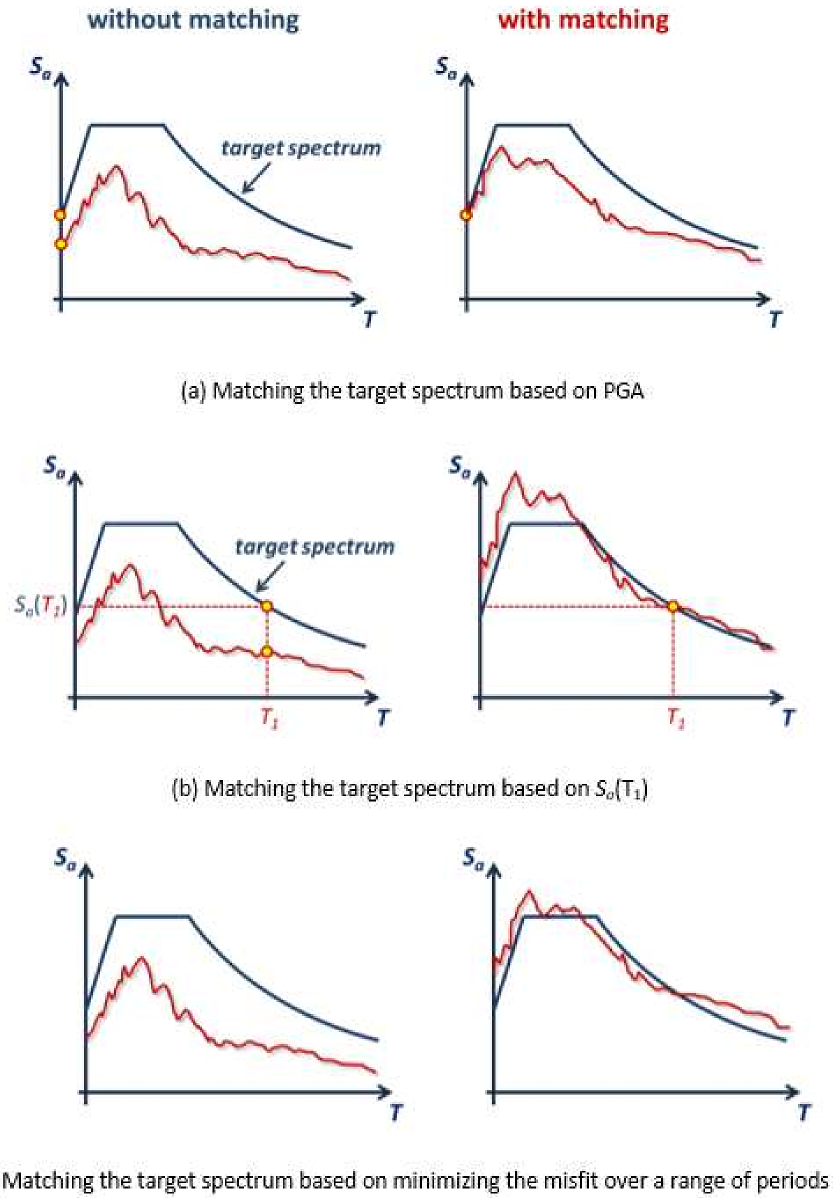

Figure 7.2 Matching of ground motion to a given elastic response spectrum

7.1.2 Number of Ground Motion Records

The calculated response can be very sensitive to the characteristics of the individual ground motion used as seismic input; therefore, several analyses are required using different ground motion records to achieve a reliable estimation of the probabilistic distribution of structural response. The minimum number of ground motions that should be used to provide stable estimates of the medians capacity (Figure 7.3); analysts are required to consider the following parameters that can strongly influence the stability in median capacity:

- Type of analysis: non-linear dynamic, non-linear static, simplified methods;
- Assumption used in selecting ground motion records;
- Type of structure and structural characteristics

For non-linear dynamic analysis, the use of 11 pairs of motions has been recommended (i.e. 22 motion set, including two orthogonal components of motion) as per ATC-58 [FEMA P-58, 2012].

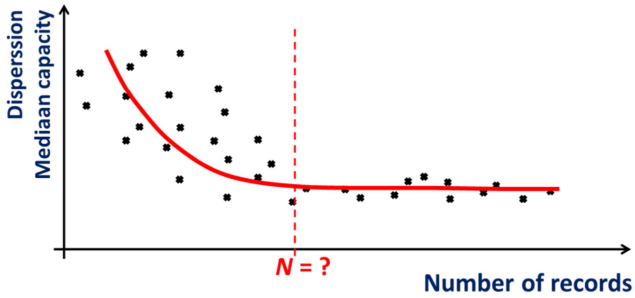

Figure 7.3 Number of ground motions for a stable prediction of median collapse capacity

In the following for each procedure we present the method for computing the median EDPs damage state threshold from backbone or capacity curves, and a discussion of which uncertainty parameters should be accounted for and how can this be computed.

7.2 Non-Linear Dynamic Analysis (NLD)

Incremental Dynamic Analysis (IDA) is the dynamic equivalent to a pushover analysis, and has been recommended in ATC-63 [FEMA P-695, 2008] and ATC-58 [FEMA P-58, 2012]. This procedure can be implemented to any building typology to estimate the different medians capacity. The analyst should note that the implementation of IDA requires defining a complete hysteretic behaviour of the materials and repeating the analysis for a large number of acceleration time histories. Depending on the level of complexity and material type of the building the length of time required to perform a computation process might be significant.

With regards to the model type to be employed, the analyst should make sure that it is consistent with the type of analysis, i.e. that sufficient model complexity is retained. To this end it is necessary to define hysteretic curves for structural and non-structural elements, to use median values for structural characteristics-related parameters, to simulate all possible modes of component damage and failure (or account for them a posteriori), to define permanent gravity actions. More details regarding the process for the development of models are provided in Section 5.

7.2.1 Procedure 1.1: Incremental Dynamic Analysis (IDA)

Incremental Dynamic Analysis (IDA, Vamvatsikos and Cornell 2002) is a comprehensive method for extracting the conditional distribution of structural response (e.g., peak interstorey drifts or peak floor accelerations) given the IM for any number of IM levels, from elasticity to global collapse. This is done by subjecting a structural model to non-linear time history analysis under a suite of ground motion accelerograms that are scaled to increasing levels of the IM until collapse is reached (see Figure 7.4).

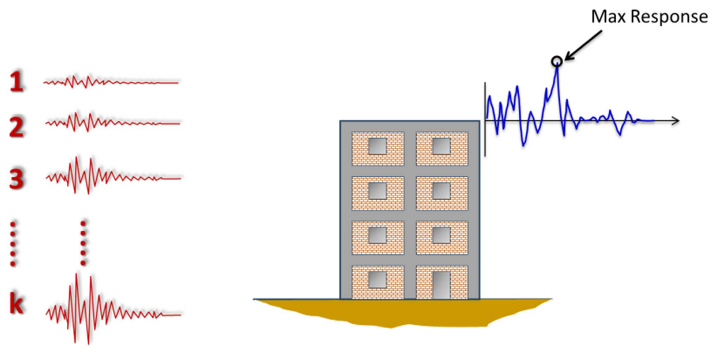

Figure 7.4 Incremental Dynamic Analysis using ground motion scaling

Regarding the application of the procedure, the amplitude of each selected ground motion should be incremented, and non-linear response history analysis performed until either global dynamic or numerical instability occurs in the analysis, indicating that either collapse, or storey drift exceeding non-simulated collapse limits, or large increase in storey drift associated with small increments in spectral acceleration is affecting the structure (see Figure 7.5). As shown in Figure 7.5, the output of IDA is a set of discrete points, (obtained by scaling each of the selected ground motions), of the IM versus the demand parameter of interest, for instance the first mode spectral acceleration $S_{a,ds_4}(T_1)$, and the maximum interstorey drift, respectively.

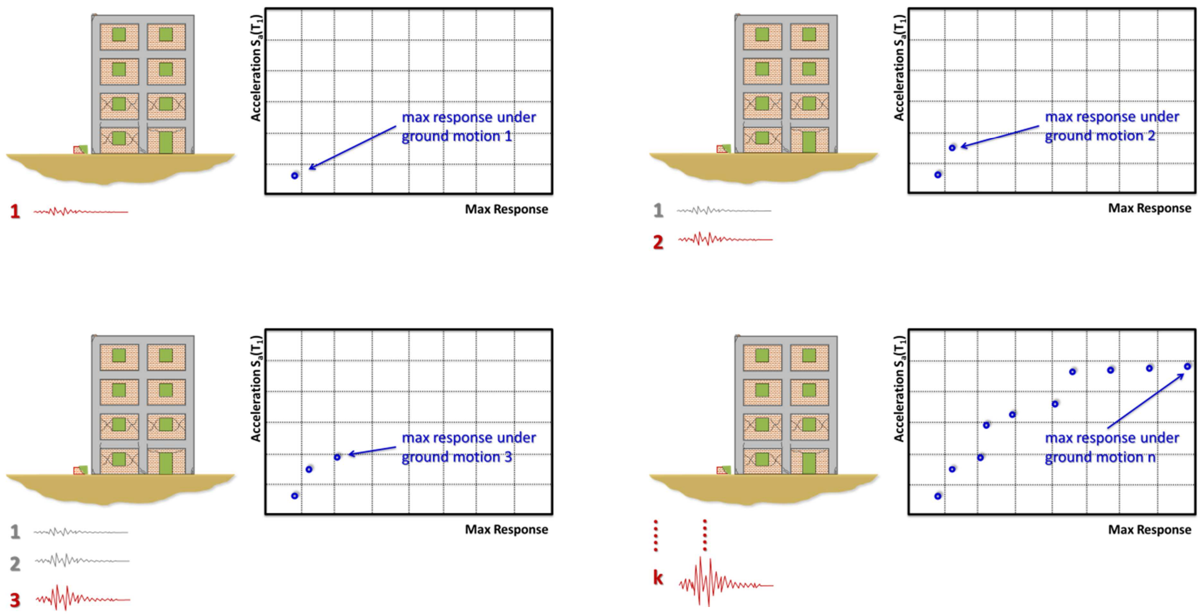

Figure 7.5 Steps of incremental dynamic analysis using ground motion scaling

To obtain continuous curves, Cubic Spline interpolation technique is made use of, in order to save computational time. This technique ensures continuity of first and second derivative at the merging points (see Figure 7.6).

The location where each IDA curve becomes flat identifies the IM level beyond which it is assumed that global collapse will occur.

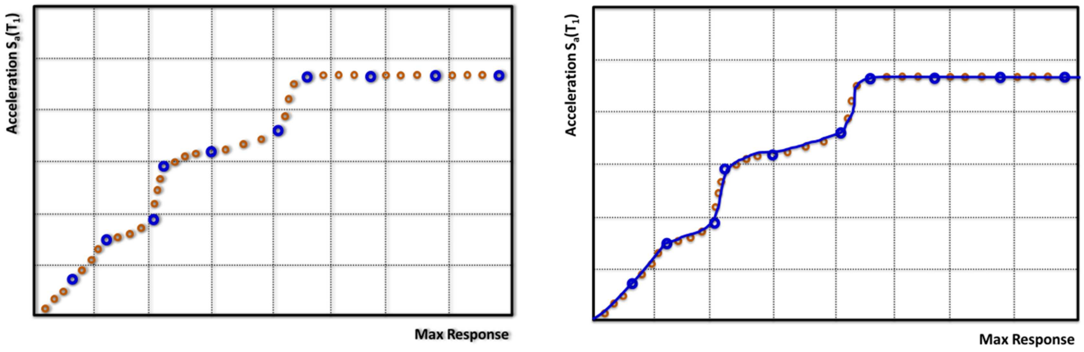

Figure 7.6 Generating IDA curve using cubic spline interpolation

The smooth IDA curve provided by the interpolation scheme offers much to observe, as shown in Figure 7.7. The IDA curve starts as a straight line in the elastic range where there is direct proportionality and correlation between IM and DM (Figure 7.7a). Beyond this first linear portion the curve can be seen as a series of steps, where the IM is increased until a new damage state threshold is reached, and the low slope portion beyond this point represents the variability in response associated to small changes of the IM, representative of the uncertainties of damage thresholds (Figure 7.7b). The last portion of the curve (Figure 7.7c), as already stated above, represent the achievement of global dynamic instability, when a small increment in the IM-level results in unlimited increase of the DM-response.

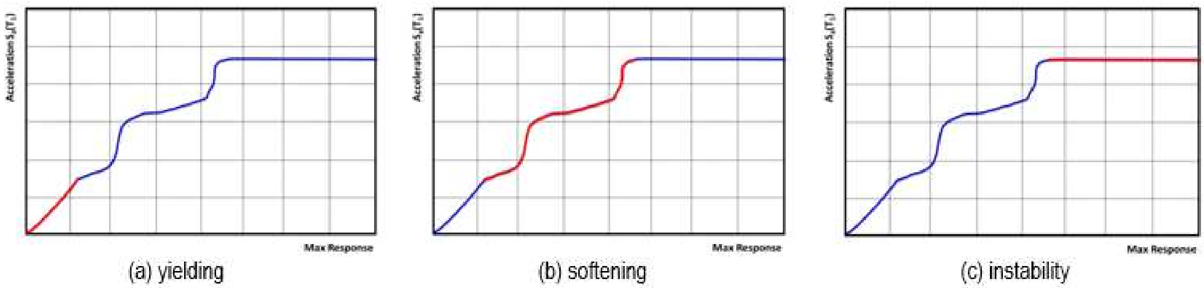

Figure 7.7 Interpretation of building response and performance from IDA curve

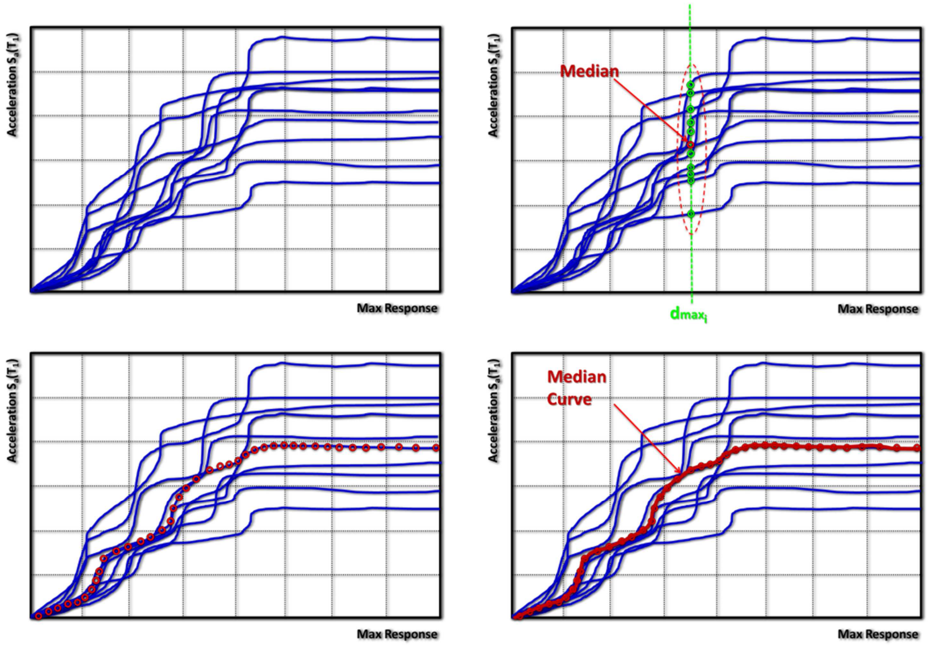

Figure 7.8 Incremental Dynamic Analysis curves using different ground motions and derivation of median curve

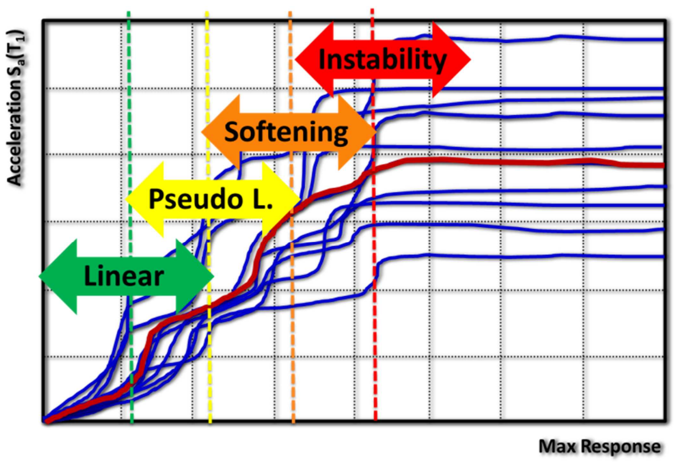

Figure 7.9 Strength and stiffness degradation

The process should be repeated for the selected suite of ground motions. The median IDA curve is defined as the 50% of all the maximum responses recorded at each level of IM, as shown in Figure 7.8.

Figure 7.9 shows the median values and range of each damage threshold. With regards to the Slight, Moderate, and Extensive damage thresholds, the analyst can estimate them as a progression of local damage through several elements (by a combination of the structural performance level and the non-structural performance level), as described in Section 6, and assign their associated interstorey drifts (ID) values in the IDA plot to extract the corresponding median capacity in terms of spectral acceleration, $\hat{S}_{a,ds_i}(T_1)$.The median collapse capacity $\hat{S}_{a,ds_4}(T_1)$ is at the level of IM producing either numerical instability or a non-simulated collapse mode as mentioned above. Note that, if 2D models are used, the median collapse capacity, $\hat{S}_{a,ds_4}(T_1)$, should be taken as the smaller of the value obtained for either direction.

The record-to-record dispersion can be estimated directly, as the lognormal standard deviation for the selected records. For instance, the following formula can be used to calculate the record-to-record dispersion associated to each damage threshold [Wen et al. 2004]:

$$\beta = \sqrt{\ln\left(1 + CoV^2\right)} \quad \text{where CoV} = \frac{\text{STDEV}}{\text{Mean}} \qquad (7.1)$$

As an alternative, the EDPs damage thresholds and their corresponding record-to-record variabilities can be extracted using regression techniques as described in Section 7.3.1.1.

The non-linear dynamic analysis can be carried out using a number of alternatives.

Cloud or stripe analysis [Jalayer and Cornell 2009, Baker 2014] can be used to organize the execution of non-linear dynamic analyses to estimate the distribution of demand given the IM. In stripe analysis, analyses at performed at specified IM levels, creating characteristic stripes of points in an IM versus EDP response plot (such as the one in Figure 7.9). If the same set of records is employed to match each IM level through scaling, then this approach is practically identical to IDA. If different ground motion sets are employed at different IM levels, typically the product of careful record selection by an informed analyst (see discussion in Section 2.3) then this allows the use of relatively insufficient IMs without problems. Cloud analysis is a similar approach that does not employ specific IM levels, but instead uses either scaled or typically unscaled sets of records for analysis, resulting in a characteristic cloud of points in an IM-response plot. The main difference to the stripe approach is that a statistical (e.g., regression) model needs to be assumed to obtain the distribution of demand given the IM, or the distribution of collapse IM capacity. Striping, instead, allows a much simpler estimation, as the response estimates are already arranged at given IM levels, thus offering direct estimates of the statistics (mean/median/dispersion) of response given the IM.

Box 7.1: Calculation of the median capacity using Procedure 1.1

Step.1. *Develop an appropriate mathematical model of the building for non-linear time histories analyses. The model should be commensurate to the level of complexity of the analysis. The analyst should refer to Section 5 for details;*

Step.2. *Select pairs of ground motion records to perform dynamic response history analysis. The use of 11 pairs of motions (i.e. 22 motions set) is recommended;*

Step 3*: For each ground motion pair, run IDA analysis: the amplitude should be incremented, and non-linear response history analysis performed until the occurrence of either:* ***Mode 1****- Numerical instability or simulated collapse;* ***Mode 2****- Predicted response that would result in non-simulated collapse;* ***Mode 3****- Large increment in storey drift for small increase in* $S_a(T_1)$ *; or* ***Mode 4****- Storey drifts at which the analytical model is no longer believed to be reliable.*

 # If none of the above four modes occurs, the analysis should be repeated, with incremental amplitude adjustment for the ground motion pair until one of these modes occurs.

 # If needed, use scaling to increase the IM level of the ground motion records, until one of the model failure modes is reached as defined above. Details on scaling procedures that the analyst may implement are beyond the scope of these guidelines. Reference on this matter can be made to ATC-58 [FEMA P-58, 2012] or other relevant literature. Excessive scaling (e.g., by factors larger than about 3.0) should be avoided, especially whenever a relatively insufficient IM such as $S_a(T_1)$ *is used. Alternatively, one may employ as a sufficient IM the average spectral response acceleration* $S_{agm}(T_i)$*, i.e., the sum of the natural logarithm of spectral acceleration values computed over a range of* T_i *values appropriate for the building studied. An experienced analyst undertaking a site-specific analysis of a given structure may want to employ cloud/stripe analysis with a more rigorous selection of ground motions.*

 # At each IM level and for each ground motion record applied, if no collapse has been deemed to occur then all response parameters of interest (e.g., peak storey drifts and peak floor accelerations at each storey) should be recorded.

Step.4. *Identify the different medians capacity associated to damage thresholds:*

 # The location where this curve becomes flat is defined as the point from which the collapse occurs; i.e. $S_{a,ds_4}(T_1)$

 # The minimum of the values of $S_a(T_1)$ *at which any of the above* ***Modes*** *occurs is taken as the collapse capacity* $S_{a,ds_4}(T_1)$ *for the considered pair of ground motion.*

 # The median collapse capacity $\hat{S}_{a,ds_4}(T_1)$ *is then defined as the value at which 50% of the ground motion pairs produce either modes as mentioned above. Note that when 2D models are used, the median collapse capacity,* $\hat{S}_{a,ds_4}(T_1)$*, should be taken as the smaller of the value obtained for either direction.*

 # At each IM level, the N values (where N is the number of ground motion records) recorded for each demand parameter of interest (e.g., peak drift of any given storey or peak acceleration of any given floor) can be used to define the distribution of demand for the specific IM value. Alternatively, one can also use these results to define maximum interstorey drift (ID) values for Slight, Moderate, and Near Collapse damage thresholds that can be estimated from the progression of local damage through several elements in Section 6. Assign these ID values in IDA plot to estimate the corresponding median $\hat{I}_{M,ds_i}$ *and the associated dispersion.*

7.3 Non-Linear Static Analysis (NLS)

The procedures presented in this subsection are based on the use of capacity curves resulting from Non-linear Static Pushover analysis (see ANNEX A). The derivation of a capacity curve by use of pushover analysis, does not directly account for the specific seismic motion, as the dynamic characteristics of demand and response system are not taken into account in the analysis.

The resulting capacity curve from pushover analysis will then need to be fitted with a bilinear (an elastic-plastic) or multilinear (elastic-plastic with residual strength) curve to idealise the behaviour. The procedure for fitting capacity curves is provided in ANNEX A.

There are some cases where the analyst may prefer to use default capacity curves available in literature (e.g. documents, guidelines), for instance:

- for simplification/reduction of calculation efforts
- lack of information for the assessed structures, especially, for the older ones, where design documents are generally not available.
- when studies are conducted for large portions of the building stock and resources for direct survey and data acquisition are modest.

However, special care should be given when assigning these default curves to represent the performance of assessed structure. For instance, the existing HAZUS capacity curves [FEMA 1999] derived for buildings in the US, have been widely used to generate fragility curves of buildings located in different regions of the world and designed and built according to standards and construction practice very different from the ones employed in the USA. Indeed differences in construction techniques and detailing between different countries are significant, even when buildings are nominally designed to the same code clauses. Such detailing can substantially affect fragility and vulnerability functions. It is hence recommended that capacity curves be derived by the analyst based on directly acquired data on local building stock, using available non-linear commercial analysis programmes.

In the following we recommend a number of procedures to determine median values of damage state thresholds, depending on the shape of the capacity curve, multilinear or bilinear, and whether record-to-record dispersion is taken into account or not in the analysis.

7.3.1 Case of Multilinear Elasto-Plastic (with Residual Strength) Form of Capacity Curve

The procedures offered herein are applicable to multilinear elasto-plastic (elastic-plastic with residual strength) capacity curves (

Figure **7.10**); it is ideal for frames structures with unreinforced masonry infills.

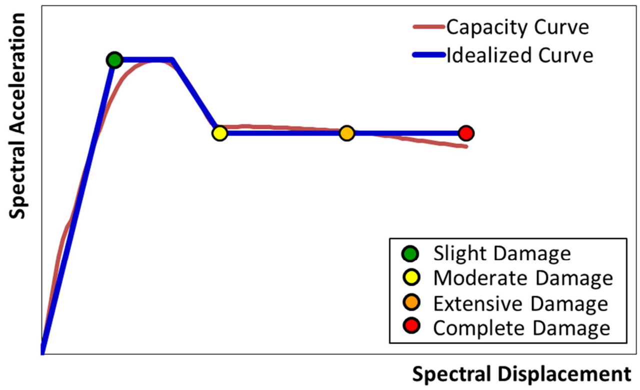

Figure 7.10 Illustrated example of multilinear elastic-plastic capacity curve with residual strength.

7.3.1.1 Procedure 2.1: N2 Method for Multilinear Elasto-Plastic Form of Capacity Curve

The procedure offered herein consists of estimating the demand given the IM level through an $R-\mu-T$ relationship: the reduction factor, R, the ductility μ, and the period T. This method, which is based on earlier work of Dolsek and Fajfar [2004], was initially proposed with the aim of directly obtaining the relationship between seismic demand and intensity measure but using elastic response spectra, hence, no estimation of the record-to-record variability can be derived by the analyses. The main improvement introduced in this document with regard to this method consists in utilizing natural records (records from real events, synthetic or artificial) in order to account for and extract the record-to-record variability from the analyses.

Determination of the performance point

The procedure is based on:

- The transformation of the MDoF system to an equivalent SDoF system, and derivation of the equivalent SDoF-based capacity curve (with defined damage state thresholds);
- Fitting of the equivalent SDoF-based capacity curve with a multilinear elasto-plastic idealization;
- For each selected 5% damped elastic response spectrum, the inelastic response spectrum ($S_a(T)$, $S_d(T)$) is derived by means of an $R-\mu-T$ relationship.

The inelastic displacement corresponding to the performance target from the equivalent SDoF system S_d^* is then derived directly from the following formula (Figure 7.11):

$$S_d^* = \frac{\mu}{\mathrm{R}} S_{de}(T^*) \tag{7.2}$$

Graphically, the performance point can be obtained by the extension of the horizontal yield plateau of the idealized capacity curve up to the intersection with the computed inelastic demand spectrum. See Figure 7.11. Note that, the inelastic acceleration $S_a(T)$ and displacement $S_d(T)$ are defined as:

$$S_a(\mathrm{T})=\frac{\mathrm{S}_{ae}(T)}{R} \tag{7.3}$$

$$S_d(\mathrm{T})=\frac{\mu}{R}S_{de}(T)=\frac{\mu}{\mathrm{R}}\frac{T^2}{4\pi^2}S_{ae}(T)=\mu\frac{\mathrm{T}^2}{4\pi^2} \tag{7.4}$$

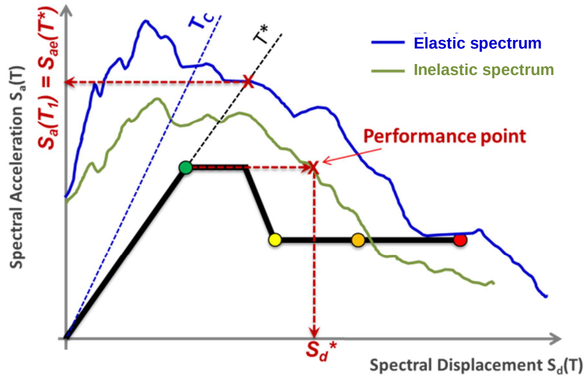

Figure 7.11 Illustrated example on the steps of the Procedure 2.1 for the evaluation of the performance point given an earthquake record.

Once the performance point (inelastic displacement) for a given earthquake (with a specific value of PGA) is calculated, then the corresponding acceleration (elastic) can also be calculated using the following expression:

$$S_a(T_1)=S_{ae}(\mathrm{T}^*)=\frac{4\pi^2}{T^{*2}}S_{de}(\mathrm{T}^*) \tag{7.5}$$

Determination of inelastic response spectrum

According to the results of parametric study (using three different set of recorded and semi-artificial ground motions, for a total of 20 recorded accelerograms and 24 semi-artificial accelerograms) for the case of system with multilinear elasto-plastic capacity diagram, the ductility demand, μ , and reduction factor, R , are related through the following formula [Dolsek and Fajfar 2004]:

$$\mu=\frac{1}{\mathrm{c}}(R-\mathrm{R}_0)+\mu_0 \tag{7.6}$$

where the ductility demand is to be computed from the known reduction factor:

$$R=\frac{\mathrm{S}_{ae}(T^*)}{S_{ay}} \tag{7.7}$$

$S_{ae}(T^*)$ is the elastic spectral acceleration at the initial period of the SDoF system, T^*, S_{ay} is the yield acceleration of the given inelastic system defined as:

$$S_{ay} = \frac{F_y^*}{m^*} \tag{7.8}$$

The parameter c expresses the slope of the $R-\mu$ relation, and has been developed based on the employment of three sets of ground motions in order to consider the effect of record-to-record variability. This parameter is defined as:

$$\begin{aligned}
&c = 0.7\left(\frac{T^*}{T_C}\right) && R \le R(\mu_s), && T^* \le T_C\\
&c = 0.7 + 0.3\Delta T && R \le R(\mu_s), && T_C < T^* \le T_D^*\\
&c = 0.7\sqrt{r_u}\left(\frac{T^*}{T_C}\right)^{\frac{1}{\sqrt{r_u}}} && R > R(\mu_s), && T^* \le T_C\\
&c = 0.7\sqrt{r_u}\,(1-\Delta T) + \Delta T && R > R(\mu_s), && T_C < T^* \le T_D^*\\
&c = 1 && && T^* > T_D^*
\end{aligned} \tag{7.9}$$

$$\begin{aligned}
&\mu_0 = 1 && R \le R(\mu_s)\\
&\mu_0 = \mu_s && R > R(\mu_s)
\end{aligned} \tag{7.10}$$

$$\begin{aligned}
&R_0 = 1 && R \le R(\mu_s)\\
&R_0 = R(\mu_s) && R > R(\mu_s)
\end{aligned} \tag{7.11}$$

With:

$R(\mu_s)$ is the reduction factor interval, defined as:

$$\begin{aligned}
&R(\mu_s) = 0.7\left(\frac{T^*}{T_C}\right)(\mu_s - 1) + 1 && T^* \le T_C\\
&R(\mu_s) = (0.7 + 0.3\Delta T)(\mu_s - 1) + 1 && T_C < T^* \le T_D^*\\
&R(\mu_s) = \mu_s && T^* > T_D^*
\end{aligned} \tag{7.12}$$

μ_s is the ductility at the beginning of the strength degradation of the infills, defined as:

$$\mu_s = \frac{D_s^*}{D_y^*} \tag{7.13}$$

The parameter r_u is defined as the ratio between the residual strength, after infill collapse, and the initial maximum strength:

$$r_u = \frac{F_{\min}^*}{F_y^*} \tag{7.14}$$

The two parameters T_D^* and ΔT depend on the corner periods (T_C and T_D) of the elastic spectrum, the ratio r_u and the initial period T^*:

$$T_D^* = T_D\sqrt{2 - r_u}\ , \qquad \Delta T = \frac{T^* - T_C}{T_D\sqrt{2 - r_u} - T_C} \tag{7.15}$$

Note that:

$$\mu = R \qquad \text{if } r_u = 1.0 \text{ and } T^* \geq T_D \tag{7.16}$$

Box 7.2: Calculation of the seismic demand using Procedure 2.1

For a multilinear elasto-plastic system, the demands for different earthquake records are obtained through the following steps:

Step.1. *Develop an appropriate mathematical model of the building for non-linear static analysis. Identify your primary and secondary elements or components; define your non-structural elements; foundation flexibility; gravity loads; and P-Delta effects. Refer to Section 5, and you may also refer to ASCE/SEI 41-06 [ASCE 2007].*

Step.2. *Run a static pushover analysis; and make sure that the analysis is extended to a deformation such that collapse is judged to occur. Construct a force-displacement relationship of the MDoF system considering different damage states thresholds. See ANNEX A to perform pushover analysis and Section 6 for the identification of the four thresholds.*

Step.3. *Transform the MDoF system to an equivalent SDoF system (Estimate the equivalent SDoF mass and period), and derive the equivalent SDoF-based capacity curve (See ANNEX A).*

Step.4. *Fit the equivalent SDoF-based capacity curve via a multilinear elasto-plastic idealization. Estimate the yield base shear, the displacement at yield, and the displacement at the start of the degradation of infills (See ANNEX A).*

Step.5. *Selection and, if necessary, scaling of ground motion record.*

Step.6. *The ductility demand to be computed from the known reduction factor, using Equation 4.19.*

Step.7. *Derive the inelastic response spectrum by means of* $R-\mu-T$ *relationship. Use Equations 7.3 and 7.4.*

Step.8. The inelastic displacement corresponding to the seismic performance point S_d^* is then derived directly from the Equation 7.7. *Note that,* S_d^* *can be obtained graphically by the extension of the horizontal yield plateau of the idealized capacity diagram up to the intersection with the computed inelastic demand spectrum*.

Step.9. Once the displacement (inelastic) demand for a given earthquake (with a specific value of PGA) is calculated, then the corresponding acceleration (elastic) can also be calculated using the following expression*:*

$$S_a(T_1) = S_{ae}(T^*) = \frac{4\pi^2}{T^{*2}} S_{de}(\mathrm{T}^*)$$

The analyst should repeat the process (*Step 5 – Step 9*) for all the selected and scaled earthquake records, derive the inelastic response spectrum, and re-calculate the performance point through Equation 7.7 until all the limit state are reached. Finally, clouds of structural-response (IM – EDP) are collected from the analyses.

Determination of EDPs damage state thresholds

In order to determine the structure's performance under increasing ground motion intensity (see Figure 7.12), the analysis described in Procedure 2.1 should be repeated for multiple accelerograms scaled up until all the limit state are reached. The selected number of accelerograms/ground motions should be sufficient to provide stable estimates of the median capacities. The resulting cloud of performance points (see Figure

7.13) is then used to determine the EDP for each damage state threshold and the dispersion, and then create a fragility curve by fitting a statistical model. Further details are provided in Section 8.1.

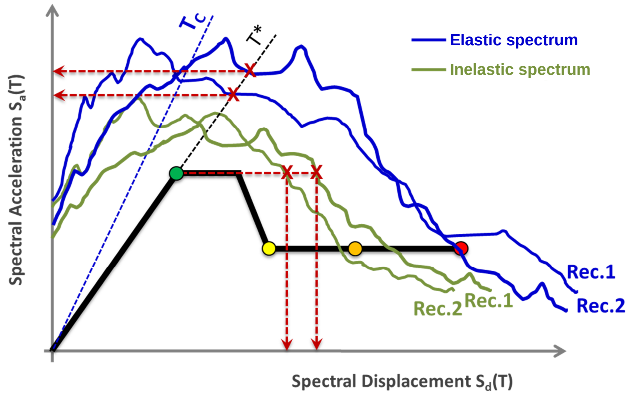

Figure 7.12 Repeat the process of Procedure 2.1 for multiple earthquake records.

	IM			EDP	
1:	Sd	$S_a(T_1)$	PGA	RDR_{max}	ISD_{max}
2:	Sd	$S_a(T_1)$	PGA	RDR_{max}	ISD_{max}
.	.	.	.		
.	.	.	.		
.	.	.	.		
n:	Sd	$S_a(T_1)$	PGA	RDR_{max}	ISD_{max}

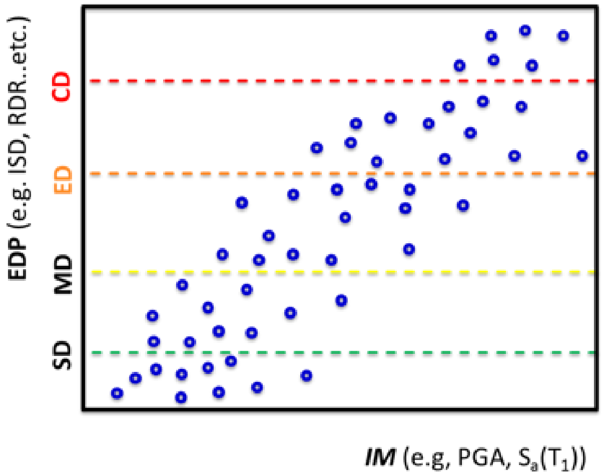

Figure 7.13 Clouds of structural-response results.

The calculation of EDPs of damage state thresholds and their corresponding dispersion can be conducted using one of the following approaches (Generalised Linear Model or Least Squares Formulation), which rely on the definition of deterministic values of EDP corresponding to damage thresholds (DS).

Generalised Linear Model (GLM)

Two generalised linear models are proposed according to whether the fragility curves of the examined building class correspond to a single or multiple damage states.

The construction of a fragility curve corresponding to a given damage state requires the determination of an indicator y_i which is assigned to each performance point EDP_i as:

$$y_i = \begin{cases} 1 & EDPi \geq EDP_k \\ 0 & EDPi < EDP_k \end{cases} \tag{7.17}$$

The curves are then obtained by fitting a generalised linear model to these binary data and their corresponding intensity measure levels (see Figure 7.14).

The indicator of a performance point for a given level of ground motion intensity ($IM = im_i$), associated with the demand spectrum, is considered to follow a Bernoulli distribution as:

$$Y \mid im \sim \binom{1}{y_i} \mu^{y_i} \left[1-\mu\right]^{1-y_i} \tag{7.18}$$

where μ is the conditional mean response which represents here the fragility curve. The fragility curve is obtained as:

$$g(\mu) = g\left(P\left(DS \geq ds \mid im\right)\right) = \theta_1 \ln\left(im\right) + \theta_0 \tag{7.19}$$

where θ_1 , θ_0 is the unknown parameters of the statistical model; $g(.)$ is the link function obtained as:

$$g(\mu) = \begin{cases} \Phi^{-1}(\mu) & \text{probit} \\ \log\left(\dfrac{\mu}{1-\mu}\right) & \text{logit} \\ \log\left[\log(1-\mu)\right] & \text{complementary loglog} \end{cases} \tag{7.20}$$

The construction of fragility curves corresponding to multiple damage states is estimated by fitting an ordered generalised linear model to the data, which ensures that the fragility curves will not cross. In this case, the EDP_i are classified in *N* + 1 discrete ordered damage states, *ds*, as:

$$ds_j = \begin{cases} 0 & EDP_1 > EDP_i \\ 1 & EDP_2 \geq EDP_i \geq EDP_1 \\ \ldots & EDP_{k+1} \geq EDP_i \geq EDP_k \\ N & EDP_i \geq EDP_N \end{cases} \tag{7.21}$$

Where *N* is the most extreme damage state. The damage states for *im* in each damage state are assumed to follow a discrete categorical distribution:

$$DS \mid im \sim \prod_{j=0}^{N} P\left(DS = ds_j \mid im\right)^{y_j} \tag{7.22}$$

where y_i is an indicator which is 1 if the building suffered damage j and 0 otherwise. Equation 8.22 shows that the categorical distribution is fully defined by the determination of the conditional probability, $P(DS = ds_j \mid im)$. This probability can be transformed into the probability of reaching or exceeding ds_j given im , $P(DS \geq ds_j \mid im)$, essentially expressing the required fragility curve, as:

$$P\left(DS = ds_j \mid im\right) = \begin{cases} 1-P\left(DS \geq dsj \mid im\right) & j=j-1 \\ P\left(DS \geq ds_j \mid im\right)-P\left(DS \geq ds_{j+1} \mid im\right) & 0<j<N \\ P\left(DS \geq ds_j \mid im\right) & j=N \end{cases} \tag{7.23}$$

The fragility curves are expressed in terms of one of the three link functions expressed in Equation 8.20, in the form:

$$g^{-1}\left[P\left(DS \geq ds_j \mid im\right)\right] = \theta_{0i} + \theta_1 \ln\left(im\right) \tag{7.24}$$

where $\theta = \left[\theta_{0i}, \theta_1\right]$ is the vector of the 'true' but unknown parameters of the model; θ_1 is the slope and θ_{0i} is the intercept for fragility curve corresponding to ds_j. Equation 8.24 assumes that the fragility curves corresponding to different damage states have the same slope but different intercepts. This ensures that the ordinal nature of the damage is taken into account leading to meaningful fragility curves, i.e. curves that do not cross.

The unknown parameters of the generalised linear models are then estimated by maximising the likelihood function as:

$$\boldsymbol{\theta}^{opt} = \arg\max\left[\log\left(L(\boldsymbol{\theta})\right)\right] = \\ = \begin{cases} \arg\max\left[\log\left(\prod_{i=1}^{M}\prod_{j=0}^{N}\frac{m_i!}{n_{ij}!}P\left(DS = ds_j \mid im_i\right)^{n_{ij}}\right)\right] & 1^{st} \text{ Stage} \\ \arg\max\left[\log\left(\prod_{i=1}^{M}\binom{m_i}{n_i}\mu_i^{n_i}\left[1-\mu_i\right]^{m_i-n_i}\right)\right] & 2^{nd} \text{ Stage} \end{cases} \tag{7.25}$$

where M is the number of performance points.

The EDPs of damage state thresholds (fragility parameters) and their corresponding dispersions can be computed as:

$$\alpha = exp\left(-\frac{\theta_0}{\theta_1}\right) \quad and \quad \beta = \frac{1}{\theta_1} \tag{7.26}$$

In addition to the mean fragility curves, their 5% - 95% confidence bounds can also be plotted, obtained by a non-parametric bootstrap analysis [Efron and Tibshirani 1994] of the data points.

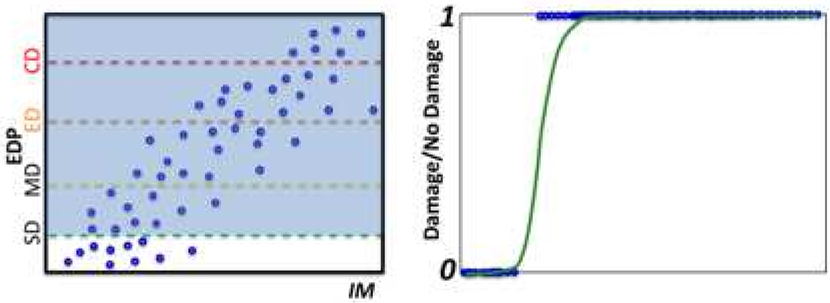

(a) Fragility curve for Slight Damage

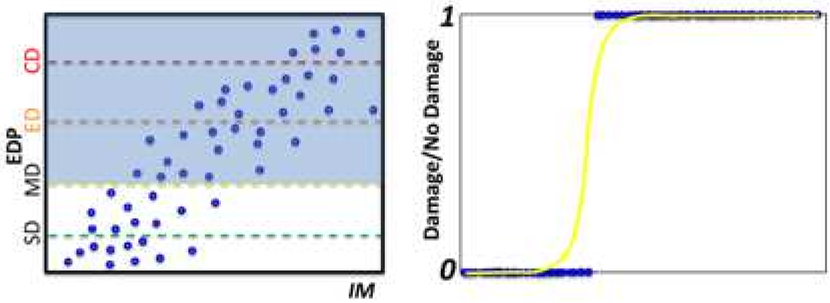

(b) Fragility curve for Modrate Damage

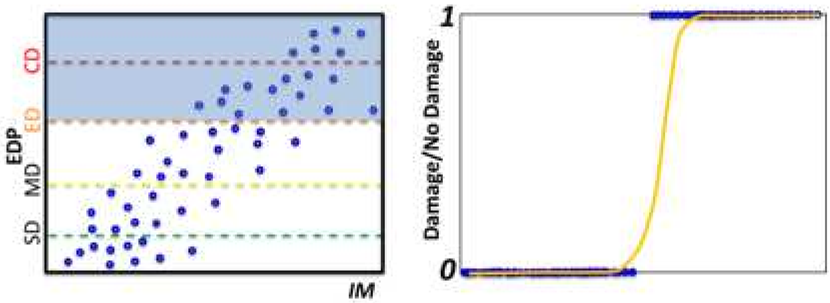

(c) Fragility curve for Extensive Damage

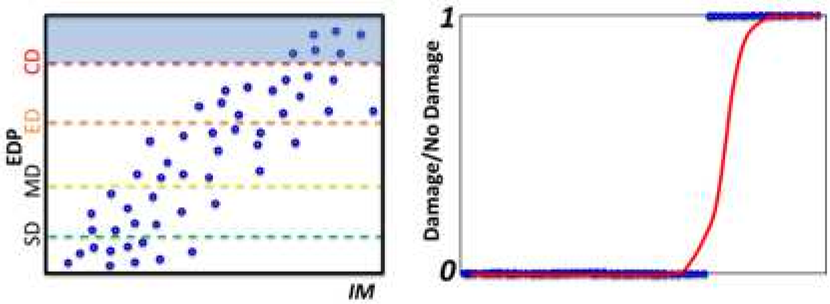

(d) Fragility curve for Complete Damage

Figure 7.14 Derivation of fragility curves using GLM regression technique.

Least Squares Formulation

Least Squares regression is a widely used technique to estimate, for each damage threshold, the probabilistic relation between EDPs and IMs (Figure 7.15) (e.g. Cornell et al. 2002; Ellingwood and Kinali 2009).

Assuming a lognormal distribution between EDP and DS [Shome and Cornell 1999], the predicted median demand is represented by a normal cumulative distribution (Figure 7.16):

$$\Phi\left[\frac{\ln IM - \ln\alpha}{\beta}\right] \tag{7.27}$$

where, Φ represents the stardard normal cumulative distribution function, β is the global standard-deviation for the predicted median demand.

For an assumed probabilistic damage threshold, IMs are chosen in a way that roughly half the points are below that damage threshold and half above, determining an interval of IMs values, which are assumed to be lognormally distributed within each interval.

Performing piece-wise regression over these different IM intervals, the fragility parameters are computed using the corresponding relation: $ln\left(\overline{EDP}\right) = a\, ln\left(IM\right) + ln\left(b\right)$. The median demand α_{ds_i} and its dispersion β_{ds_i} for each assumed threshold, ds_i , can be written as:

$$\alpha_{ds_i} = \exp\left(\ln\left(\frac{ds_i}{b}\right)\Big/a\right) \quad \text{and} \quad \beta_{ds_i} = \frac{\mathrm{STDEV}\left(\ln \mathrm{IM_i}\right)}{a} \tag{7.28}$$

For instance, the median demand of complete damage state threshold and the corresponding dispersion can be computed as (Figure 7.16):

$$\alpha_{CD} = \exp\left(\ln\left(\frac{CD}{b}\right)\Big/a\right) \quad \text{and} \quad \beta_{CD} = \frac{\mathrm{STDEV}\left(\ln \mathrm{IM_i}\right)}{a}$$

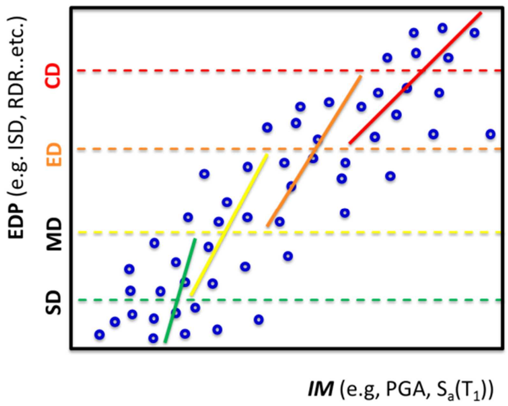

Figure 7.15 Derivation of fragility functions (median demand and dispersion) using Least Squares regression technique.

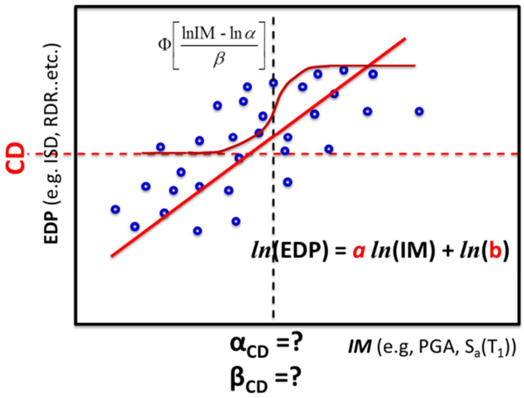

Figure 7.16 Calculation example of Median demand and dispersion for Complete Damage (CD) using Least Squares regression

Use of Smoothed Elastic Response Spectrum

The non-linear static based procedure offered in this section (Procedure 2.1) allows, as an alternative, the calculation of EDPs thresholds using smoothed elastic response spectrum. However, this type of response spectrum cannot reflect record-to-record variability as it generally represents the envelope or average of response spectra. Hence, the analyst should note that this choice is not recommended for the development of new fragility and vulnerability functions, as the uncertainty (record-to-record variability) is not appropriately considered in computing the estimated median capacity value.

When using smoothed response spectrum, the process of calculation consists of identifying the appropriate inelastic response spectrum for which the extracted performance point reaches, or is close to, the displacement capacity at the considered damage state threshold (see Figure 7.17).

The procedure is based on the selection of 5% damped elastic response spectrum appropriate for the assessment of each performance target ds_i, i.e. with return period appropriate to the considered damage state. (See Eurocode-8, CEN 2004). If the calculated performance point, from Equation 7.2, does not reach, or comes close to, the displacement capacity at the considered damage state threshold, the analyst should repeat the process by selecting another 5% damped elastic response spectrum (i.e. with return period appropriate to the considered damage state threshold as discussed above), derive the inelastic response spectrum, and re-calculate the performance point through Equation 7.2 until the condition is fulfilled, i.e. the value of S_d^* is equal or close to the value of displacement at the considered damage state, as illustrated in the example in the Figure 7.17. This process leads to the selection of a range of R -values.

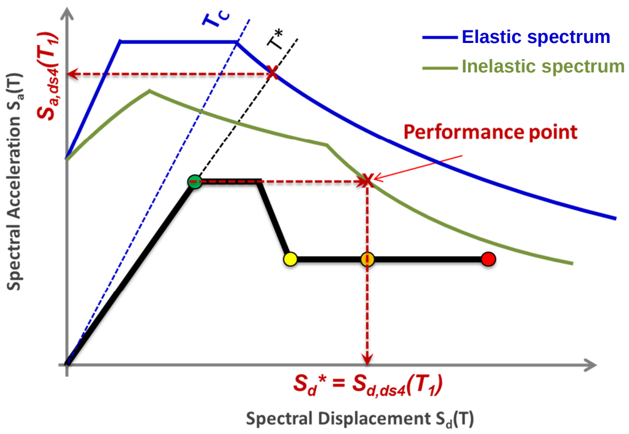

Figure 7.17 Illustrated example on the Procedure 2.1 for the calculation of performance point using smoothed elastic response spectrum.

Once the condition is fulfilled, then the calculated S_d^* will be considered as the median displacement capacity of the corresponding damage state.

$$S_{d,ds_i}(T_1) = S_d^* \tag{7.29}$$

Then, the median acceleration capacity value corresponding to the selected response spectrum with a specific value of PGA can be calculated using the following expression:

$$\hat{S}_{a,ds_i}(T_1) = \frac{4\pi^2}{T^{*2}} S_{de}(\mathrm{T}^*) \tag{7.30}$$

NOTE:

In this alternative (i.e. the use of smoothed response spectrum), the record-to-record variability is not accounted for; hence, in order to derive fragility and vulnerability functions considering the record-to-record variability, the analyst may calculate β_D through Equation 7.45b as proposed in Section 7.3.2.3 (simplified equation suggested by Ruiz-Garcia and Miranda 2007).

The analyst may also wish to assign, but with a special care, default values provided in ANNEX B, Table B-1, as suggested by ATC-58 [FEMA P-58, 2012]. Given the fundamental period of the structure and a strength ratio, the values of β_D can be chosen in a range between 0.05 and 0.45. If data on the above two parameters is lacking or uncertain, a maximum default value of 0.45 can be used.

7.3.2 Case of Bilinear Elasto-Plastic Form of Capacity Curve

The procedures presented herein are applicable to bilinear elasto-plastic capacity curve only; therefore, it is ideal for Steel or Reinforced Concrete bare frame moment-resisting structures, masonry structures with curtailed ductility, and wherever negative stiffness or reserve strength are not an issue.

7.3.2.1 Procedure 3.1: N2 Method for Bilinear Elasto-Plastic Form of Capacity Curve

This procedure is based on earlier work of Fajfar [2002], and has been recommended by Eurocode-8 [CEN 2004]. The procedure is specifically applicable only for structures that are characterised by bilinear *Elasto-Perfectly Plastic* capacity curve. The process consists of obtaining the appropriate inelastic response, i.e. performance point (defined as point of intersection of idealized SDoF system based capacity curve with the inelastic demand spectrum) for a given earthquake record (see Figure 7.18).

Similarly to the previous procedure (i.e. Procedure 2.1), Procedure 3.1 was initially proposed with the aim of obtaining directly the relationship between seismic demand and intensity measure but using a smoothed response spectrum, hence, no estimation of the record-to-record variability can be derived by the analyses. The main improvement introduced in this document with regard to this method consists in utilizing natural records (records from real events; synthetic; or artificial) in order to account for and extract the record-to-record variability from the analyses.

Determination of the performance point

The procedure is based on:

- The transformation of the MDoF system to an equivalent SDoF system, and deriving the equivalent SDoF-based capacity curve (with defined damage state thresholds);
- Fitting the equivalent SDoF-based capacity curve via a bilinear elasto-plastic idealization;
- For each selection of 5% damped elastic response spectrum ($S_{ae}(T)$, $S_{de}(T)$), the inelastic response spectrum ($S_a(T)$, $S_d(T)$) is derived by means of $R-\mu-T$ relationship (Equations 7.31 and 7.32).

$$S_a(\mathrm{T}) = \frac{\mathrm{S}_{ae}(T)}{R} \tag{7.31}$$

$$S_d(\mathrm{T}) = \frac{\mu}{R} S_{de}(T) = \frac{\mu}{\mathrm{R}} \frac{T^2}{4\pi^2} S_{ae}(T) = \mu \frac{\mathrm{T}^2}{4\pi^2} S_a(T) \tag{7.32}$$

Graphically, the seismic demand/performance point is defined by the intersection of the idealized capacity curve and the inelastic demand spectrum for the relevant ductility value. See Figure 7.18.

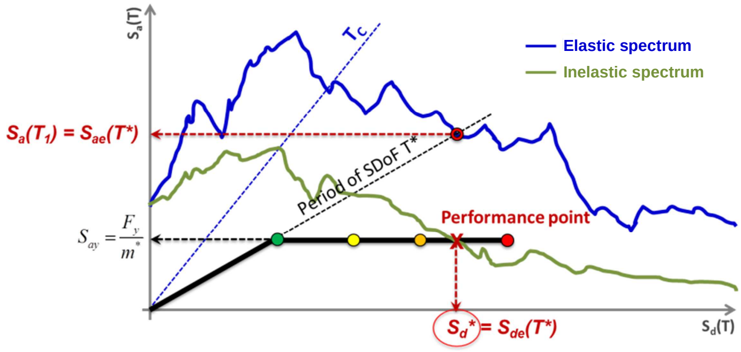

(a) for medium and long period range: $T^{*} \geq T_{C}$

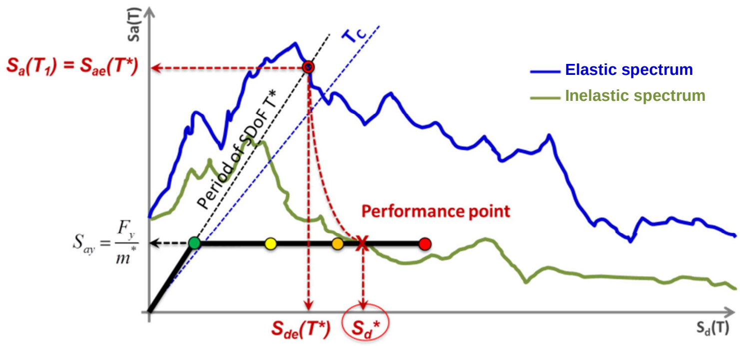

(b) for short period range: $T^{*} < T_{C}$, and $S_{ay} < S_{ae}\left(T^{*}\right)$

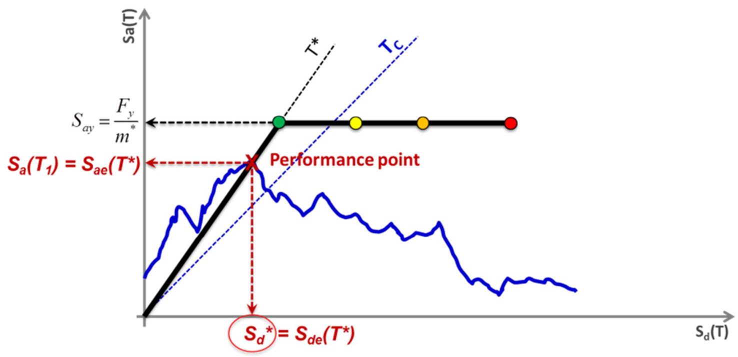

(c) for short period range: $T^{*} < T_{C}$, and $S_{ay} \geq S_{ae}\left(T^{*}\right)$

Figure 7.18 Illustrated example on the steps of Procedure 3.1 for the evaluation of performance point for a given earthquake record.

For a given earthquake ground record, the performance point of the equivalent SDoF system can be calculated with respect to the following conditions (see Figure 7.18):

- For medium and long period range: $T^* \geq T_C$

  If the elastic period T^* is larger or equal to the corner period T_C , the ductility demand μ is equal to the reduction factor R . According to Equation 7.32, it follows that the inelastic displacement demand is equal to the elastic displacement demand (see Figure 7.18a):

$$S_d^* = S_{de}(T^*) \tag{7.33a}$$

- For short period range: $T^* < T_C$

  - If $S_{ay} < S_{ae}(T^*)$, the response is non-linear and thus, the target performance displacement can be determined from the following expression:

$$S_d^* = \frac{S_{de}(T^*)}{R}\left(1 + (\mathrm{R} - 1)\frac{T_C}{T^*}\right) \geq \mathrm{S_{de}}(T^*) \tag{7.33b}$$

  - If $S_{ay} \geq S_{ae}(T^*)$, the response is elastic and thus, the inelastic displacement demand is equal to the elastic displacement demand:

$$S_d^* = S_{de}(T^*) \tag{7.33c}$$

T_C (also termed corner period) is the characteristic period of the ground motion, which identifies the transition from constant acceleration (corresponding to the short-period range) to constant velocity (the medium-period range) section of the elastic spectrum.

$S_{ae}(T^*)$ is the elastic spectral acceleration at the initial period of the SDoF system, T^*, S_{ay} is the yield acceleration of the given inelastic system defined as:

$$S_{ay} = \frac{F_y^*}{m^*} \tag{7.34}$$

μ is the ductility factor, determined by employing a specific $R\!-\!\mu\!-\!T$ relation, appropriate for bilinear elasto-plastic system.

The following formula allows the ductility factor μ to be computed from the known reduction factor R , as per Eurocode-8 [CEN 2004]:

$$\mu = (R-1)\frac{T_C}{T^*} + 1 \qquad T^* < T_C$$

$$\mu = R \qquad T^* \geq T_C \tag{7.35}$$

Once the performance point (inelastic displacement) for a given earthquake (with a specific value of PGA) is calculated, then the corresponding acceleration (elastic) can also be calculated using the following expression:

$$S_a(T_1) = S_{ae}(T^*) = \frac{4\pi^2}{T^{*2}} S_{de}(T^*) \tag{7.36}$$

Box 7.3: Calculation of the seismic demand using Procedure 3.1

For a multilinear elasto-plastic system, the demands for different earthquake records are obtained through the following steps:

Step.1. *Develop an appropriate mathematical model of the building for non-linear static analysis. Identify your primary and secondary elements or components; define your non-structural elements; foundation flexibility; gravity loads; and P-Delta effects. Refer to Section 5, and you may also refer to ASCE/SEI 41-06 [ASCE 2007].*

Step.2. *Run a static pushover analysis; and make sure that the analysis is extended to a deformation such that collapse is judged to occur. Construct a force-displacement relationship of the MDoF system considering different damage states thresholds. See ANNEX A to perform pushover analysis and Section 6 for the identification of the four thresholds.*

Step.3. *Transform the MDoF system to an equivalent SDoF system (Estimate the equivalent SDoF mass and period), and derive the equivalent SDoF-based capacity curve (See ANNEX A).*

Step.4. *Fit the equivalent SDoF-based capacity curve via a multilinear elasto-plastic idealization. Estimate the yield base shear, the displacement at yield, and the displacement at the start of the degradation of infills (See ANNEX A).*

Step.5. *Selection and, if necessary, scaling of ground motion record.*

Step.6. *The ductility demand to be computed from the known reduction factor, using Equation 4.19.*

Step.7. *Derive the inelastic response spectrum by means of an R-μ-T relationship. Use Equations 7.31 and 7.32.*

Step.8. The inelastic displacement corresponding to the seismic performance point S_d^* is then derived directly from the Equation 7.7. *Note that,* S_d^* *can be obtained graphically as the intersection of the idealized capacity diagram and the computed inelastic demand spectrum*.

Step.9. Once the displacement (inelastic) demand for a given earthquake (with a specific value of PGA) is calculated, then the corresponding acceleration (elastic) can also be calculated using the following expression*:*

$$S_a(T_1) = S_{ae}(T^*) = \frac{4\pi^2}{T^{*2}} S_{de}(\mathrm{T}^*)$$

The analyst should repeat the process (*Step 5 - Step9*) for all the selected and scaled earthquake records, derive the inelastic response spectrum, and re-calculate the performance point through Equation 7.27 until all the limit states are reached. Finally, clouds of structural-response (IM – EDP) are collected from the analyses.

Determination of EDPs damage state thresholds

In order to determine the structure's performance under increasing ground motion intensity (see Figure 7.19), the analysis described in Procedure 3.1 should be repeated for multiple accelerograms scaled up until all the limit state are reached. The selected number of accelerograms/ground motions should be sufficient to provide stable estimates of the median capacities. The resulting cloud of performance points (similarly to the

Procedure 2.1, see Figure 7.13) is then used to determine the EDP for each damage state threshold and the dispersion, and then create a fragility curve by fitting a statistical model. Further details are provided in Section 8.1.

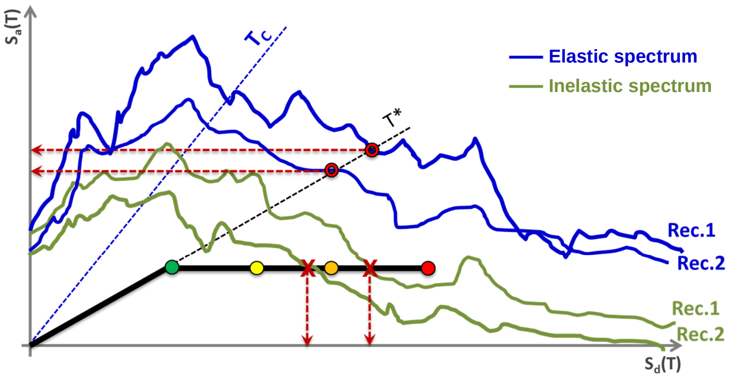

Figure 7.19 Repeat the process of the Procedure 2.1 for multiple earthquake records.

The calculation of EDPs of damage state thresholds and their corresponding dispersion can be conducted using one of the following approaches (Generalised Linear Model or Least Squares Formulation), which rely on the definition of deterministic values of EDP corresponding to damage thresholds (DS).

Generalized Linear Model (GLM)

Details are provided in Section 7.3.1.1

Least Squares Formulation

Details are provided in Section 7.3.1.1

Use of smoothed elastic response spectrum

Similarly to the Procedure 2.1, the non-linear static based procedure offered in this section (Procedure 3.1) allows, as an alternative, the calculation of EDPs thresholds using smoothed elastic response spectrum. However, this type of response spectrum cannot reflect record-to-record variability as it generally represents the envelope or average of response spectra. Hence, the analyst should note that this choice is not recommended for the development of new fragility and vulnerability functions, as the uncertainty (record-to-record variability) is not appropriately considered in computing the estimated median capacity value.

When using smoothed elastic response spectrum, the process of calculation consists of identifying the appropriate inelastic response spectrum for which the extracted performance point reaches, or is close to, the displacement capacity at the considered damage state threshold (see Figure 7.20).

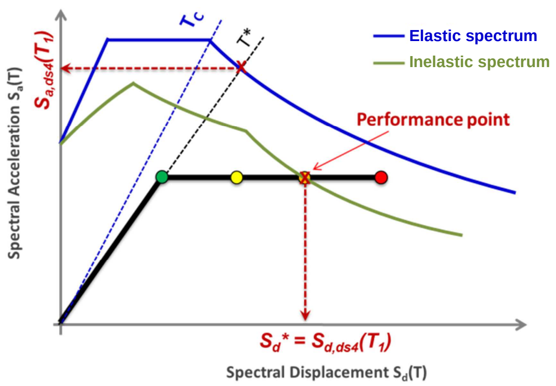

Figure 7.20 Illustrated example on the Procedure 3.1 for the calculation of performance point using smoothed elastic response spectrum.

If the calculated performance point, from Equation 7.33, does not meet, or is close to, the displacement capacity at the considered damage state threshold, the analyst should repeat the process by selecting another 5% damped elastic response spectrum (i.e. with return period appropriate to the considered damage state threshold as discussed above), derive the inelastic response spectra, and re-calculate the performance point through Equation 7.33 until the condition is fulfilled, i.e. the value of S_d^* is equal or close to the value of displacement at the considered damage state, as illustrated in the example in the Figure 7.20.

Once the condition is fulfilled, then the calculated S_d^* will be considered as the median displacement capacity of the corresponding damage state threshold, given the considered intensity.

$$S_{d,ds_i}(T_1) = S_d^* \tag{7.37}$$

Then, the median acceleration capacity value corresponding to the selected response spectrum with a specific value of PGA can be calculated using the following expression:

$$\hat{S}_{a,ds_i}(T_1) = \frac{4\pi^2}{T^{*2}} S_{de}(\mathrm{T}^*) \tag{7.38}$$

NOTE:

In this alternative (i.e. the use of smoothed response spectrum), the record-to-record variability is not accounted for; hence, in order to derive fragility and vulnerability functions considering the record-to-record variability, the analyst may calculate β_D through Equation 7.45b as proposed in the Section 7.3.2.3 (simplified equation suggested by Ruiz-Garcia and Miranda 2007).

The analyst may also wish to assign, but with a special care, default values provided in ANNEX B, Table B-1, as suggested by ATC-58 [FEMA P-58, 2012]. Given the fundamental period of the structure and a strength ratio, the values of β_D can be chosen in a range between 0.05 and 0.45. If data on the above two parameters is lacking or uncertain, a maximum default value of 0.45 can be used.

7.3.2.2 Procedure 3.2: FRAgility through Capacity ASsessment (FRACAS)

FRACAS is a displacement-based procedure, originally developed by Rossetto and Elnashai (2005). The procedure is applicable for structures that are characterised by Elastic-Perfectly Plastic (EPP), Linear Strain Hardening (EST) or Tri-Linear Model (TLM); therefore, can cover different types of buildings with any number of storeys. The proposed methodology for vulnerability curve derivation, prescribes the analysis of a population of frames with different structural properties, subjected to a number of earthquake records with distinct characteristics. In this way, the method is able to account for the effect of variability in seismic input and structural characteristics on the damage statistics simulated for the building class, and evaluate the associated uncertainty in the vulnerability prediction. The procedure has been implemented in a Matlab programme through a collaborative effort between University College London (UCL) and Bureau de Recherches Géologiques et Minières (BRGM), France. The FRACAS executable can be freely obtained by e-mailing t.rossetto@ucl.ac.uk.

Determination of the performance point

The determination of performance point using FRACAS procedure is based on the following steps (Figure 7.21):

- Transformation of the pushover curve (force-displacement format), resulting from non-linear static analysis, to ADRS format.
- Idealisation of the capacity curve
- Discretisation of the idealised capacity curve and definition of a suite of SDoF for inelastic demand analysis
- Inelastic demand calculation
- Determination of the performance point.

It is important to note that, in contrast to other capacity spectrum methods, FRACAS does not rely on reduction factors or indices to estimate the inelastic spectrum from the elastic one. Instead, it carries out, for each target ductility and period, a simplified dynamic analysis on the idealized non-linear SDOF model corresponding to the capacity curve.

This process proves to be more time-consuming than the commonly used static approaches but it remains faster and more robust than performing full time-history analyses on finite element models. This feature also has the advantage of permitting the use of various natural accelerograms that generate unsmoothed spectra as opposed to standardized design spectra. Therefore, the record-to-record variability can be directly introduced and the resulting cloud of performance points leads to fragility curves that account for the natural variability in the seismic demand.

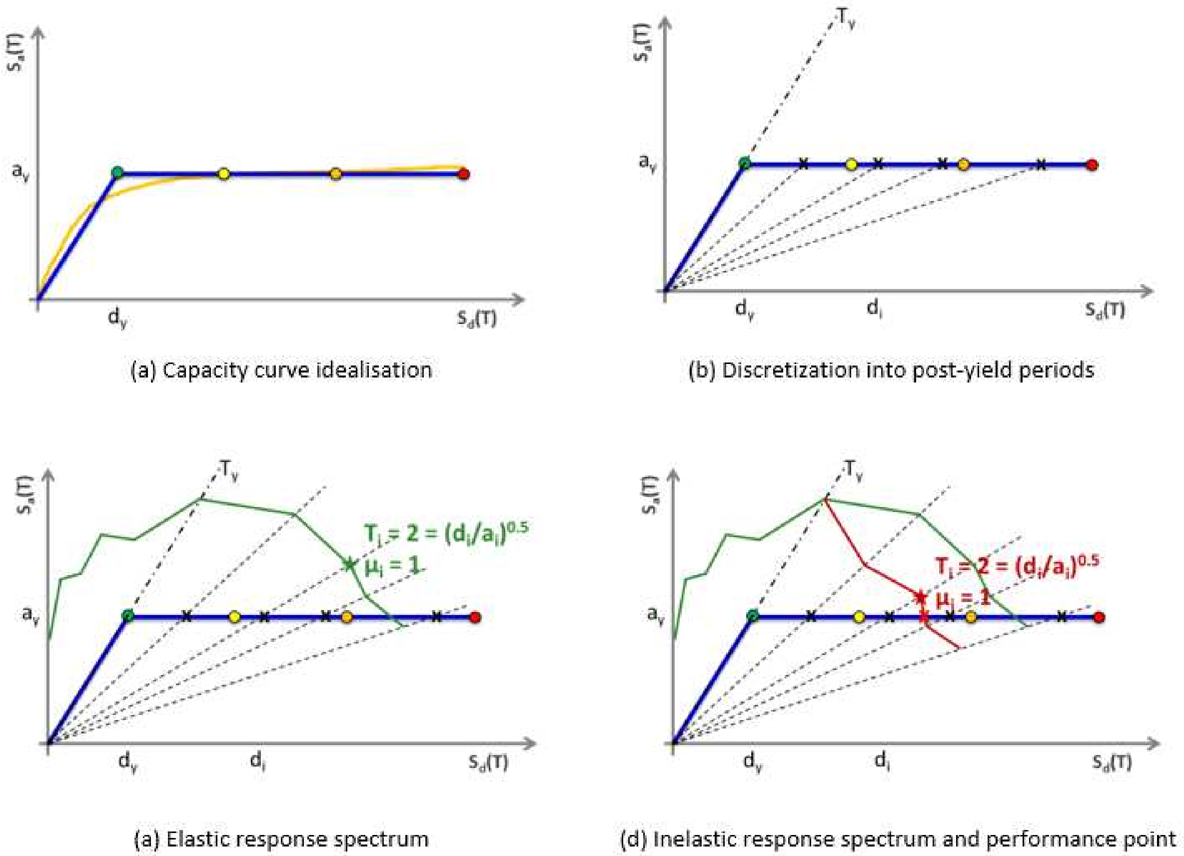

Figure 7.21 Summary of the main steps carried out by FRACAS for a bilinear capacity curve

Transformation of the pushover curve to ADRS format

Details are provided in ANNEX A.

Idealisation of the capacity curve

In FRACAS, the capacity curve is directly idealised as a multi-linear curve that: a) is used to represent the capacity curve when it is compared to the demand values in the determination of the performance points and b) is used to define the hysteretic behaviour of an inelastic single degree of freedom system for the demand calculation explained in the next sub-section. Various curve-fitting options can be implemented within the FRACAS programme: elastic-perfectly plastic (EPP), linear strain hardening (EST) or tri-linear model (MLM). See ANNEX A**.** The choice of model depends on the type of structure and shape of the resulting capacity curve, with for example, EST being better suited to steel frames without infill and MLM to reinforced concrete frames with infill.

Discretisation of the idealised capacity curve and definition of a suite of SDoF for inelastic demand analysis

In order to improve efficiency of performance point calculation, the FRACAS approach discretises the capacity curve into a number of pre and post-yield periods, which are used as analysis points. The number of points is left to the user but it is recommended that points defining changes of slope in the idealised curve (e.g. yield point) should be adopted as analysis points. Each analysis point is characterised by its S_d and S_a

coordinates, and a ductility value, defined by the S_d coordinate of the analysis point divided by the S_d coordinate of global yield of the structure (S_{dy}). Together with the elastic period of the idealised curve, this ductility value is used to define a single degree of freedom system from which the inelastic demand is calculated. The hysteretic behaviour of the SDoF is also defined by the shape of the idealised curve to the analysis point.

Inelastic demand calculation

For a given earthquake record and scale factor, the inelastic seismic demand corresponding to each analysis point is calculated through analysis of the SDOF associated with that analysis point (see above). The earthquake record used in the analysis is discretised into time increments less than $(1/50)^{th}$ of the smallest vibration period of interest. The acceleration record is applied in these time steps to the SDoF and a *Newton-Raphson* iterative scheme is used to solve the dynamic non-linear equilibrium equation for the evaluation of the SDoF response. It is noted that only one inelastic dynamic analysis of the SDoF is required under the applied accelerogram at each analysis point, increasing the rapidity of the assessment.

Determination of the performance point

Each analysis point represents an effective period (defined by a line passing from the origin through the analysis point) along which the inelastic demand and capacity curve can be directly compared, as they have the same ductility. Hence, the performance point is determined directly from the intersection of the capacity curve with the demand curve obtained by joining together the demand values of S_a and S_d calculated at each analysis point (see Figure 7.21d).

In order to determine the EDPs corresponding to each performance point, the capacity curve coordinates at the performance point are used to determine the corresponding load step of the non-linear static analysis file, and relevant response parameters (e.g. maximum interstorey drift) are read from this file. Damage thresholds of EDP should be determined from an appropriately selected damage scale for the structure being analysed. See Section 6.

Box 7.4: Calculation of the median capacity using Procedure 3.2

*The FRACAS procedure is based on the following steps (*Figure 7.21*):*

Step.1. *Develop an appropriate mathematical model of the building for non-linear static analysis. Identify primary and secondary elements or components; define your non-structural elements; foundation flexibility; gravity loads; and P-Delta effects. Refer to Section 5, and you may also refer to ASCE/SEI 41-06 [ASCE 2007].*

Step.2. *Run a static pushover analysis; and make sure that the analysis is extended to a deformation such that collapse is judged to occur. Construct a force-displacement relationship considering different damage states thresholds (capacity curve). See ANNEX A to perform pushover analysis and Section 6 for the identification of the four thresholds.*

Step.3. *The capacity curve is transformed from Force-displacement (FD) to Acceleration-Displacement Response Spectra (ADRS) space. See ANNEX A.*

Step.4. *Provide additional input information: floor displacement, floor masses, building height, and fundamental period.*

Using the FRACAS tool

Step.5. *An idealised shape is fit to the capacity curve making various choices regarding the selection of the yield and ultimate points, the number of segments (bilinear or trilinear) and the presence of strain hardening. For more details see ANNEX A.*

Step.6: *The idealized curve is discretized into a number of analysis points, each representing an SDoF with the elastic stiffness, ductility and hysteretic properties shown by the capacity curve to the analysis point.*

Step 7. *At each analysis point, the inelastic response of the corresponding SDoF under the selected ground motion record is assessed through solution of a Newton-Raphson iteration scheme. (NB: the elastic response is calculated for all analysis points preceding yield in the capacity curve). The maximum response under the entire record, defines the spectral displacement and acceleration values used to characterise the demand at the analysis point.*

Step.8. *The selected accelerogram the performance point is determined directly from the intersection of the capacity curve with the demand curve obtained by joining together the demand values of* S_a *and* S_d *calculated at each analysis point (see* Figure 7.21*).*

Step.9. *The capacity curve coordinates at the performance point are used to determine the corresponding load step of the non-linear static analysis file, and relevant response parameters (e.g. maximum interstorey drift) are read from this file.*

Determination of EDPs damage state thresholds

In order to determine the structure’s performance under increasing ground motion intensity, the analysis described in this procedure (Procedure 3.2) should be repeated for the same accelerogram scaled up until all the limit state are reached, and/or for multiple accelerograms (Figure 7.22). The selected number of accelerograms/ground motions should be sufficient to provide stable estimates of the medians capacity. The use of 11 pairs of motions (i.e. 22 motion set, including two orthogonal components of motion), should be sufficient to provide stable estimates of the medians capacity [Gehl et al. 2014]. The resulting cloud of performance points (similarly in the Procedure 2.1, see Figure 7.13) is then used to determine the EDP for each damage state thresholds and the dispersion, and then create a fragility curve by fitting a statistical model. Further details are provided in Section 8.1.

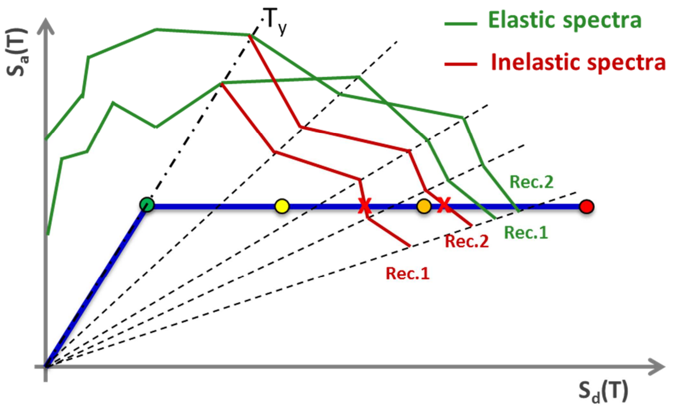

Figure 7.22 Repeat the process of the Procedure 3.2 for multiple earthquake records.

The calculation of EDPs of damage state thresholds and their corresponding dispersion can be conducted using one of the following approaches (Generalised Linear Model or Least Squares Formulation), which rely on the definition of deterministic values of EDP corresponding to damage thresholds (DS).

Generalized Linear Model (GLM)

Details are provided in Section 7.3.1.1

Least Squares Formulation

Details are provided in Section 7.3.1.1

7.3.2.3 Procedure 3.3: Alternative Method for Considering Record-to-Record Variability

The process consists of the evaluation of inelastic demand in terms of *IM* $\hat{S}_{a,ds_i}(T_1)$ considering the dispersion due to the record-to-record variability in the system's non-linear response. It estimates both the median and the dispersion of the lognormally distributed responses given an IM level through relationships between the inelastic displacement ratio C_R (where $C_R = \mu(R)/R$), the ductility μ, and the period T ($C_R - \mu - T$ relationship).

Determination of the performance point

The implementation of the procedure requires the transformation of the Multi Degree of Freedom (MDoF) system, characterized by storey masses m_i and mode shapes ϕ_i, to an equivalent Single Degree of Freedom (SDoF) system, characterized by an equivalent mass m^* (for more details see ANNEX A).

For MDoF system dominated by the first-mode shape, the roof lateral displacement response, δ_{roof,ds_i}, is related to the lateral displacement response of an equivalent elastic SDoF system, $S_d(T_1)$, corresponding to the building's fundamental period of vibration, T_1, as follows [FEMA 440 2005]:

$$\delta_{roof,ds_i} = S_d(T_1) \cdot \Gamma_1 \phi_1 \tag{7.39}$$

where $\Gamma_1 \phi_1$ is the first mode participation factor, estimated for the first-mode shape normalized by the roof displacement.

Determination of EDPs damage state thresholds

The central value of roof displacement corresponding to the median EDP capacity can be estimated using the following expression as per ATC-55 [FEMA-440 2005]:

$$\hat{\delta}_{roof,ds_i} = C_R \cdot \hat{S}_d(T_1) \cdot \Gamma_1 \phi_1 \tag{7.40}$$

C_R is the inelastic displacement ratio computed for non-linear SDoF systems having hysteretic behaviour representative of the analysed structure, which is a function of the first-mode period of vibration and the relative lateral strength of the system, R.

The roof displacement of a MDoF system corresponding to a damage state threshold ds_i, $\hat{\delta}_{roof}(ds_i)$, can easily be estimated from the result of pushover analysis. Considering the following relation between spectral acceleration and displacement:

$$S_d(T_1) = \frac{T_1^2}{4\pi^2} S_a(T_1) \tag{7.41}$$

the median spectral acceleration of the equivalent SDoF can be estimated as follows:

$$\hat{S}_{a,ds_i}(T_1) = \frac{4\pi^2}{C_R T^2 \Gamma_1 \phi_1} \hat{\delta}_{roof,ds_i} \tag{7.42}$$

Providing the relationship between the median IM and the corresponding median EDPs structural response.

For the use of Equation 7.42 it is convenient to have a simplified equation to estimate C_R for SDoF systems having hysteretic behaviour representative of the global force-deformation response. The following functional form proposed by Ruiz-Garcia and Miranda [2005] and later incorporated in ATC-55 [FEMA-440 2005] recommendations is proposed to estimate the central tendency of C_R :

$$\hat{C}_R = \frac{\mu(R)}{R} = 1 + \frac{R-1}{\theta_1 \cdot T_1^{\theta_2}} \tag{7.43a}$$

where $\hat{\theta}_1$ and $\hat{\theta}_2$ are parameters whose estimates are obtained through non-linear regression analysis. This regression analysis would require the analyst to employ a significant number of ground motions representative of the location of the assessed building or class of buildings. Most probably, this option may not be always possible because of lacking of ground motions data from the same location.

Default values of parameter estimates are provided by Ruiz-Garcia and Miranda [2007] as result of non-linear regression analysis of three different measures of central tendency computed from 240 ground motions:

$$\hat{C}_R = 1 + \frac{R-1}{79.12 \cdot T_1^{1.98}} \tag{7.43b}$$

The lateral strength ratio, R , can be estimated using the following relation:

$$R = \frac{S_a(T_1)/g}{F_y/W} = \frac{S_a(T_1)/g}{C_y} = \frac{m^*}{F_y} S_a(T_1) \tag{7.44}$$

where m^* is the total seismic mass (the equivalent SDoF mass), F_y is the yield base shear extracted from the linear idealization of the system capacity curve (See ANNEX A). C_y is the building's yield strength coefficient and represent the ratio between the yield base shear and the weight of the structure, *W*.

Finally, the following simplified non-linear equation, as suggested by Ruiz-Garcia and Miranda [2007], shall be used to estimate the record-to-record dispersion β_D that accompanies the median value of $\hat{C}_R$ computed in Equation 7.43a:

$$\beta_D = \sigma_{\ln \hat{C}_R} = \left[\frac{1}{\hat{\beta}_1} + \frac{1}{\hat{\beta}_2 \cdot (T+0.1)} \right] \cdot \hat{\beta}_3 \cdot \left[1 - \exp\left(-\hat{\beta}_4 (R-1) \right) \right] \tag{7.45a}$$

where $\hat{\beta}_1$, $\hat{\beta}_2$, $\hat{\beta}_3$ and $\hat{\beta}_4$ are parameters that the analyst can obtain through non-linear regression. Alternatively, the analyst may use the default values of parameter estimates provided by Ruiz-Garcia and Miranda [2007], and for which Equation 7.6a becomes:

$$\beta_D = \left[\frac{1}{5.876} + \frac{1}{11.749 \cdot (T+0.1)}\right] \cdot 1.957 \cdot [1 - \exp(-0.739(R-1))] \quad (7.45b)$$

Box 7.5: Calculation of the median capacity using Procedure 3.3

For a bilinear elasto-plastic system the medians capacity for different damage thresholds are obtained through the following steps:

Step.1. *Develop an appropriate mathematical model of the building for non-linear static analysis. Identify primary and secondary elements or components; define non-structural elements contributing to lateral capacity; foundation flexibility; gravity loads; and P-Delta effects. Refer to Section 5, and you may also refer to ASCE/SEI 41-06 [ASCE 2007].*

Step.2. *Run a static pushover analysis; and make sure that the analysis is extended to a deformation such that collapse is judged to occur. Construct a force-displacement relationship considering different damage states thresholds (capacity curve). See ANNEX A to perform pushover analysis and Section 6 for the identification of the four damage thresholds.*

Step.3. *Transformation of MDoF system to an equivalent SDoF system, and derive the equivalent SDoF-based capacity curve. Estimate the equivalent SDoF mass and period (see ANNEX A).*

Step.4. *Fit the SDoF system based capacity curve via a bilinear elasto-plastic idealization. Estimate the yield base shear, and the displacement at yield,*

Step.5. *From pushover analysis, estimate* $\hat{\delta}_{roof,ds_i}$*, the median roof displacement of MDoF system corresponding to a damage threshold* ds_i*. Estimate* $S_{d,ds_i}(T_1)$ *and* $S_{a,ds_i}(T_1)$ *from the equivalent SDoF-based capacity curve*

Step.6. *Compute the lateral strength ratio* R *from Equation 7.44*

Step.7. *Compute* C_R *the inelastic displacement ratio from Equation 7.43*

Step.8. *Estimate the median IM capacity,* $\hat{S}_{a,ds_i}(T_1)$ *from Equation 7.42.*

$$\hat{S}_{a,ds_i}(T_1) = \frac{4\pi^2}{C_R T^2 \Gamma_1 \phi_1} \hat{\delta}_{roof,ds_i}$$

7.4 Non-Linear Static Analysis Based on Simplified Mechanism Models (SMM-NLS)

The non-linear static based procedure offered in this section allows the calculation of the EDPs thresholds for most of masonry construction typologies (unreinforced masonry and adobe structures). The calculation of the EDPs thresholds can be done using smoothed elastic response spectrum only. Hence, the analyst should note that when using this method the uncertainty associated to record-to-record variability is not appropriately considered in computing the estimated median capacity value. Smoothed elastic response spectrum cannot reflect record-to-record variability as it generally represents the envelope or average of response spectra.

7.4.1 *Procedure 4.1: Failure Mechanism Identification and Vulnerability Evaluation (FaMIVE)*

The *Failure Mechanism Identification and Vulnerability Evaluation* (FaMIVE) procedure is based on previous work presented in D'Ayala and Speranza [2003] and D'Ayala [2005]. The FaMIVE method uses a non-linear pseudo-static structural analysis with a degrading pushover curve to estimate the performance points, as it has been described in Procedure 2.1 and Procedure 3.1. It yields as output collapse multipliers which identify the occurrence of possible different mechanisms for a given masonry construction typology, given certain structural characteristics. The FaMIVE algorithm produces capacity curves, performance points and outputs fragility curves for different seismic scenarios in terms of intermediate and ultimate displacements or ultimate acceleration. Figure 7.23 shows the workflow of the FaMIVE method for the seismic vulnerability assessment.

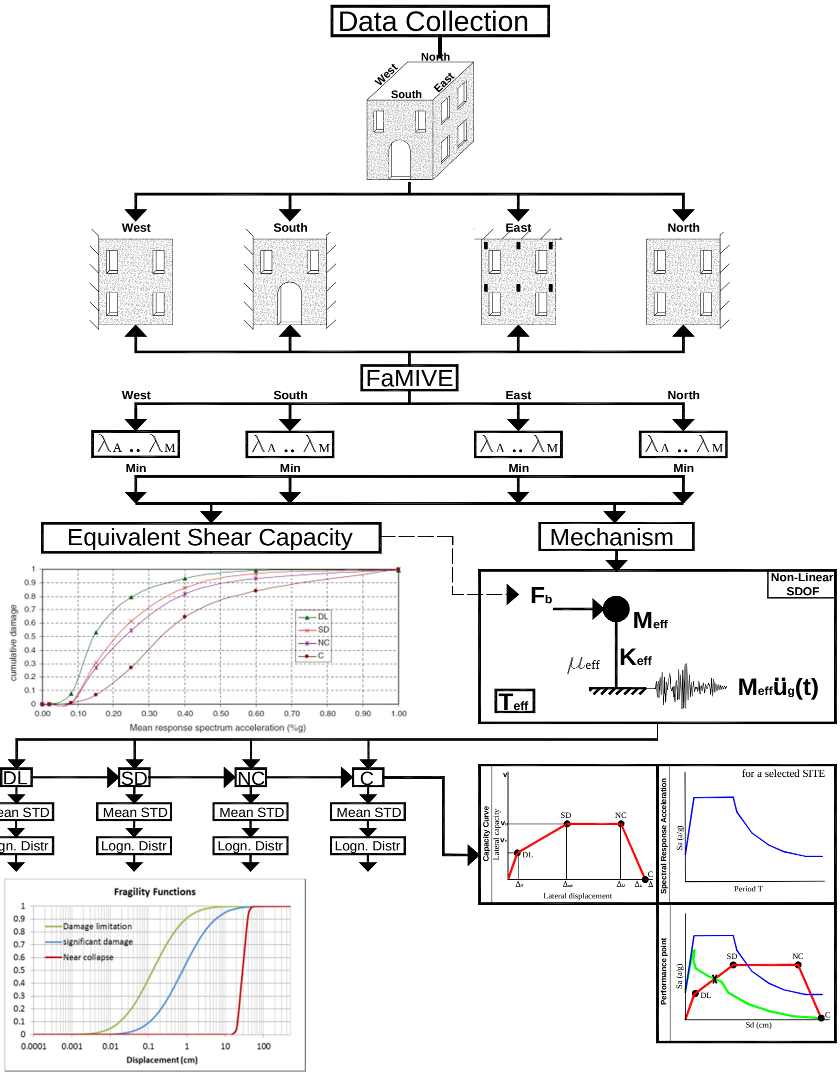

Figure 7.23 Workflow of the FaMIVE method for derivation of fragility functions

Within the FaMIVE database capacity curves and fragility functions are available for various unreinforced masonry typologies, from adobe to concrete blocks, for a number of reference typologies in a number of regions of the world [D'Ayala and Kishali 2012, D'Ayala 2013]. The FaMIVE executable can be freely obtained by e-mailing d.dayala@ucl.ac.uk.

Derivation of capacity curve and determination of the performance point

The capacity curve for the structure is directly related to the collapse mechanism identified by the analysis as the critical one. The construction of the capacity curve is obtained by first calculating the lateral effective stiffness for each wall and its tributary mass. The effective stiffness for a wall is calculated on the basis of the type of mechanism attained, the geometry of the wall and layout of opening, the constraints to other walls and floors and the portion of other walls involved in the mechanism:

$$K_{eff} = k_1 \frac{E_t I_{eff}}{H_{eff}^3} + k_2 \frac{E_t A_{eff}}{H_{eff}} \tag{7.46}$$

where H_{eff} is the height of the portion involved in the mechanism, E_t is the estimated modulus of the masonry as it can be obtained from experimental literature for different masonry typologies, I_{eff} and A_{eff} are the second moment of area and the cross sectional area, calculated taking into account extent and position of openings and variation of thickness over height, k_1 and k_2 are constants which assume different values depending on edge constraints and whether shear and flexural stiffness are relevant for the specific mechanism.

The tributary mass Ω_{eff} is calculated following the same approach and it includes the portion of the elevation activated by the mechanisms plus the mass of the horizontal structures involved in the mechanism:

$$\Omega_{eff} = V_{eff}\gamma_m + \Omega_f + \Omega_r \tag{7.47}$$

where V_{eff} is the solid volume of the portion of wall involved in the mechanism, γ_m is the density of the masonry, Ω_f and Ω_r are the masses of the horizontal structures involved in the mechanism. Effective mass and effective stiffness are used to calculate a natural period T_{eff} , which characterises an equivalent SDoF oscillator:

$$T_{eff} = 2\pi\sqrt{\frac{\Omega_{eff}}{K_{eff}}} \tag{7.48}$$

The mass is applied at the height of the centre of gravity of the collapsing portion with respect to the ground h_0 and a linear acceleration distribution over the wall height is assumed. The elastic limit acceleration S_{ay} is also computed depending on the failure mechanism identified; for failure mechanisms involving flexural strain limit (assuming no tensile capacity in the material), for instance, S_{ay} will be the value of lateral acceleration that combined with gravitational load resultant, will cause a triangular distribution of compression stresses at the base of the overturning portion, just before the onset of partialisation:

$$S_{ay} = \frac{t_b^2}{6h_0} g \quad \text{with corresponding displacement } S_{de} = \frac{S_{ay}}{4\pi^2} T_{eff} \tag{7.49}$$

where, t_b is the effective thickness of the wall at the base of the overturning portion, h_0 is the height to the ground of the centre of mass of the overturning portion, and T_{eff} the natural period of the equivalent SDoF oscillator. In the case of in-plane mechanism the geometric parameter used for the elastic limit is, rather than the wall thickness, the width of the pier where the flexural strain limit is first attained.

The maximum lateral capacity S_{au} is defined as:

$$S_{au} = \frac{\lambda_c}{\alpha_1} \tag{7.50}$$

where λ_c is the load factor of the collapse mechanism chosen, calculated by FaMIVE, and α_1 is the proportion of total mass participating to the mechanism. This is calculated as the ratio of the mass of the façade and sides or internal walls and floor involved in the mechanism Ω_{eff} , to the total mass of the involved macro-elements (i.e. walls, floors, and roof). The displacement corresponding to first attainment of the peak lateral force S_{au} , identifying the damage threshold of structural damage, is S_{ds} set as:

$$3S_{dy} \le S_{ds} \le 6S_{dy} \tag{7.51}$$

as suggested by Tomazevic et al. [2007]. The range in Equation 7.51 is useful to characterize masonry fabric of variable regularity and its integrity at ultimate conditions, with the lower bound better describing the behaviour of adobe, rubble stone and brickwork in mud mortar, while the upper bound can be used for massive stone, brickwork set in lime or cement mortar and concrete blockwork.

Finally the near collapse condition is determined by the displacement S_{du} identified by the condition of loss of vertical equilibrium which, for overturning mechanisms, can be computed as a lateral displacement at the top or for in plane mechanism by the loss of overlap of two units in successive courses, i.e.:

$$S_{du} \ge t_b/3 \quad \text{or} \quad S_{du} \ge l_u/2 \tag{7.52}$$

where t_b is the thickness at the base of the overturning portion and l_u is the typical length of units forming the wall.

Equations 7.49 to 7.52 identify the threshold points on the idealised capacity curve corresponding to the damage limit states ds_1 to ds_4 defined in Table 6.6.

To calculate the coordinates of the performance point in the displacement-acceleration space, the intersection of the capacity curve with the non-linear demand spectrum for an appropriate level of ductility μ can be determined as shown in Equation 7.53, given the value of ultimate lateral capacity of the equivalent SDoF oscillator, S_{au} :

- For short period range: $T^* < T_C$
  - If $S_{au} \geq S_a(T^*)$

$$S_d^*(\mu) = \frac{T_C^2 \left(S_{ae}(T^*) - S_a(T^*)\right)^2}{(\mu - 1)^2} \cdot \frac{g\mu}{4\pi^2 S_a(T^*)} \tag{7.53a}$$

  - If $S_a(T_C) < S_{au} < S_a(T^*)$

$$S_d^*(\mu) = \frac{T_C^2 \left(S_{ae}(T^*) - S_{au}\right)^2}{(\mu - 1)^2} \cdot \frac{g\mu}{4\pi^2 S_{au}} \tag{7.53b}$$

  - If $S_{au} \leq S_a(T_C)$

$$S_d^*(\mu) = \frac{gT_C^2 \left(S_{ae}(T^*)\right)^2}{4\pi^2 \mu S_{au}} \tag{7.53c}$$

- For medium and long period range: $T^* \geq T_C$
  - If $S_{au} \geq S_a(T^*)$

$$S_d^*(\mu) = \frac{gT_C^2 \left(S_{ae}(T^*)\right)^2}{4\pi^2 \mu S_a(T^*)} \tag{7.53d}$$

  - If $S_{au} < S_a(T^*)$

$$S_d^*(\mu) = \frac{gT_C^2 \left(S_{ae}(T^*)\right)^2}{4\pi^2 \mu S_{au}} \tag{7.53e}$$

where two different formulations are provided for values of ultimate lateral capacity S_{au} greater or smaller than the non-linear spectral acceleration $S_a(T_C)$ associated with the corner period T_C marking the transition from constant acceleration to constant velocity section of the parent elastic spectrum.

Figure 7.24 shows an example of calculation of performance points for median capacity curves for some different types of mechanisms (see Figure 5.3).

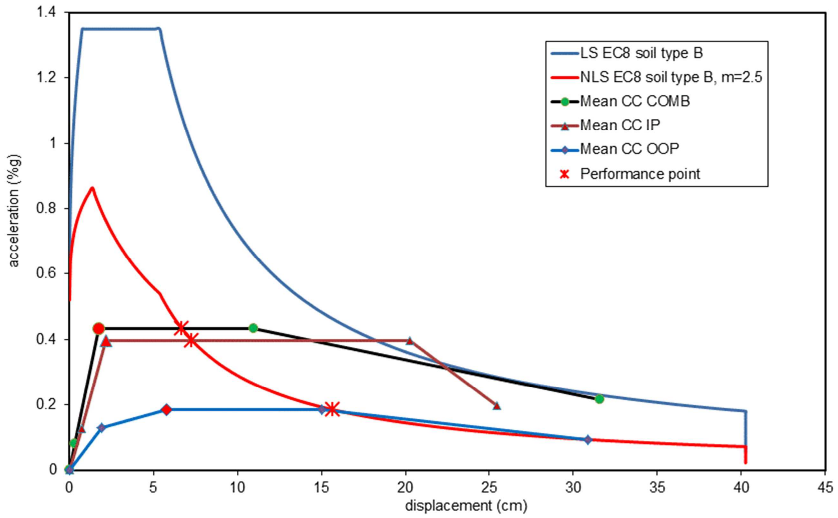

Figure 7.24 Example of calculation of performance points for median capacity curves for types of mechanisms triggered (COMB= combined mechanism, IP= in-plane mechanism, OOP= Out-of-plane mechanism; see also Figure 5.3).

Determination of EDPs damage state thresholds

In the above procedure (i.e. FaMIVE approach), EDPs damage state thresholds are obtained by computing the median values of the performance point displacements for each index building in a given sample and by deriving equivalent lognormal distributions.

$$\hat{S}_{d,ds_i} = e^{\overline{\mu}_i} \qquad \text{with} \qquad \overline{\mu}_i = \frac{1}{n}\sum_{j=1}^{n} \ln S^j_{d,ds_i} \tag{7.54}$$

Smoothed elastic response spectrum cannot reflect record-to-record variability as it generally represents the envelope or average of response spectra. Hence, in order to derive fragility and vulnerability functions considering the record-to-record variability, the analyst may refer to Equation 7.45b to estimate β_D as proposed in the Section 7.3.2.3 (simplified equation suggested by Ruiz-Garcia and Miranda 2007).

The analyst may also wish to assign, but with a special care, default values provided in ANNEX B, Table B-1, as suggested by ATC-58 [FEMA P-58, 2012]. Given the fundamental period of the structure and a strength ratio, the values of β_D can be chosen in a range between 0.05 and 0.45. If data on the above two parameters is lacking or uncertain, a maximum default value of 0.45 can be used.

In case a given set of buildings surveyed on site or created through randomisation of the input parameters to characterise the exposure of a urban centre or district, then, having run FaMIVE and having generated a capacity curve for each building in the physical sample, the standard deviation (associated to structural characteristics) of the median capacity for each limit state can be calculated as:

$$\beta_{M,ds_i} = e^{\overline{\mu}_i + \frac{1}{2}\sigma_i^2}\sqrt{e^{\sigma_i^2} - 1} \qquad \text{with} \qquad \sigma_i = \sqrt{\frac{\sum_{j=1}^{n}(\ln S^j_{d,ds_i} - \ln \overline{S}^j_{d,ds_i})^2}{n}} \tag{7.55}$$

To account for the reliability of the input parameters, three levels of reliability are considered, high, medium, and low, respectively, to which three confidence ranges of the value given for a parameter can be considered corresponding to 10% variation, 20% variation, and 30% variation. The parameter value is considered central to the confidence range so that the interval of existence of each parameter is defined as $\mu \pm 5\%$, $\mu \pm 10\%$, $\mu \pm 15\%$, depending on highest or lowest reliability. The reliability applied to the output parameters, in particular, equivalent lateral acceleration and limit states' displacement, is calculated as a weighted average of the reliability of each section of the data form, with minimum 5% confidence range to maximum 15% confidence range.

8 STEP F: Vulnerability Curves Derivation

Vulnerability curves translate the physical damage into monetary loss (estimation of repair and reconstruction cost), given a level of intensity measure, *im*. Options are offered to the analyst to generate different forms of vulnerability curves:

- vulnerability curve evaluated on the damage indicators of one index building,
- vulnerability curve evaluated on the damage indicators of three index buildings, and
- vulnerability curve evaluated on the damage indicators of multiple index buildings.

In order to generate these curves, two approaches can be used, depending on available data, project requirement, and analyst's skills:

Building-based vulnerability assessment approach:

In this approach, widely used in literature, the vulnerability functions are obtained by convolving building level fragility curves with the cumulative cost of a given damage state ds_i (damage-to-loss functions). In general, the implementation of this approach would be more reasonable, in terms of calculation effort and the availability of detailed data, when performing studies of large population of buildings.

Component-based vulnerability assessment approach:

In this approach, comprehensively presented in ATC-58 [FEMA P-58, 2012], the vulnerability functions are obtained by correlating the components level-based drifts directly to loss. In general, this approach is appropriate when performing loss analysis for single buildings, or when the majority of the economic losses are related to content and non-structural components. The analyst will have to ascertain that the relevant information on specific component loss is available and that time and monetary resources are at hand to perform such detailed analysis.

Note: within this approach, the vulnerability curve can be generated at the storeys level, and at the entire building-level.

8.1 STEP F-1: Building-Based Vulnerability Assessment Approach

The transformation of the fragility curves into vulnerability can be conducted through the following total probability relation:

$$E(C > c \mid im) = \sum_{i=0}^{n} E(C > c \mid ds_i) \cdot P(ds_i \mid im) \tag{8.1}$$

Where, n is the number of damage states considered, $P(ds_i \mid im)$ is the probability of a building sustaining damage state ds_i given intensity im; $E(C > c \mid ds_i)$ is the complementary cumulative distribution of the cost (loss) given ds_i ; $E(C > c \mid im)$ is the complementary cumulative distribution of cost (or loss) given a level of intensity im.

The transformation expressed by Equation 8.1 requires the calculation of damage probabilities from the fragility curves for specific level of intensity:

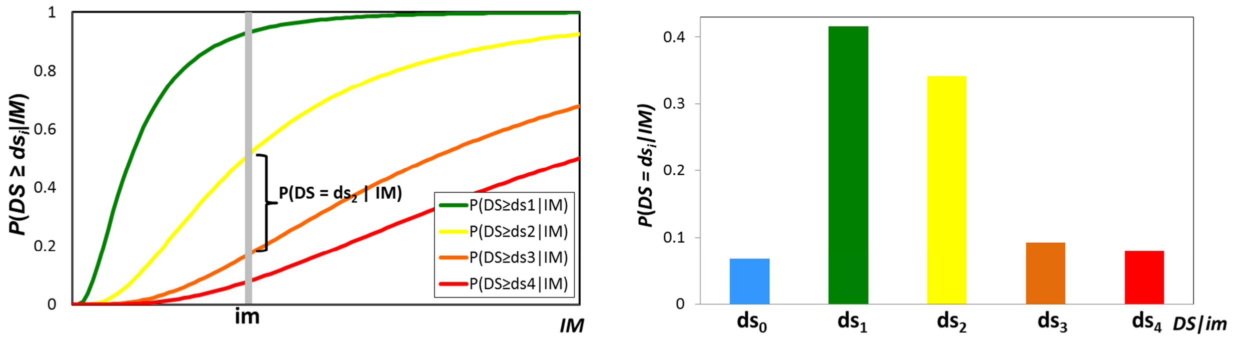

(a) Fragility curves corresponding to n =4 damage states (b) Column of a damage probability for intensity *im*

ds_0 = No Damage; ds_1 = Slight Damage; ds_2 = Moderate Damage; ds_3 = Near Collapse; ds_4 = Collapse

Figure 8.1 Calculation of damage probabilities from the fragility curves for a specific level of intensity measurement, *im*.

Each element (or bar) in the damage probabilities is defined as the distance between two successive fragility curves for a given intensity im, as shown in Figure 8.1. The mean, $E(C \mid im)$, and the variance, $\mathrm{var}(C \mid im)$, of the vulnerability can be then obtained by the following expressions (where *n* = is the number of damage states considered):

$$E(C \mid im) = \sum_{i=0}^{n} E(C \mid ds_i) \cdot P(ds_i \mid im) \tag{8.2}$$

$$\mathrm{var}(C \mid im) = \sum_{i=0}^{n} \left[\mathrm{var}(C \mid ds_i) + E^2(C \mid ds_i) \right] \cdot P(ds_i \mid im) - E^2(C \mid im) \tag{8.3}$$

Repeating the process of calculation (using Equations 8.2 and 8.3) for a range of values for intensity measure $im \in$ {0.01, 0.02, ...3.0g}, will result in the vulnerability curve, as shown in the example of

Figure **8.2**, where the variance will provide the confidence boundary.

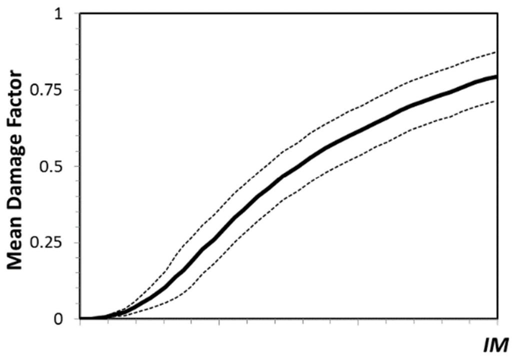

Figure 8.2 Example of illustration of transformation of the fragility curves into vulnerability, with confidence boundaries

8.1.1 Building-Based Fragility Curves

Fragility curves express the probability of a damage state, ds_i, sustained by an examined building class, being reached or exceeded given a level of ground motion intensity measure, IM. As commonly done in seismic vulnerability studies, the curves are assumed to take the form of lognormal cumulative distribution functions having a median value and logarithmic standard deviation, or dispersion. The mathematical form for such a fragility curves is:

$$P(DS \geq ds_i \mid IM) = \Phi\left(\frac{ln(IM) - \alpha_{DS|IM}}{\beta}\right) \quad (8.4)$$

where Φ is the standard normal cumulative distribution function; $\alpha_{DS|IM}$ is the lognormal mean of the generic structural response conditioned on the ground motion intensity, IM; and β is the lognormal standard deviation of $DS|IM$.

For instance, considering the spectral acceleration, $S_a(T)$, as the choice of intensity measure to be used, the above Equation 8.4 may take the following form:

$$P(DS \geq ds_i \mid S_a) = \Phi\left(\frac{1}{\beta}\ln\left(\frac{S_a(T)}{\hat{S}_{a,ds_i}(T_1)}\right)\right) \quad (8.5)$$

Where the pertinent quantities are defined as follows

- ***Median Capacity*** $\hat{S}_{a,ds_i}(T_1)$

The different values of median capacity, $\hat{S}_{a,ds_i}(T_1)$, corresponding to different damage states, should be obtained using one of the alternatives that are offered in Section 7, where a step by step procedure is provided for each method of calculation.

- ***Total Dispersion*** β

The total dispersion parameter β, defined as the lognormal standard deviation, should include: the randomness in the demand imposed on the structure by the earthquake ground motion, the randomness in the values of structural parameters, the uncertainty associated with the mathematical modeling; the building-to-building variability when a class of buildings is considered, the uncertainty associated with the definition of the damage thresholds [D'Ayala and Meslem 2013a].

A number of different formulae exist to represent the contributions of each of these uncertainties to the total dispersion parameter β [FEMA P-58, 2012; FEMA, 2003]. Depending on the refinement of the procedure used for the calculation of EDPs (Section 7), these uncertainties are accounted for implicitly or explicitly. It should be kept in mind that the dispersions associated with record-to-record variability, β_D, total modelling dispersion, β_M, and damage threshold variability, β_{ds}, all are dependent on the damage state considered, with increasing value of dispersion as the damage state increase.

According to ATC-58 [FEMA P-58, 2012], the following Equation could be used for the calculation of total variability:

$$\beta = \sqrt{\beta_D^2 + \beta_M^2} \tag{8.6a}$$

where, β_D is the dispersion associated with uncertainty in the demand (record-to-record variability); β_M is the total modelling dispersion associated with uncertainty in the definition of structural characteristics of building, quality and completeness of mathematical model (definition of different mechanisms, geometric configuration…etc.), and building-to-building variability.

According to HAZUS-MH [FEMA 2003], the following Equation could be used for the calculation of total variability:

$$\beta = \sqrt{\left(CONV\left[\beta_C, \beta_D, \overline{S_{d,Sds}}\right]\right)^2 + \left(\beta_{ds}\right)^2} \tag{8.6b}$$

where, β_C is the dispersion associated with variability in the capacity curve; β_D is the uncertainty in the demand (record-to-record variability); β_{ds} is the uncertainty in the estimate of the median value of the threshold of structural damage state *ds*. The function "CONV" in Equation (8.6b) implies a complex process of convolving probability distributions of the demand spectrum and the capacity curve, respectively.

Record-to-record dispersion, β_D

The demand dispersion associated with ground motion uncertainty, β_D, represents the variability in the distribution of the recorded response at a given level of intensity IM due to different ground motion records. It highly depends on the structure but also on the type of IM used. Shorter periods, higher levels of system ductility, increased influence of higher modes but also the use of a less efficient IM (Section 2.3) will generally result in increased values of β_D :

- If natural records (records from real events; synthetic; or artificial) with different level of IM are used, β_D should be estimated directly from the computation as the lognormal standard deviation for the selected records. Details are provided in Section 7.
- If smoothed elastic response spectrum (which generally represents the envelope or average of response spectra) is used, the uncertainty in demand will not be appropriately considered, as this type of response spectrum cannot reflect record-to-record variability. In this case, β_D should be calculated using the simplified relation offered in Equation 7.45b (Details are provided in Section 7.3.2.3):

$$\beta_D = \left[\frac{1}{5.876} + \frac{1}{11.749 \cdot (T + 0.1)}\right] \cdot 1.957 \cdot \left[1 - \exp(-0.739(R-1))\right]$$

Alternatively, but with special care, β_D can be assumed through default values that are provided in ANNEX B, Table B-1, as suggested by ATC-58 [FEMA P-58, 2012]. Given the fundamental period of the structure and a strength ratio, the values of β_D can be chosen in a range between 0.05 and 0.45. If data on the above two parameters is lacking or uncertain, a maximum default value of 0.45 can be used.

Total modelling dispersion, β_M

Given the selected approach of modelling (from one index building to multiple index buildings) and analysis, alternatives are offered to account for the total dispersion in modelling:

- In case a given set of buildings surveyed on site or created through randomisation of the input parameters to characterise the exposure of an urban centre or district, then, having run selected analysis type and having generated a capacity curve for each building in the physical sample, the dispersion associated to the structural characteristics variability and building-to-building variability, β_M , should be estimated directly from the computation as standard deviation of the median capacity for each limit state using one of the techniques (i.e. regression techniques) offered in Section 7.
- β_M is obtained by using First-Order Second-Moment (FOSM) procedure (Lee and Mosalam 2005; Baker and Cornell 2008b, Vamvatsikos and Fragiadakis 2010). β_M is computed based on the structural responses obtained from the assigned Central, Lower and Upper Bound values (Figure 3.1) of the modelling parameters, the type of distribution for the structural characteristics-based parameters, and model variability. Assuming that the logarithm of the median capacity is a function of the random parameters, the standard deviation of the logs (i.e., the dispersion) is estimated using a first-order derivative:

$$\beta_M^2 \approx \sum_{k=1}^{K}\left(\frac{\ln S_a^{X_k{}^{Upper}} - \ln S_a^{X_k{}^{Lower}}}{X_k{}^{Upper} - X_k{}^{Lower}}\right)^2 \cdot \sigma_{X_k}^2 \approx \sum_{k=1}^{K}\left(\frac{\ln S_a^{\max} - \ln S_a^{\min}}{X_k{}^{Upper} - X_k{}^{Lower}}\right)^2 \cdot \sigma_{X_k}^2 \quad (8.7)$$

where, K is the total number of random modelling parameters considered in the analyses (selected from Table 3.1); X_k is the lower or upper value of the random modelling parameter k ; σ_{X_k} is the standard deviation for each parameter considered, and should be obtained from result of structural characteristics assessment. Further details are provided in D'Ayala and Meslem 2013b, 2013c.

- When conducting a single analysis without extracting lower and upper bound values corresponding to the parameter variability (one index building only central value), then a default value of β_M can be used, as summarised in ANNEX B, Table B-1. These values have been suggested by ATC-58 (FEMA P-58, 2012), and are defined as the uncertainty due to ambiguity in building definition and construction quality. These values range between 0.25 and 0.50 depending on the fundamental period of the structure and its strength ratio.

Damage threshold dispersion, β_{ds}

According to HAZUS-MH [FEMA 2003], the lognormal standard deviation parameter that describes the uncertainty in the estimate of the median value of the threshold of structural damage state ds, β_{ds} , is assumed to be independent of capacity and demand. The values of dispersion of this parameter available in HAZUS-MH are computed in terms of spectral displacement.

8.1.2 Building-Based Repair Cost Given Damage State

For a reliable estimation of total repair cost it is quite important that the analyst accounts for the type of occupancy of the assessed building. In addition to that, the analysts will need to provide their local estimates of repair and reconstruction costs in order to reach a better level of accuracy for the derived vulnerability curves.

If such data is available, the analyst can calculate the total repair cost, given damage threshold:

$$E(C \mid ds_i) = E(LabCost \mid Area\_ds_i) + E(MatCost \mid Area\_ds_i) \quad (8.8)$$

where

$E(C \mid ds_i)$ = is the complementary cumulative distribution of the total repair cost given ds_i .

$E(LabCost \mid Area\_ds_i)$ = is the local labour cost in the considered region (cost per percentage of damaged area given ds_i).

$E(MatCost \mid Area\_ds_i)$ = is the local material cost in the considered region (cost per percentage of damaged area given ds_i).

Table 8.1 identifies the type of repair and reconstruction cost input data that the analyst should provide for generating building level vulnerability functions.

Default values for Damage Factors at global level

A compendium of existing Damage Factors (DF) values (including material and labour costs), given damage threshold, collected from vulnerability literature is provided in ANNEX C. The DF values are at the entire building level, and are presented as a function of:

Building typology, developed within the framework of GEM-VEM [Rossetto et al. 2014]. The data was collected from different sources, and includes material and labour costs for structural and non-structural components (see Rossetto 2014).

Building occupancy class, from HAZUS-MH [FEMA 2003]:

- Default DF values which include material and labour cost for only structural components. The DF values are related to 33 occupancy classifications.
- Default DF values which include material and labour cost for only non-structural components. The DF values are provided in terms of acceleration sensitive and drift sensitive.

Given these default values the relation between DF and repair cost can be expressed as:

$$DF_{ds_i} = \mathrm{E}(\mathrm{C} \mid \mathrm{ds_i}) / CC \tag{8.9}$$

and the analyst can estimate the repair cost $E(C/ds_i)$, for given damage threshold, ds_i , knowing the Construction Cost *CC* in the considered region.

Table 8.1 Repair cost input data for generating building-level vulnerability functions using global level approach

Repair Cost Input Data of Index Building - global building level vulnerability assessment				
	Slight Damage	Moderate Damage	Extensive Damage	Complete Damage
Local Labour cost in the considered region (cost per m2)				
Material cost in the considered region (cost per m2)				
Total building floors area (m2)				
Total building construction cost (covers total structural and non-structural components)				

8.1.3 Building-Based Vulnerability Curve

8.1.3.1 One Index Building Based Vulnerability Curve

Using equations 8.2 and 8.3, the process leads to estimating vulnerability functions at the entire building level (Total Cost given IM per entire building level) by convolving building-level fragility curves with the cumulative distribution of the total cost. The values chosen from the response analysis for generating the vulnerability functions should correspond to the ***Typical Quality*** case for a building class as defined in **Section 3.1**.

Repair cost given damage state

The cumulative distribution of the total repair cost given ds_i , $E(C \mid ds_i)$, should be calculated usingEquation 8.8. The input data should be prepared as shown in Table 8.1, and must be representative of the considered region. In the absence of relevant regional or local data, the analyst may directly use default damage factor values provided in ANNEX D (estimated for the entire building) and Equation 8.9, to estimate repair cost given ds_i .

Fragility curves

The analyst will be required to run a non-linear analysis (or use any existing relevant default capacity curves); the fragility curves should be derived using one of the alternatives presented above. The process of the assessment should include the use of ***Central, Lower, and Upper*** bound values for the structural characteristics-related parameters as described in Table 3.2 (see also Table 3.1).

Vulnerability Curve

Repeating the process of calculation for a range of values for intensity measure $im \in$ {0.01, 0.02, ...3.0g}, using Equations 8.2 and 8.3, will result in the vulnerability curve.

Box 8.1: Derivation of Building-level Vulnerability Curve

The steps for generating the building-level vulnerability curve should be applied considering a Typical Quality for the index building. The steps are as followings:

Step.1. *Given the structural analysis choices made run the analysis assuming Central values, and Lower/Upper bound values (see Section 3). Further guidance on the modelling and analysis type is provided in Section 5 and Section 7.*

Step.2. *Obtain the median capacities at roof level,* $\hat{S}_{a,ds_i}$ *, from non-linear analysis (See* ***Section 7****).*

Step.3*. Derive the building-level fragility curves,* $P(DS \geq ds_i \mid S_a)$*, using one of the suggested alternatives.*

Step.4. *Use Equation 8.8 to calculate the cumulative distribution of the total repair cost given* ds_i *,* $E(C \mid ds_i)$*. The different parameters' cost input data in Table 8.1 must be representative for the considered region. In case of lacking in advanced regional data, the analyst may use default Damage Factors (DF) values in ANNEX C and Equation 8.9.*

For a given intensity im:

Step.5. *Estimate the damage probability matrices,* $P(ds_i \mid im)$*, from the fragility curves (see Figure 8.1).*

Step.6. *The Mean* $E(C \mid im)$*, and the variance,* $\mathrm{var}(C \mid im)$ *of the vulnerability can be then obtained using Equations 8.2 and 8.3.*

$$E(C \mid im) = \sum_{i=0}^{n} E(C \mid ds_i) \cdot P(ds_i \mid im)$$

$$\mathrm{var}(C \mid im) = \sum_{i=0}^{n} \left[\mathrm{var}(C \mid ds_i) + E^2[C \mid ds_i] \right] \cdot P(ds_i \mid im) - E^2[C \mid im]$$

Repeating the process of calculation (using Equations 8.2 and 8.3) for a range of values for intensity measure im *∈ {0.01, 0.02, ...3.0g}, will result in the vulnerability curve.*

8.1.3.2 Three Index Buildings Based Vulnerability Curve

As a simple means to quantify the specific uncertainty in constructing a vulnerability function associated with a given building typology, the analyst can consider the EDPs obtained from the analysis of 3 Index buildings associated to the same typology, but different quality of construction and materials, and generate vulnerability functions as a simple average of the results from three index buildings (see Section 3.2) as suggested in Porter et al [2013] for non-structural components vulnerability. These three index buildings should represent the case ***of Poor Quality***, ***Typical Quality***, and ***Good Quality***, in terms of structural characteristics-related parameters (i.e. level of design base shear …etc.), as shown in Table 3.3.

The mean vulnerability function for the considered three index buildings can be calculated through the following Equation:

$$E(C \mid im) = \frac{1}{3}\sum_{j=1}^{3} E_j(C \mid im) \tag{8.10}$$

where, $E_j(C \mid im)$ is the mean vulnerability function for each index building (each value of *j*) and is given by Equation 8.2, i.e.:

$$E_j(C \mid im) = \sum_{i=0}^{n} E_j(C \mid ds_i) \cdot P_j(ds_i \mid im) \tag{8.11}$$

$E_j(C \mid ds_i)$ is the cumulative distribution of the repair cost given ds_i , for each index building (each value of *j*);

$P_j(ds_i \mid im)$ is the fragility function for each index building (each value of *j*).

Repair cost given damage state

For each index building (each value of *j*), the cumulative distribution of the repair cost given ds_i , $E_j(C \mid ds_i)$, can be calculated using *Equation 8.8*, i.e.,:

$$E_j(C \mid ds_i) = E_j(LabCost \mid Area\_ds_i) + E_j(MatCost \mid Area\_ds_i) \tag{8.12}$$

The input data should be prepared as shown in Table 8.1, and must be representative of the considered region. In the absence of relevant regional or local data, the analyst may directly use default damage factor values provided in ANNEX C and Equation 8.9, to estimate repair cost given ds_i .

The Poor, Typical, and Good-quality index buildings should represent cases where repair cost would be exceeded respectively by 10%, 50%, and 90% of buildings of the same class/category.

Fragility curves

For each index building (each value of *j*), fragility curves $P_j(DS \geq ds_i \mid S_a)$ should be derived in a similar way to one index building-level fragility curves, described in Section 8.1.3.1. The process of analysis, for each index building, should be conducted for: ***Central*** value, ***Lower Bound*** value, and ***Upper Bound*** value for the structural characteristics-related parameters as described in Table 3.3 (see also Table 3.1).

Then for a given intensity im, the analyst should estimate the column of a damage probability, $P_j(ds_i \mid im)$, from the generated fragility curves of each index building as shown in Figure 8.1.

Box 8.2: Derivation of Three Index Buildings-based Vulnerability Curve

The steps for generating the three index buildings-based vulnerability curve should be applied considering the case of: Poor, Typical, and Good quality. The steps are as followings:

For each index building j (j =1,2,3):

Step.1. *Given the structural analysis choices made run the analysis assuming central values, lower values, and upper values. Further guidance on the modelling and analysis type is provided in Section 5 and Section 7.*

Step.2. *Obtain the medians capacity at roof level,* $\hat{S}_{a,ds_i}$ *, from non-linear analysis (See Section 7).*

Step.3. *Derive the building-level fragility curves,* $P_j\left(DS \geq ds_i \mid S_a\right)$*, using one of the suggested alternatives.*

Step.4. *Use Equation 8.12 to calculate the cumulative distribution of the total repair cost given* ds_i *,* $E_j\left(C \mid ds_i\right)$*. The different parameters' cost input data in Table 8.1 must be representative for the considered region. In case of lacking in advanced regional data, the analyst may use default damage factors values provided in ANNEX C, and Equation 8.9.*

For a given intensity im and from each index building:

Step.5. *Estimate the column of different damage probability,* $P_j\left(ds_i \mid im\right)$*, from the fragility curves (see Figure 8.1).*

Step.6. *The mean* $E_j(C|im)$ *of the vulnerability for each building can be then obtained using Equation 8.11.*

$$E_j(C \mid im) = \sum_{i=0}^{n} E_j\left(C \mid ds_i\right) \cdot P_j\left(ds_i \mid im\right)$$

Repeating the process of calculation (using Equation 8.11) for a range of values for intensity measure {0.01, 0.02, ...3.0g}, will result in the mean vulnerability curve for each index building.

Step.7. *The three index buildings-based Mean Vulnerability curve can simply be calculated through the following Equation 8.10:*

$$E(C \mid im) = \frac{1}{3}\sum_{j=1}^{3} E_j(C \mid im)$$

8.1.3.3 Multiple Index Buildings Based Vulnerability Curve

The implementation of this approach would require a greater calculation effort, depending on the number of properties considered (i.e. number of parameters that will be considered as significant). The process will require the use of a large number of numerical simulations by implementing one of the following sampling approaches: Moment-Matching, Class Partitioning, or Monte Carlo simulation. Further details are provided in Section 3.3.

8.2 STEP F-2: Component-Based Vulnerability Assessment Approach

The derivation of vulnerability functions using component level approach will require detailed information for each structural and non-structural component, in terms of fragility functions and unit repair cost. The selected non-structural components should be identified as the most dominant contributing to construction cost.

Note that, the list of these dominant non-structural components might vary substantially between building types (especially in terms of occupancy) and countries. An example of the selection and classification of the most dominant non-structural components for the case of US building is shown in Table 4.4. More details are provided in the Section 4.2.

8.2.1 Component-Based Fragility Curve

The component-level fragility curves can either be derived or estimated by adopting one the following alternatives:

- ***Alternative 1:*** Provide a definition of the performance criteria (e.g. plastic rotation values...etc.) for each structural and non-structural component and then run analyses to derive the component-level fragility curves. This option would require the availability of necessary data/information and would be considered cumbersome for general use. Further guidance on defining the performance criteria of different components, depending on their material type, can be found in literature, such as, ATC-58 (FEMA P-58, 2012) and Eurocode-8 (CEN 2004).
- ***Alternative 2:*** The use of existing component-level fragility curves from literature. As default source of the data, ATC-58 PACT (FEMA P-58, 2012), NISTIR 6389 (NIST 1999) are suggested, where more than 700 fragility curves for different type and category of components are provided. However, it is quite important to keep in mind that these default component-level fragility curves are mostly derived for US buildings.

Table 8.2 and Table 8.3 show an illustrative example of input data, in terms of component-level fragility functions (medians capacity and log STD deviation), that the analyst should consider for asset definition of structural and non-structural components.

Table 8.2 Example of asset definition for structural components and existing fragility functions by damage state as per literature, for the generation vulnerability functions

Specifications for Structural Components												
Component Name	RC shear walls		RC columns		RC beams		....		....		....	
Unit	Each (900 sf)											
NISTIR 6389 class ID	B1040		....		....		....		....		....	
FEMA P-58 class ID	B1044.043		....		....		....		....		....	
Demand parameter	PTD		....		....		....		....		....	
Ref (default PACT 1.0)	PACT 1.0		PACT 1.0		PACT 1.0		....		....		....	
Fragility Function												
Damage state (ds)	Median Capacity	Log STD Deviation	Median Capacity	Log STD Deviation	Median Capacity	Log STD Deviation	Median Capacity	Log STD Deviation	Median Capacity	Log STD Deviation	Median Capacity	Log STD Deviation
1												
2												
3												
4												

Table 8.3 Example of asset definition for non-structural components and existing fragility functions by damage state as per literature, for the generation vulnerability functions

Specifications for Non-structural Components												
Component Name	Terminal & package units		Plumbing fixtures		Lighting branch wiring		Partitions		Interior doors		Exterior windows	
Unit	Ea		N/A		Ea		100 lf = 30m		Each		Each (4' by 8' panel)	
NISTIR 6389 class ID	D3050		D2010		D5020		C1010		C1020		B2020	
FEMA P-58 class ID	D3052.011d				C3034.001		C1011.001d		C1020.001		B2022.035	
Demand parameter	PFA		PFA		PTD		PTD		PTD		PTD	
Ref (default PACT 1.0)	PACT 1.0		N/A		PACT 1.0		PACT 1.0		Porter judgment		PACT 1.0	
Fragility Function												
Damage state (ds)	Median Capacity	Log STD Deviation	Median Capacity	Log STD Deviation	Median Capacity	Log STD Deviation	Median Capacity	Log STD Deviation	Median Capacity	Log STD Deviation	Median Capacity	Log STD Deviation
1												
2												
3												
4												

8.2.2 *Component-Based Repair Cost Given Damage State*

To generate vulnerability functions based on component approach, the damage cost is needed for each structural and non-structural component. Table 8.4 and Table 8.5 show an example on how the repair cost should be assigned for each structural and non-structural component depending on damage state.

In order to obtain these, reference can be made to cost manuals that estimate the cost of repair or construction of a component given a damage state. However, it is worth to recall that the provided information may vary substantially between countries. For instance, the analyst can use values from ATC-58 PACT 1.0 [FEMA P-58, 2012], RS Means [2009], developed for US buildings. The database provided in PACT is defined mainly for a construction industry and construction standards that do not apply worldwide.

Once all the structural and non-structural components have been categorized, the analyst should conduct an inventory of these components for each storey, as shown in Table 8.6 and Table 8.7.

Table 8.4 Repair cost by damage state; example for structural component, RC elements

Component Specification, Partitions				
NISTIR Class	B1040		Component Name	RC elements
FEMA P-58 Class	B1044.043		Unit	
Demand Parameter	PTD		Ref. (default PACT 1.0)	PACT 1.0
Fragility Function			**Repair cost by damage state**	
Damage State (ds)	Median Capacity	Log STD Deviation	P_{50} (median cost)	Log STD Deviation
1				
2				
3				
4				

Table 8.5 Repair cost by damage state; example for non-structural component, Partitions

Component Specification, Partitions				
NISTIR Class	C1010		Component Name	Partitions
FEMA P-58 Class	C1011.001d		Unit	
Demand Parameter	PTD		Ref. (default PACT 1.0)	PACT 1.0
Fragility Function			**Repair cost by damage state**	
Damage State (ds)	Median Capacity	Log STD Deviation	P_{50} (median cost)	Log STD Deviation
1				
2				
3				
4				

Table 8.6 Structural components inventory by storey, for low- and mid-rise buildings

Structural components inventory						
Component Name	RC shear walls	RC columns	RC beams	….	….	….
Unit	Each (900 sf)					
Storey	**Quantity (total)**					
1						
2						
3						
4						
5						
6						
7						

Table 8.7 Non-structural components inventory by storey, for low- and mid-rise buildings

Non-structural components inventory						
Component Name	Terminal & package units	Plumbing fixtures	Lighting branch wiring	Partitions	Interior doors	Exterior windows
Unit	Ea	N/A	Ea	100 lf = 30m	Each	Each (4' by 8' panel)
Storey	Quantity (total)					
1						
2						
3						
4						
5						
6						
7						

8.2.3 Component-Based Vulnerability Curve

8.2.3.1 One Index Building Based Vulnerability Curve

Two levels for the construction of vulnerability functions can be derived: Storey-level vulnerability functions and Building-level vulnerability functions.

8.2.3.1.1 Storey-Level Vulnerability Functions

The procedure offered here allows the calculation of storey-level vulnerability functions for all acceleration-sensitive components on each individual storey, and all drift-sensitive components on each individual storey (sum of different components repair costs on each storey). Any of the non-linear dynamic approaches described in Section 7.1 can be used to obtain the needed distribution of peak storey drift and peak floor acceleration at each storey/floor. The non-linear static pushover methods of Section 7.2.1 can also be employed to obtain peak storey drift distributions, while simplified methods described in Porter et al. (2014) should be used for extracting peak floor acceleration estimates. The use of pushover methods that do not account for record-to-record dispersion (Section 7.2.2) is also possible.

When implementing the component-based vulnerability assessment approach, the generation of storey-level vulnerability functions does not require the definition of different global damage states (i.e. STEP D/Section 6 is not mandatory).

The storey-level vulnerability function is derived for a discrete number of levels of floor acceleration or drift, as follows:

- The storey-level mean vulnerability for acceleration-sensitive components should be estimated from the following relation:

$$E\left[C_a \mid S_{h,a} = S_a\right] = \sum_{i=1}^{N_a} E\left[C_i \mid S_{h,a} = S_a\right] \quad (8.13)$$

- The storey-level mean vulnerability for drift-sensitive components should be estimated from the following relation:

$$E\left[C_d \mid S_{h,d} = S_d\right] = \sum_{i=1}^{N_d} E\left[C_i \mid S_{h,d} = S_d\right] \tag{8.14}$$

where C_a = repair cost of acceleration-sensitive components on the given storey

C_d = repair cost of drift-sensitive components on the given storey

$S_{h,a}$ = storey-level acceleration at floor h .

S_a = a particular value of $S_{h,a}$; i.e. peak floor acceleration at floor h , to be evaluated at {0, 0.01, 0.02, ...3.00g}

$S_{h,d}$ = storey-level drift ratio at storey h .

S_d = a particular value of $S_{h,d}$; i.e. peak transient drift at storey h , to be evaluated at $\in$ {0, 0.005, 0.010, ...0.20}. Note: the drifts reach 0.20 because wood frame buildings can tolerate drifts in excess of 10% without collapse.

i = an index to the component categories present on the storey.

N_a = number of acceleration-sensitive components categories present on the storey

N_d = number of drift-sensitive components categories present on the storey

The mean vulnerability function per component of category i (in terms of either acceleration or drift) is given by:

$$E\left[C_i \mid S_{h,i} = S_i\right] = N_{i,h} \cdot \sum_{ds=1}^{N_{ds}} P_{i,ds}(s) \cdot m_{i,ds} \tag{8.15}$$

where,

N_{ds} = number of the possible component damage state, ds (see Table 8.4 - Table 8.5).

$N_{i,h}$ = quantity of components of category i on storey h , from Table 8.6 (for structural components) or Table 8.7 (for non-structural components).

$m_{i,ds}$ denotes the mean repair cost per unit of component category i, component damage state ds. It can be calculated from the median unit repair cost $P_{50,i,ds}$ and logarithmic standard deviation of unit repair cost b , as follows:

$$m_{i,ds} = P_{50,i,ds}\, exp\left(0.5 \cdot b^2\right) \tag{8.16}$$

$P_{i,ds}(s)$, which is the expected per-specimen failure probability, is defined as the mean fraction of specimens of type i that are damaged in damage state ds, and given by the following equation:

$$P_{i,ds}(s) = \Phi\left(\frac{\ln\left(S/\theta'_{i,ds}\right)}{\beta'_{i,ds}}\right) - \Phi\left(\frac{\ln\left(S/\theta'_{i,ds+1}\right)}{\beta'_{i,ds+1}}\right) \qquad \mathrm{d} < \mathrm{N_{ds}}$$

$$P_{i,ds}(s) = \Phi\left(\frac{\ln\left(S/\theta'_{i,ds}\right)}{\beta'_{i,ds}}\right) \qquad \mathrm{d} = \mathrm{N_{ds}} \tag{8.17}$$

where,

$$\beta'_{i,ds} = \sqrt{\beta^2_{i,ds} + \beta^2_m} \tag{8.18}$$

$$\theta'_{i,ds} = \theta_{i,ds} \cdot \exp\left(1.28 \cdot \left(\beta'_{i,ds} - \beta_{i,ds}\right)\right) \tag{8.19}$$

In Equation 8.17, S denotes peak floor acceleration in the case of acceleration-sensitive components and peak transient drift in the case of drift-sensitive components; $\theta_{i,ds}$ and $\beta_{i,ds}$ are median and logarithmic standard deviation of the fragility function for component category i, damage state ds, taken from Table 8.2 (for structural components) or Table 8.3 (for non-structural components).

The parameter β_m in Equation 8.18 adds uncertainty associated with approximations in the structural model. In the case of a pushover structural analysis, β_m = 0.3 as in ATC-63 [FEMA P-695 2009], which accounts for the approximation of using a pushover rather than multiple non-linear dynamic analyses. If the analyst employs non-linear dynamic structural analysis, then β_m = 0 as in ATC-58 [FEMA P-58, 2012].

Box 8.3: Derivation of storey-level vulnerability based on component level approach

The storey-level vulnerability functions can be estimated through the following steps:

Step.1. *In addition to the structural components (see Section 4.1), Identify the most dominant non-structural components, in terms of contribution to construction cost (see Section 4.2).*

Step.2 *Conduct inventory to categorize all the structural and dominant non-structural components by storey. Use **Table 8.6** and **Table 8.7**.*

Step.3 *For each structural and non-structural component, assign the fragility functions as shown in Table 8.2 and Table 8.3.*

Step.3. *Estimate the corresponding repair cost input data. For each structural and non-structural component, repair cost should be assigned for different damage state, as shown in Table 8.4 and Table 8.5.*

Step.4. *For the estimation of fragility functions and repair cost, analyst may refer to several sources' e.g. ATC-58 PACT 1.0 (FEMA P-58, 2012).*

S***tep.5.*** *At each storey and for a given damage state, estimate the peak acceleration and peak transient drift (should be obtained from analysis; go to Section 7).*

Step.6. *For each unit of component category i, calculate at storey level:*

- $m_{i,ds}$ *: the mean repair cost at damage state ds. Use Equation 8.16*
- $P_{i,ds}(s)$ *: the mean fraction damaged at damage state ds. Use Equation 8.17*

Step.5. *The mean vulnerability function per component of category i (in terms of either acceleration or drift) can then be calculated using the Equation 8.15:*

$$E[C_i \mid S_{h,i} = S_i] = N_{i,h} \cdot \sum_{ds=1}^{N_{ds}} P_{i,ds}(s) \cdot m_{i,ds}$$

8.2.3.1.2 Building-Level Vulnerability Functions

The expected value of Damage Factor (corresponding to the *Mean Vulnerability Function* for the case of one index building), at each value of intensity measure, im, should be calculated using the following relation, where *RCN* is the Replacement Cost New of the building:

$$DF(im) = P_c(im) + (1 + P_c(im)) \cdot \frac{E[C \mid S = s(im), NC]}{RCN} \qquad (8.20)$$

The implementation of the above expression to generate *Building-Level Vulnerability Functions*, will require the definition of median collapse capacity only from STEP D in Section 6. In the Equation 8.20, $P_c(im)$ is the collapse probability at intensity measure im, defined as:

$$P_c(im) = \Phi\left(\frac{\ln\left(im / \hat{S}_{a,ds_4}(T_1)\right)}{\beta}\right) \tag{8.21}$$

with $\hat{S}_{a,ds_4}(T_1)$ being the median collapse capacity of the building calculated by one of the procedures specified in Section 7.

For non-linear dynamic structural analysis or user-selected analyses that require multiple structural analyses per intensity measure level:

$$E[C \mid S = s(im), NC] =$$

$$= \frac{1}{\left(f_1 \cdot n^*(im)\right)} \cdot \sum_{m=1}^{n^*(im)} \sum_{h=1}^{N} \left(E\left[C_a \mid S_{h,a} = s_{h,a,m}(im)\right] + E\left[C_d \mid S_{h,d} = s_{h,d,m}(im)\right]\right) \quad \text{if} \leq 0.6 \tag{8.22a}$$

$$= 1.0 \qquad \text{otherwise}$$

For simplified structural analysis

$$E[C \mid S = s(im), NC] = \frac{1}{f_1} \cdot \sum_{h=1}^{N} \left(E\left[C_a \mid S_{h,a} = s_{h,a}(im)\right] + E\left[C_d \mid S_{h,d} = s_{h,d}(im)\right]\right) \quad \text{if} \leq 0.6 \tag{8.22b}$$

$$= 1.0 \qquad \text{otherwise}$$

Where, *N* is the number of stories, f_1 is the fraction of total building replacement cost (new) represented by components in the inventory, $n^*(im)$ is the number of ground motion pairs that did not result in collapse at intensity measure level im, $s_{h,a,m}(im)$ is the geometric mean floor acceleration at floor h in ground motion pair m (excluding cases of collapse), and $s_{h,a,m}(im)$ is the peak transient drift ration at storey h in ground motion pair m (excluding cases of collapse). When repair cost exceeds 0.6, the building is commonly considered a total loss, hence the jump to a damage factor of 1.0 when the repair cost exceeds 0.6·*RCN*.

Finally, the Coefficient of Variation (CoV) of loss at each value of im should be calculated using the functions suggested by Porter [2010]:

$$v(im) = \frac{0.25}{\sqrt{DF(im)}} \tag{8.23}$$

Repeating the process of calculation (using Equations 8.20 and 8.23) for a range of values for intensity measure $im \in \{0.01, 0.02, ...3.0g\}$, will result in the vulnerability curve as shown in the example of Figure 8.3 [Porter et al 2014].

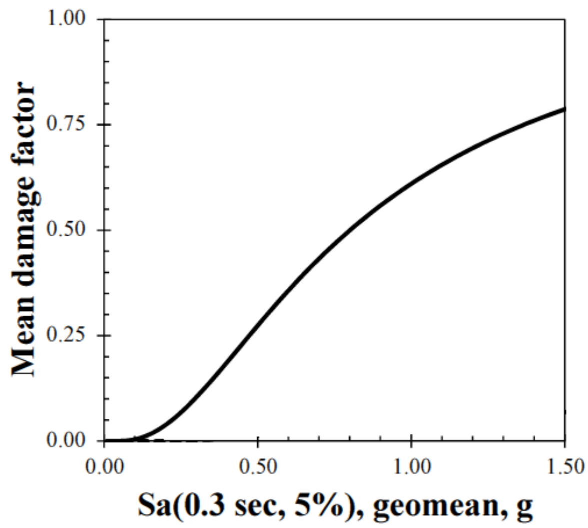

Figure 8.3 Example of derived one index-based building-level vulnerability curve for collapse damage state: case of mid-rise storey RC shear wall office building, in region of 0.17 ≤S_{MS} <0.5g for USA.

8.2.3.2 *Three Index Buildings Based Vulnerability Curve*

The approach offered here will require from the analyst to identify three variants which should be associated to the quality of the buildings as discussed in Section 3.2. For component level assessment, the different quality classes can be defined as followings (see Table 8.8):

- Poor quality, with relatively low design base shear and fragile components;
- Typical quality that should be characterized as a median quality in terms of design base shear and fragile components; and
- Superior quality, with relatively rugged or seismically restrained components and relatively design high base shear.

Table 8.8 Example of configuration of the three index variants, Poor, Typical, and Superior quality, using ATC-58 component types

Three Index Buildings			
Component Description	**Poor**	**Typical**	**Superior**
Exterior Windows	B2022.032	B2022.035	B2022.071
Partitions	C1011.001a	C1011.001c	C1011.001b
Interior Doors	C1021.001	C1021.001	C1021.001
Plumbing Fixtures			
Terminal & Package Units	D3052.011b	D3052.011d	D3052.013k
Lighting & Branch Wiring	C3034.001	C3034.001	C3034.002
RC shear walls	B1044.073	B1044.013	B1044.041
Other attributes			
Sa, g	0.2	0.3	0.4

The analyst should identify other variables, considered as the most dominant in terms of response capacity, to differentiate between these three indexes, which can be different from country to country, and from typology to typology. For instance: number of stories, presence of vertical irregularity, and presence of plan irregularity. The three variant Poor, Typical, and Superior-quality index buildings should represent cases where repair cost would be exceeded respectively by 10%, 50%, and 90% of buildings of similar occupancy.

In this approach, the mean vulnerability function for the considered building class is given by the average of the three variants, as shown in Equation 8.24:

$$DF(im) = \frac{1}{3} \cdot \sum_{j=1}^{3} DF_j(im) \tag{8.24}$$

where, $DF_j(im)$ for each index building (each value of *j*) is given by Equation 8.24.

The Coefficient of Variation (CoV) of loss at each value of im should be calculated using the following relation:

$$v(im) = 1.4 \cdot \frac{\sqrt{\frac{1}{2} \cdot \sum_{j=1}^{3} \left(DF_j(im) - DF(im)\right)^2}}{DF(im)} \tag{8.25}$$

The conditional distribution of loss can be taken as lognormal with mean and coefficient of variation as described above, or as beta with bounds 0 and 1 and the same mean and coefficient of variation. Figure 8.4 shows the resulting three index based vulnerability functions [Porter et al. 2014].

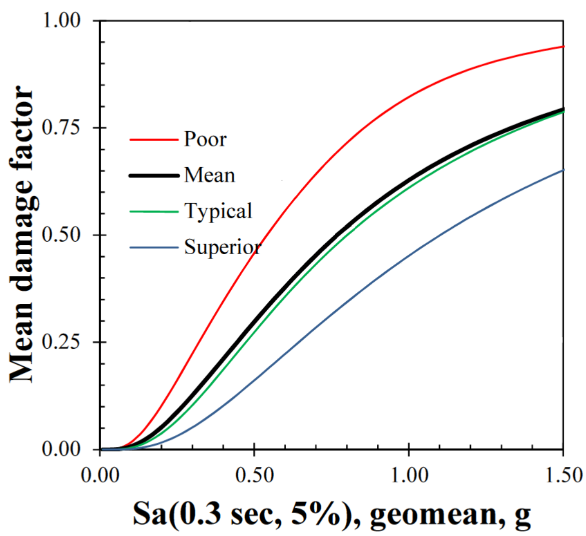

Figure 8.4 Example of derived three index-based seismic vulnerability curve for collapse damage state: case of mid-rise storey RC shear wall office building, in region of 0.17 ≤S_{MS} <0.5g for USA.

8.2.3.3 Multiple Index Buildings Based Vulnerability Curve

This process requires advanced skills to implement Monte Carlo simulation. The analyst will need to identify the key attributes to construct an asset class and quantify the probability distribution. The Mean and Coefficient of Variation of the vulnerability function at excitation im for the asset class can be obtained by the following expressions:

$$DF(im) = \sum_{k=1}^{K} w_k \cdot DF_k(im) \tag{8.26}$$

$$v(im) = \frac{1}{DF(im)} \cdot \sqrt{\sum_{k=1}^{K} w_k \cdot \left(\sigma_k^2(im) + \left(DF_k(im) - DF(im)\right)^2 \right)} \tag{8.27}$$

In Equations 8.26 and 8.27, $DF_k(im)$ and $\sigma_k(im)$ are the mean and standard deviation, respectively, of the vulnerability function at excitation im for index building *k*, defined as follows:

$$DF_k(im) = \frac{1}{N_{sim}} \cdot \sum_{sim=1}^{N_{sim}} DF_{k,sim}(im) \tag{8.28}$$

$$\sigma_k(im) = \sqrt{\frac{1}{(N_{sim}-1)} \cdot \sum_{sim=1}^{N_{sim}} \left(DF_{k,sim}(im) - DF_k(im)\right)^2} \tag{8.29}$$

where:

k = index to index buildings, $k \in \{1,2, ...K\}$;

$DF_k(im)$ = mean damage factor for index building *k* at excitation *im*;

$DF(im)$ = mean damage factor for the asset class at excitation *im*;

$\sigma_k(im)$ = standard deviation of damage factor for index building *k* at excitation *im*;

$v(im)$ = coefficient of variation of damage factor for the asset class at excitation *im*;

N_{sim} = number of simulations of structural response, component damage, and repair cost per index building per level of excitation *m*; It is suggested that N_{sim} should be between 20 and 100 [Porter et al. 2014];

w_k = weight (participation percentage) of index building *k* in the population;

sim = index to Monte Carlo simulations, $sim \in \{1, 2, \ldots N_{sim}\}$

$DF_{k,sim}(im)$ = damage factor for index building *k* in simulation *sim* at excitation *im*;

REFERENCES

Abo El Ezz, A. (2008), Deformation and strength based assessment of seismic failure mechanisms for existing RC frame buildings, *MSc Thesis*, ROSE School, Pavia, Italy.

American Society of Civil Engineers (ASCE) (2007), Seismic Rehabilitation of Existing Buildings, *ASCE/SEI 41-06*, American Society of Civil Engineers, Reston, Virginia.

Applied Technology Council (ATC) (2003), Preliminary Evaluation of Methods for Defining Performance, *ATC-58-2*, Redwood City, CA.

Asteris, P., Antoniou, S., Sophianopoulos, D., and Chrysostomou, C. (2011). Mathematical Macromodeling of Infilled Frames: State of the Art, J. Struct. Eng, 137(12), 1508–1517.

Bal, I.E., Crowley, H. and Pinho, R., (2008), Detail assessment of structural characteristics of Turkish RC buildings stock for loss assessment models, Soil Dynamic and Earthquake Engineering, 28, 914-932.

Bal, I.E., Crowley, H., and Pinho, R., (2010), Displacement-based earthquake loss assessment: Method development and application to Turkish building stock, *ROSE Research Report 2010/02*, IUSS Press, Pavia, Italy.

Baker, J.W., (2007), Probabilistic structural response assessment using vector-valued intensity measures, Earthquake Engineering and Structural Dynamics, 36, 1861-1883.

Baker, J.W, and Cornell C.A., (2008a), Spectral shape, epsilon and record selection, Earthquake Engineering and Structural Dynamics, 35,1077–1095.

Baker, J.W., and Cornell, C.A. (2008b), Uncertainty propagation in probabilistic seismic loss estimation, Structural Safety 30, 236-252.

Baker, J.W. (2014), Efficient analytical fragility function fitting using dynamic structural analysis, Earthquake Spectra, in press, doi: 10.1193/021113EQS025M

Bernardini, A., D'Ayala, D., Modena, C., Speranza, E., and Valluzzi, M.R., (2008), Vulnerability assessment of the historical masonry building typologies of Vittorio Veneto, Special issue of Bollettino di Geofisica Teorica e Applicata Vol.49, n.3-4, 463-484.

Berryman, K., Wallace, L., Hayes, G., Bird, P., Wang, K., Basili, R., Lay, T., Stein, R., Sagiya, T., Rubin, C., Barreintos, S., Kreemer, C., Litchfield, N., Pagani, M., Gledhill, K., Haller, K., and Costa C., (2013), The GEM Faulted Earth Subduction Characterisation Project, Version 1.0, GEM Faulted Earth Project.

Bianchini, M., Diotallevi, P., and Baker, J.W., (2009), Prediction of Inelastic Structural Response Using an Average of Spectral Accelerations, *Proceedings of 10th International Conference on Structural Safety and Reliability (ICOSSAR09)*, Osaka, Japan.

Borzi, B., Crowley, H., and Pinho, R. (2008), Simplified pushover-based earthquake loss assessment (SP-BELA) method for masonry buildings, International Journal of Architectural Heritage; Conservation, Analysis, and Restoration, 2(4), 353-376

Brzev, S, Scawthorn, C., Charleson, A.W., and Jaiswal, K. (2012), GEM basic building taxonomy. Report produced in the context of the GEM Ontology and Taxonomy Global Component project, 45 pp.

Calvi, G.M. (1999), A displacement-based approach for the vulnerability evaluation of classes of buildings. Journal of Earthquake Engineering, 26, 1091–1112.

Canadian Standards Association (CSA) (2004), Design of masonry structures (CSA-S304.1), Ontario, Canada.

Casapulla, C. and D'Ayala, D. F. (2006), In plane collapse behaviour of masonry walls with frictional resistance and openings. In: Structural Analysis of Historical Construction V, 2006-11-01, Delhi.

Ching, J., Porter, K.A., and Beck, J.L. (2009), Propagating uncertainties for loss estimation in performance-based earthquake engineering using moment matching, Structure and Infrastructure Engineering, 5(3), 245-262.

Cho, I.H., and Porter, K.A. (2013), Three techniques for modelling building classes using moment matching, Structural Engineering and Structural Mechanics Program, SESM 13-01, University of Colorado, UCB 428.

Computers & Structures Inc (CSI) (2009), SAP2000, Integrated Software for Structural Analysis & Design, Berkeley, CA.

Cornell C.A, Jalayer F., Hamburger R.O., and Foutch D.A., (2002), Probabilistic Basis for 2000 SAC Federal Emergency Management Agency Steel Moment Frame Guidelines. Journal of Structural Engineering, 128(4), 526–533.

Crowley, H., Pinho, R., and Bommer, J., (2004), A probabilistic displacement-based vulnerability assessment procedure for earthquake loss estimation, Bulletin of Earthquake Engineering, 2, 173–219.

Crowley, H., and Pinho, R. (2004), Period-height relationship for existing European reinforced concrete buildings. Journal of Earthquake Engineering, 893-119.

Crowley, H., and Pinho, R. (2006), Simplified equations for estimating the period of vibration of existing buildings, *Proceedings of the 1st European Conference on Earthquake Engineering and Seismology*, Geneva, Switzerland, Paper No. 1122.

Crowley, H., Borzi, B., Pinho, R., Colombi, M., and Onida, M. (2008), Comparison of two mechanics-based methods for simplified structural analysis in vulnerability assessment, Advances in Civil Engineering, doi:10.1155/2008/438379.

D'Ayala, D. (2005), Force and Displacement Based Vulnerability Assessment for Traditional Buildings; Bulletin of Earthquake Engineering, Vol.3, Springer, pp. 235-265.

D'Ayala, D. (2013), Assessing the seismic vulnerability of masonry buildings, In: Handbook of Seismic Risk analysis and management of civil infrastructure systems , Woodhead publishing, 334-365.

D'Ayala, D., and Kishali, E. (2012), Analytically derived fragility curves for unreinforced masonry buildings in urban contexts, 15th World Conference of Earthquake Engineering, Lisbon, Portugal.

D'Ayala, D., and Meslem, A. (2013a), Guide for selection of existing fragility curves and compilation of the database", GEM Technical Report 2013-X, GEM Foundation.

D'Ayala, D., and Meslem, A. (2013b), Sensitivity of analytical fragility functions to capacity-related parameters", GEM Technical Report 2013-X, GEM Foundation.

D'Ayala, D., and Meslem, A. (2013c), Derivation of analytical vulnerability functions considering modeling uncertainties, *Proceedings of the 11th International Conference on Structural Safety & Reliability*, New York.

D'Ayala, D., and Speranza E. (2003), Definition of collapse mechanisms and seismic vulnerability of historic masonry buildings, Earthquake Spectra, 19, 479-509

D Ayala, D., Kappos, A., Crowley, H., Antoniadis, P., Colombi, M., and Kishali, E. (2012), Providing building vulnerability data and analytical fragility functions for PAGER, *Technical Report*, Earthquake Engineering Research Institute..

Dolsek, M., and Fajfar, P. (2004), Inelastic spectra for infilled reinforced concrete frames, Earthquake Engineering and Structural Dynamics, 33, 1395-1416.

Dolsek, M., and Fajfar, P. (2008), The effect of masonry infills on the seismic response of a four-storey reinforced concrete frame – a deterministic assessment, Engineering Structures, 30, 1991-2001.

Douglas, J., Cotton, F., Abrahamson, N.A., Akkar, S., Boore, D.M., and Di Alessandro, C. (2013), Pre-selection of ground motion prediction equations, Report produced in context of GEM GMPE project.

Efron, B., and Tibshirani, R.J. (1994), An Introduction to the Bootstrap, Chapman and Hall/CRC, 456 pages.

Ellingwood, B.R., and Kinali, K. (2009), Quantifying and communicating uncertainty in seismic risk assessment. Structural Safety 31, 179–187, doi:10.1016/j.strusafe.2008.06.001.

Ellul, F.L., and D'Ayala, D. (2012), Realistic FE models to enable push-over nonlinear analysis of masonry infilled frames, The Open Construction and Building Technology Journal, 6, 213-235.

Erberik, M.A. (2008), Generation of fragility curves for Turkish masonry buildings considering in-plane failure modes, Earthquake Engineering and Structural Dynamics, 37, 387-405

Erdik, M., Aydinoglu, N., Fahjan, Y., Sesetyan, K., Demircioglu, M., Siyahi, B., Durukal, E., Ozbey, C., Biro, Y., Akman, H., and Yuzugullu, O. (2003), Earthquake Risk Assessment for Istanbul Metropolitan Area, Earthquake Engineering and Engineering Vibration, 2(,1), 1-25.

European Committee for Standardization (CEN) (2004), Design of structures for earthquake resistance, Part 1: General rules, seismic actions and rules for buildings, Eurocode-8, ENV 1998-1-1, Brussels, Belgium.

European Committee for Standardization (CEN) (2005), Design of structures for earthquake resistance, Part 3: Strengthening and repair of buildings, Eurocode 8, EN 1998-3, Brussels, Belgium.

Fajfar, P. (2002), Structural analysis in earthquake engineering- a breakthrough of simplified nonlinear methods, *Proceedings of the 12th European Conference on Earthquake Engineering*, London, paper 843.

Federal Emergency Management Agency (FEMA P-58) (2012), Seismic Performance Assessment of Buildings, ATC-58, Applied Technology Council, Washington, D.C.

Federal Emergency Management Agency (FEMA P-695) (2009), Quantification of Building Seismic Performance Factors, ATC-63, Applied Technology Council, Redwood City, CA.

Federal Emergency Management Agency (FEMA-440) (2005), Improvement of Nonlinear Static Seismic Analysis Procedures, ATC-55, Applied Technology Council, Washington, D.C.

Federal Emergency Management Agency (FEMA-445) (2006), Next-Generation Performance-Based Seismic Design Guidelines: Program Plan for New and Existing Buildings. Applied Technology Council, Washington, D.C.

Federal Emergency Management Agency – National Institute of Building Sciences (FEMA-NIBS) (2003), Multi-hazard loss estimation methodology – earthquake model: HAZUS-MH Advanced engineering building module - Technical and user's manual, Washington, DC.

Federal Emergency Management Agency (FEMA) (1999), HAZUS 99 - Technical and user's manual, Washington, DC.

Federal Emergency Management Agency (FEMA) (2003), HAZUS-MH - Multi-hazard loss estimation methodology, Technical and user's manual, Washington, DC.

Galasco, A., Lagomarsino, S., Penna, A., and Resemini, S. (2004), Non-Linear Seismic Analysis of Masonry Structures, *Proceedings of the 13th World Conference on Earthquake Engineering*, Vancouver, Canada.

Galasco, A., Lagomarsino, S., Penna, A. and Cattari, S. (2009), TREMURI program: Seismic Analyses of 3D Masonry Buildings, University of Genoa.

Gehl, P., Douglas, J., Rossetto, T., Macabuag, J., Nassirpour, A., Minas, S., and Duffour, P. (2014). Investigating the use of record-to-record variability in static capacity approaches. *Proceedings of the Second International Conference on Vulnerability and Risk Analysis and Management (ICVRAM2014) & Sixth International Symposium on Uncertainty Modelling and Analysis (ISUMA2014)*, Liverpool, UK.

Glaister, S., and Pinho, R. (2003), Development of a simplified deformation based method for seismic vulnerability assessment, Journal of Earthquake Engineering, 7, 107–140.

Huyck, C., Esquivias, G., Gamba, P., Hussain, M., Odhiambo, O., Jaiswal, K., Chen, B., Becker, M., and Yetman, G. (2011), Survey of available input databases for Global Exposure Database, GED4GEM, Global Earthquake Model.

Jaiswal, K., and Wald, D.J. (2008), Creating a Global Building Inventory for Earthquake Loss Assessment and Risk Management, *USGS Open File Report*, OF 2008-1160 , 103 pp., http://pubs.usgs.gov/of/2008/1160/.

Jaiswal, K.S., Wald, D.J., Perkins, D., Aspinall, W.P., and Kiremidjian, A.S. (2013), Estimating structural collapse fragility of generic building typologies using expert judgement, *Proceedings of 11th International Conference on Structural Safety & Reliability*, New York, USA.

Jalayer, F. and Cornell, C.A. (2009), Alternative non-linear demand estimation methods for probability-based seismic assessments, Earthquake Engineering and Structural Dynamics, 38, 951–972.

Lagomarsino, S., and Giovinazzi, S. (2006), Macroseismic and Mechanical Models for the Vulnerability and Damage Assessment of Current Buildings, Bulletin of Earthquake Engineering, 4(4).

Lagomarsino, S., Penna, A., Galasco, A., and Cattari, S. (2013), TREMURI program: An equivalent frame model for the nonlinear seismic analysis of masonry buildings, Engineering Structures, 56, 1787-1799.

Lang, K., and Bachmann, H. (2004), On the seismic vulnerability of existing buildings: a case study of the city of Basel, Earthquake Spectra, 20(1), 43–66.

Lee, T.H., and Mosalam, K.M. (2005), Seismic demand sensitivity of reinforced concrete shear-wall building using FOSM method, Earthquake Engineering and Structural Dynamics, 34, 1719-1736.

Luco, N., and Cornell, C.A. (2007), Structure-Specific Scalar Intensity Measures for Near-Source and Ordinary Earthquake Ground Motions, Earthquake Spectra, 23(2), 357–392.

Luco N., and Bazzurro, P. (2007), Does amplitude scaling of ground motion records result in biased nonlinear structural drift responses? Earthquake Engineering and Structural Dynamics, 36, 1813–1835.

Luco, N., Mori, Y., Funahashi, Y., Cornell, C.A., and Nakashima, M. (2003), Evaluation of predictors of non-linear seismic demands using 'fishbone'models of SMRF buildings, Earthquake Engineering and Structural Dynamics, 32(14), 2267–2288.

Mainstone, R. J., and Weeks, G. A. (1970), The influence of bounding frame on the racking stiffness and strength of brick walls, *Proceedings of the 2nd International Brick Masonry Conference*, Stoke-on-Trent, UK.

Masonry Standards Joint Committee (MSJC) (2010), Building Code Requirements for Masonry Structures, Commentary Working Draft, Building Code Requirements for Masonry Structures.

Meslem, A., and D'Ayala, D. (2012), Toward Worldwide Guidelines for the Development of Analytical Vulnerability Functions and Fragility Curves at Regional Level", *Proceedings of the 15th World Conference on Earthquake Engineering*, Lisbon, Portugal.

Meslem, A., and D'Ayala, D. (2013), Investigation into analytical vulnerability curves derivation aspects considering modelling uncertainty for infilled buildings, *Proceedings of the 4th International Conference on Computational Methods in Structural Dynamics and Earthquake Engineering (COMPDYN'13)*, Kos Island, Greece.

Nakashima, M., Ogawa, K., and Inoue, K. (2002), Generic frame model for simulation of earthquake responses of steel moment frames, Earthquake Engineering and Structural Dynamics, 31(3), 671– 692.

National Institute of Standards and Technology (NIST) (1999), UNIFORMAT II Elemental Classification for Building Specifications, Cost Estimating, and Cost Analysis, *NISTIR 6389*, Washington, D.C.

National Institute of Standards and Technology (NIST) (2011), Selecting and Scaling Earthquake Ground Motions for Performing Response-History Analyses, Prepared for the US National Institute of Standards and Technology by the NEHRP Consultants Joint Venture, Gaithersburg, Maryland.

National Earthquake Hazards Reduction Program (NEHRP) (2010), Nonlinear structural Analysis for seismic design: A guide for practicing engineers (NIST GCR 10-917-5), *NEHRP Seismic Design Technical Brief No. 4*, National Institute of Standards and Technology.

New Zealand Society for Earthquake Engineering (NZSEE) (2006), Assessment and Improvement of the Structural Performance of Buildings in Earthquakes. New Zealand.

Newmark, N.M. (1959), A method of computation for structural dynamics. Journal of the Engineering Mechanics Division, ASCE, 85, EM3, 67-94.

Paulay, T., and Priestley, M.J.N. (1992), Seismic Design of Reinforced Concrete and Masonry Buildings, John Wiley and Sons, Inc., New York.

Pinho, R., Bommer, J.J., and Glaister, S. (2002), A simplified approach to displacement-based earthquake loss estimation analysis. *Proceedings of the 12th European Conference on Earthquake Engineering*, London, UK, Paper N. 738.

Priestley, M.J.N., Calvi, G.M., and Kowalsky, M.J. (2007). *Displacement-based Seismic Design of Structures*, IUSS Press, Pavia, Italy.

Porter, K.A., Farokhnia, K., Cho, I.H., Rossetto, T., Ioannou, I., Grant, D., Jaiswal, K., Wald, D., D'Ayala, D., Meslem, A., So, E., Kiremidjian, A.S. and Noh, H. (2012a), Global Vulnerability Estimation Methods for the Global Earthquake Model, *Proceedings of the 15th World Conference on Earthquake Engineering*, Lisbon.

Porter, K.A., Farokhnia, K., and Cho, I. (2012b), Nonstructural seismic vulnerability estimation guidelines, Global Vulnerability Consortium.

Porter, K.A., Farokhnia, K., and Cho, I. (2012c), Contents seismic vulnerability estimation guidelines, Global Vulnerability Consortium.

Porter, K.A., G. Johnson, R. Sheppard, and R. Bachman (2010), Fragility of mechanical, electrical, and plumbing equipment. Earthquake Spectra, 26(2), 451-472.

Porter, K., Farokhnia, K., Vamvatsikos, D., and Cho, I., (2014), Analytical Derivation of Seismic Vulnerability Functions for Highrise Buildings, Global Vulnerability Consortium, GEM Foundation.

Porter, K.A., R.P. Kennedy, and R.E Bachman (2007), Creating fragility functions for performance-based earthquake engineering, Earthquake Spectra, 23(2), 471-489,

Porter, K.A. (2010), Cracking an open safe: uncertainty in HAZUS-based seismic vulnerability functions, Earthquake Spectra, 26(3), 893-900.

Porter, K., Hu, Z., Huyck, C., and Bevington, J. (2014), User guide: Field sampling strategies for estimating building inventories, *GEM Technical Report 2014-02 V1.0.0*, 42 pp., GEM Foundation, Pavia, Italy.

Rezaeian, S., Bozorgnia, Y., Idriss, I. M., Campbell, K., Abrahamson, N., and Silva, W. (2012), Spectral Damping Scaling Factors for Shallow Crustal Earthquakes in Active Tectonic Regions, *PEER Report No 2012/01*, Pacific Earthquake Engineering Research Center, California, USA.

Roca P., Molins C., and Marí A.R. (2005) Strength capacity of masonry wall structures by the equivalent frame method, Journal of Structural Engineering, 131(10), 1601-1610

Rossetto, T. (2004), Vulnerability Curves for the Seismic Assessment of Reinforced Concrete Structure Populations, *PhD Thesis*, Imperial College London. April 2004. pp.330.

Rossetto, T. (2014), The Conversion of Damage to Loss in GEM VEM Indirect Vulnerability Curve Derivation, GEM Technical Report 2013-X, GEM Foundation.

Rossetto, T., and Elnashai, A. (2005), A new analytical procedure for the derivation of displacement-based vulnerability curves for populations of RC structures, Engineering Structures, 27, 397-409.

Rossetto, T., Ioannou, I., Grant, D. N., and Maqsood, T. (2014). Guidelines for Empirical Vulnerability Assessment, Global Vulnerability Consortium.

R S Means Engineering (2009), RSMeans Building Construction Cost Data, R. S. Means Company, Incorporated, pp. 869.

SYNER-G (2011), Fragility functions for common RC building types in Europe, *Deliverable 3.1,*. Available from URL: http://www.vce.at/SYNER-G/.

Ruiz-Garcia, J., and Miranda, E. (2005), Performance-based assessment of existing structures accounting for residual displacements, The John A. Blume earthquake Engineering Center, *Report No. 153*, Stanford University.

Ruiz-Garcia, J., and Miranda, E. (2007), Probabilistic estimation of maximum inelastic displacement demands for performance-based design, Earthquake Engineering and Structural Dynamics, 36, 1235-1254.

Shome, N., and Cornell, C.A. (1999), Probabilistic seismic demand analysis of nonlinear structures, *Tech. Rep. RMS–35*, RMS Program, Stanford University, CA.

Silva, V., Crowley, H., Pinho, R., and Varum, H. (2013), Extending displacement-based earthquake loss assessment (DBELA) for the computation of fragility curves, Engineering Structures, 56, 343-356.

Tomazevic, M. (2007), Damage as a measure for earthquake-resistant design of masonry structures: Slovenian experience, Canadian Journal of Civil Engineering, 34(11), 1403-1412.

Turnsek, V., and Cacovic, F. (1970), Some experimental results on the strength of brick masonry walls, *Proceedings of the 2nd international brick masonry conference*, Stoke on Trent, United Kingdom, 149-156.

Vamvatsikos D., and Cornell C.A. (2005), Developing efficient scalar and vector intensity measures for IDA capacity estimation by incorporating elastic spectral shape information, Earthquake Engineering and Structural Dynamics, 34(13), 1573–1600.

Vamvatsikos, D., and Cornell, C.A. (2006), Direct estimation of the seismic demand and capacity of oscillators with multi-linear static pushovers through IDA, Earthquake Engineering and Structural Dynamics, 35(9), 1097-1117.

Vamvatsikos, D., and Fragiadakis, M. (2010), Incremental dynamic analysis for estimating seismic performance sensitivity and uncertainty, Earthquake Engineering and Structural Dynamics, 39, 141-163.

Vamvatsikos, D., and Kazantzi, A.K (2015), Developing analytical vulnerability curves for Western US low-rise steel frame buildings, *Technical Report*, Global Vulnerability Consortium, GEM Foundation.

Wasserman L. (2004), All of statistics: a concise course on statistical inference. New York, USA: Springer.

Wen Y.K, Ellingwood B.R, and Bracci J. (2004), Vulnerability Function Framework for Consequence-based Engineering, MAE Center Project DS-4 Report.

APPENDIX A Derivation of Capacity Curves

A.1 Perform Pushover Analysis

The pushover analysis of a structure is a static nonlinear analysis under permanent vertical loads and gradually increasing lateral loads (incremental loads) up to failure. The equivalent static lateral loads approximately represent earthquake-induced forces. A plot of the total base shear versus top displacement in a structure is obtained by this analysis allowing the determination of collapse load and ductility capacity (see Figure A.1).

To implement a pushover analysis, the analyst will need to develop an appropriate mathematical model and define the following parameters:

- Define structural model: 3D or a simplified 2D model; identify your primary and secondary elements or components; define your non-structural elements; foundation flexibility; and P-Delta effects. Procedures for performing a structural model are provided in Section 5.
- Define loads:
  - Gravity: This is permanent gravity actions, i.e. dead load, live load;
  - Lateral load pattern (vertical distribution): incremental loads consist of horizontal forces at each storey level.
- Select increment control: different strategies may be employed: load control (force control), response control.

For further details regarding the procedure to perform non-linear static analysis, analyst may refer to ASCE/SEI 41-06 (ASCE 2007).

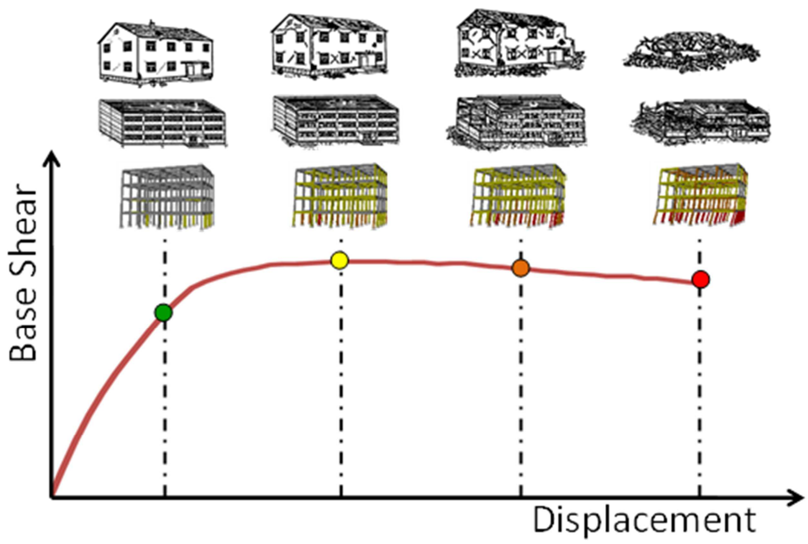

Figure A.1. Plot of pushover curve and evaluation of different damage thresholds

Box A.1: Perform pushover analysis

The pushover analysis can be performed as follows:

***Step 1**: Develop an appropriate mathematical model of the building for non-linear static analysis. Refer to Section 5, and you may also refer to ASCE/SEI 41-06.*

***Step 2:** Select and determine the horizontal force pattern to be applied for each storey mass;*

***Step 3**: Selection of control node: Roof node shall be selected as the control node;*

***Step 4**: Selection of deformation level (target displacement): as ATC-40 (ATC 1996) requires, the capacity curve shall be determined up to 4% of total height of the building; as Eurocode-8 (CEN 2005), the capacity curve shall be determined up to Up to 150% of the control node displacement that corresponds to the limit-state of interest;*

***Step 5**: Gravity loading is applied (with no lateral loads).*

***Step 6**: At constant vertical load, gradually increase one-parameter lateral loads up to the attainment of the target displacement.*

***Step 7**: Make sure that the analysis is extended to a deformation such that collapse is judged to occur.*

The output of this analysis is the capacity curve (force-displacement relationship) of MDoF system with the estimated damage states.

A.2 Derivation of Equivalent SDoF-Based Capacity Curves

For some non-linear static-based procedures suggested in the guidelines, the analyst should, firstly, derive the equivalent SDoF-based capacity curves of the MdoF-based curve obtained from pushover analysis (see Figure A.2), in order to conduct vulnerability assessment. The transformation of the Force-Displacement (Base shear-Top Drift) curve to ADRS space is done using the modal participation factors and effective modal weight ratios, determined from the fundamental mode of the structure.

The different steps for the derivation of equivalent SDoF-based capacity curve are provided in Box A.2.

Box A.2: Equivalent SDoF-based capacity curve

The equivalent SDoF-based capacity curve is obtained through the following steps:

***Step 1**: Run Eigenvalue analysis and extract the fundamental mode shapes,* ϕ *, of MDoF system.*

***Step 2**: Obtain the Base Shear – Displacement relationship (capacity curve) as result of non-linear static (pushover) analysis of MDoF system. See Section A.1.*

***Step 3**: Derive the equivalent SDoF-based capacity curve (Figure A.2) by dividing the base shear and displacement of the MDoF-based capacity curve with a Transformation Factor.*

The mass of an equivalent SDoF system m^* is determined as:

$$m^* = \sum m_i \cdot \phi_i, \quad \text{where } i = 1,2,\ldots n \text{ denotes roof level} \tag{A.1}$$

The transformation to an equivalent SDOF model is made by dividing the base shear, F_b, and top displacement, d_n, of the MDOF model with a transformation factor Γ:

$$F^* = \frac{F_b}{\Gamma} \qquad d^* = \frac{d_n}{\Gamma} \tag{A.2}$$

where F^* and d^* are, respectively, the base shear force and the displacement of the SDoF system. The transformation factor is given by:

$$\Gamma = \frac{\phi^T \cdot \mathrm{M} \cdot 1}{\phi^T \cdot \mathrm{M} \cdot \phi} = \frac{\mathrm{m}^*}{\sum m_\mathrm{i} \cdot \phi_\mathrm{i}^2} \tag{A.3}$$

Note that:

- For the calculation of an equivalent mass m^* and the constant Γ, the assumed displacement shape ϕ is normalized – the value at the top is equal to 1. Usually a triangular shape for the first mode is assumed, however any reasonable shape can also be used for ϕ .
- For the transformation from MDoF to SDoF system, both force and displacement must be divided by the same constant Γ, so that the initial stiffness of the equivalent SDoF system remains the same as that defined by the base shear – displacement diagram of the MDoF system.

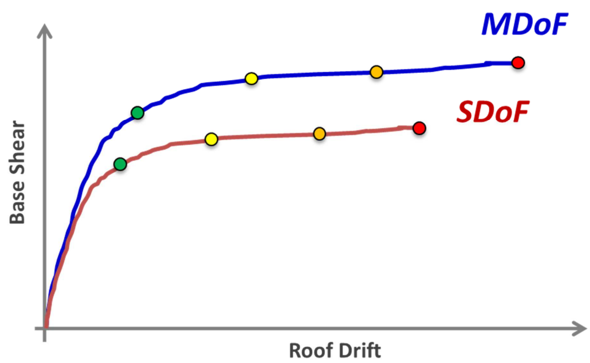

Figure A.2. Example of transformation of MDoF-based pushover curve to an equivalent SDoF.

A.3 Fitting the Capacity into Idealised Representation

The implementation of some non-linear static-based procedures requires the determination of an approximate idealized form for the derived capacity curve of the equivalent SDoF system.

To derive the idealized capacity diagram of the SDoF system the equal energy principle is used, by which the idealised curved is determined by imposing that the areas under the actual curve of SDoF and the idealized curve are equal. Two forms of idealization are provided (see Figure A.3):

- Multilinear elasto-plastic form, which may be used, for instance, in the case of capacity curve derived from infilled frames structures. The use of multilinear elasto-plastic form requires providing the following segments (Figure A.3a):
    - from the ordinate to point 1: defined as the elastic segment, where point 1 is defined as the yield point;
    - from point 1 to point 2: termed the hardening segment, where point 2 is defined as the point of peak strength or initial degradation point;
    - from point 2 to point 3: termed the softening segment, where point 3 represents the onset of residual strength response (e.g. complete failure of the infill for infilled frames);
    - from point 3 to point 4: represents the residual strength plateau, where point 4 represents the ultimate deformation at collapse.
- Simple bilinear elasto-perfectly plastic form, which may be used, for instance, in the case of capacity curve derived from bare frames structures, masonry buildings. The use of bilinear elasto-plastic form requires providing the following segments (Figure A.3b):
    - from the ordinate to point 1: defined as the elastic segment, where point 1 is defined as the yield point;
    - from point 1 to point2: the hardening and softening plateau up to the residual strength, where point 2 represents the ultimate deformation at collapse.

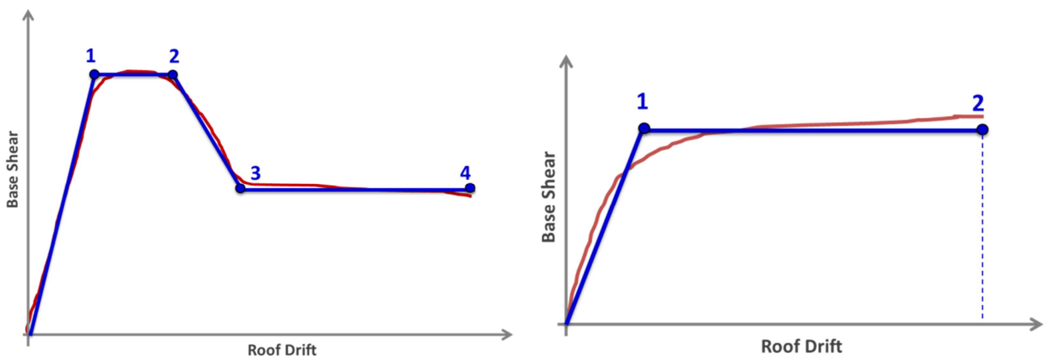

Figure A.3. Idealization of capacity curves. (a) Multilinear elasto- plastic form; (b) Bilinear elasto-perfectly plastic form.

The subsections below present some examples for the calculation of these different segments and points characterizing an idealized capacity curve. Note that these examples are one possibility, and the analyst may perform any other procedure through which the different segments and points are accurately defined.

Indeed, at the level of yielding point, the choice of the yield displacement (D_y) and yield force (F_y) might have a significant influence. The period of the idealized equivalent SDoF system, T^*, is determined by:

$$T^* = 2\pi \cdot \sqrt{\frac{m^* \cdot D_y}{F_y}} \quad \text{(A.4)}$$

A.3.1 Multilinear Elasto-Perfectly Plastic Form

Infilled frames are typically characterized by substantial strength degradation after the infill fails. To take into account this feature, the capacity curve has to be idealized as a multi-linear force-displacement relation rather than a simple bilinear elasto-plastic one. The idealization of pushover curve can be performed as follows (see Figure A.4):

- Definition of point (D_{max}, F_{max}) corresponding to the maximum strength of the structure;
- Definition of point (D_{max}, F_{min}) corresponding to the minimum strength of the structure; this point is related to the complete failure of the infill in one or more stories. After that, only the frame resists the horizontal loading;
- Once the above characteristic points of the idealized pushover curve are defined, the yield point (D_y^*, F_y^*) is determined by assuming the yield force F_y^* of the idealized system to be equal to the maximum strength of the structure F^*_{max}; Displacement at yield D_y^* is determined by applying the equal energy rule (i.e., the area under the pushover curve and idealized curve are equal) for the interval from 0 to D^*_{max};
- Determination of the displacement at the start of the degradation D^*_s by applying the equal energy rule for the interval from D^*_{max} to D^*_{min}.

$$D_y = 2 \cdot \left(D_{max} - \frac{E_{D_{max}}}{F_{max}} \right) \tag{A.5}$$

$$D_s = \frac{2}{F^*_{max} - F^*_{min}} \left(E^*_{D^*_{Fmin}} - \left(\left(D^*_{min} - D^*_{max} \right) \cdot F^*_{max} \right) + \left(\frac{1}{2} \left(F^*_{max} - F^*_{min} \right) \cdot D^*_{min} \right) \right) \tag{A.6}$$

where:

$E_{D_{max}}$ = is the area under the pushover curve in the intervals from 0 to D_{max}.

E_{D_u} = is the area under the pushover curve in the intervals from 0 to D_u .

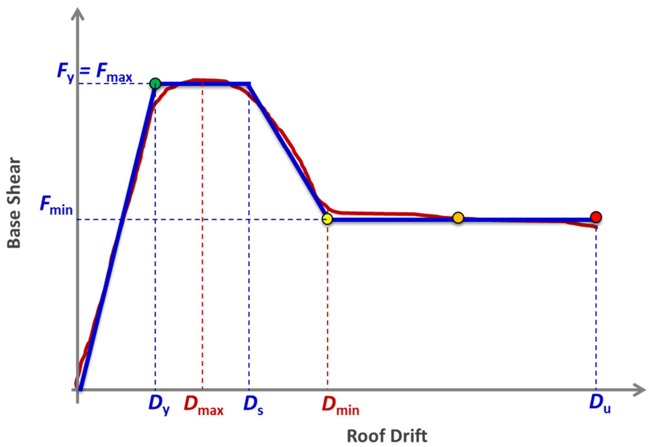

Figure A.4. Idealization of capacity curve using multilinear elasto-plastic form.

A.3.2 Bilinear Elasto-Perfectly Plastic Form

For bilinear elasto-perfectly plastic form, the idealization of capacity curve can be performed as follows (
Figure A.5):

- Define the yield force of the idealized SDoF system F_y, so that it will coincide with the maximum capacity load of the equivalent SDoF system;
- Define the maximum (ultimate) displacement of the idealized SDoF system D_u , which coincide with the formation of plastic mechanism or collapse for global level of the equivalent SDoF system.
- The yield displacement of the idealized system D_y , to be computed from the known F_y and D_u , using the following relation:

$$D_y = 2\left(D_u - \frac{E_{area}}{F_y} \right) \quad \text{(A.7)}$$

where E_{area} is the actual deformation energy up to the formation of the plastic mechanism (i.e. the area under the pushover curve in the interval from 0 to D_u).

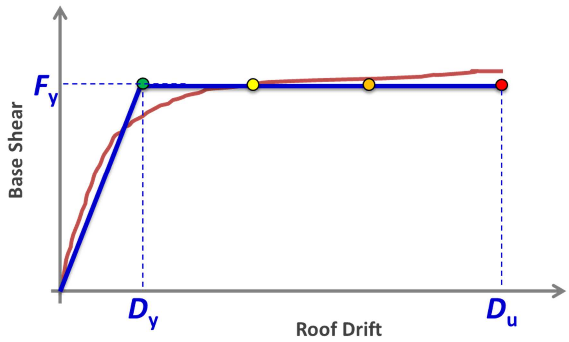

Figure A.5. Idealization of capacity curve using bilinear elasto-perfectly plastic form.

A.4 Acceleration-Displacement Response Spectra (ADRS) Format

The Force-Displacement relationship can be transformed to Acceleration-Displacement Response Spectra (ADRS) format by simply dividing the forces in the diagram by the equivalent mass m*:

$$S_a = \frac{F}{m^*} \quad \text{(A.8)}$$

NOTE:

In the case of adaptive pushover analysis (APO), the transformation must include the combined effect of multiple response modes. A single transformation cannot be applied to the adaptive pushover curve as the relative contribution of each mode changes with each applied load increment. Hence, an approximate method for the transformation is used, where the instantaneous displaced shape and storey forces at each increment step of the APO, are used to transform the force displacement curves into ADRS space (for further details see Rossetto, 2004 Chapter 7, Figure 7.11).

APPENDIX B Average Values of Dispersions for Response Analysis, FEMA P-58

Table B. 1. Default dispersions for record-to-record variability and modelling uncertainty (Table 5-6, Volume 1, FEMA P-58, 2012)

T_1 (sec)	$S = \frac{S_a(T_1) \cdot W}{V_{y1}}$	$\beta_{a\Delta}$	β_m
0.2	≤ 1.0	0.05	0.25
	2	0.35	0.25
	4	0.40	0.35
	6	0.45	0.50
	≥ 8	0.45	0.50
0.35	≤ 1.0	0.10	0.25
	2	0.35	0.25
	4	0.40	0.35
	6	0.45	0.50
	≥ 8	0.45	0.50
0.5	≤ 1.0	0.10	0.25
	2	0.35	0.25
	4	0.40	0.35
	6	0.45	0.50
	≥ 8	0.45	0.50
0.75	≤ 1.0	0.10	0.25
	2	0.35	0.25
	4	0.40	0.35
	6	0.45	0.50
	≥ 8	0.45	0.50
1.0	≤ 1.0	0.15	0.25
	2	0.35	0.25
	4	0.40	0.35
	6	0.45	0.50
	≥ 8	0.45	0.50
1.50	≤ 1.0	0.15	0.25
	2	0.35	0.25
	4	0.40	0.35
	6	0.45	0.50
	≥ 8	0.45	0.50
2.0	≤ 1.0	0.25	0.25
	2	0.35	0.25
	4	0.40	0.35
	6	0.45	0.50
	≥ 8	0.45	0.50

$\beta_{a\Delta}$ dispersion for record-to-record variability; β_m dispersion for modelling uncertainty; T_1 is the fundamental period of the building in the direction under consideration, S is a strength ratio, V_{y1} is the estimated yield strength of the building in first mode response; and W is the total weight.

APPENDIX C Compendium of Existing Building-Level Damage Factor (DF) Values

C.1 Damage Factors Function of Building Typology (GEM Damage-to-Loss Report – Rossetto, 2011)

C.1.1 General Damage Factor Values

Damage Scale	HAZUS (1999)				Comments
Reference/Damage State	**Slight**	**Moderate**	**Extensive**	**Complete**	
HAZUS99 (1999)	2%	10%	50%	100%	**Country:** USA **DF Definition:** Repair / Replacement Cost. Structural and non-structural damage included **Comment:** Defined independently of structure type, but taking into account occupancy and use (in HAZUS-MR4). Derived using empirical and judgement-based methods. Despite more complex method, HAZUS-MR4 total DFs for residential structures do not vary much from HAZUS99 ones (only variation observed in the "Moderate" damage state.
HAZUS-MR4 (2003) – Single family dwelling (RES1)					
Structural DF	0.5%	2.3%	11.7%	23.4%	
Acceleration sensitive non-structural DF	0.5%	2.7%	8.0%	26.6%	
Drift sensitive non-structural DF	1.0%	5.0%	25.0%	50.0%	
Total DF	2%	10%	44.7%	100%	
HAZUS-MR4 (2003) – Multiple family dwelling (RES3a-f)					
Structural DF	0.3%	1.4%	6.9%	13.8%	
Acceleration sensitive non-structural DF	0.8%	4.3%	13.1%	43.7%	
Drift sensitive non-structural DF	0.9%	4.3%	21.3%	42.5%	
Total	2%	10%	41.3%	100%	

Roca (2004), Mouroux et al. (2004) and Vacareanu et al. (2004)	2%	10%	50%	100%	**Country:** Spain, France and General European **DF Definition:** Repair / Repalcement cost **Comment:** Part of RISK-UE project. DFs mainly based on expert judgement and national "experience" with no stated method. Values are identical to HAZUS99.

Damage Scale	MSK						Comments
Reference/Damage State	DS0	DS1	DS2	DS3	DS4	DS5	
Chavez (1998)	0%	5%	20%	50%	80%	100%	**Country:** Spain **DF Definition:** Repair cost / Replacement Cost. Non-structural damage is assumed to be included. **Comment:** Based on judgement as a "rough average of different equivalences obtained in different countries ".
Timchenko (2002)	0%	2%	10%	30%	80%	100%	**Country:** Georgia and Russia **DF Definition:** Repair cost / Replacement Cost. Non-structural damage is assumed to be included. **Comment:** Unclear methodology of derivation. Assumed to have been derived from judgement. No distinction made between structure types.
Masi et al. (2002) – parameter "q" of Beta pdf	0.015	0.604	5.587	4.942	9.224	11.585	**Country:** Italy **DF Definition:** Repair cost / Replacement Cost. Non-structural damage is assumed to be included. **Comment:** Based on data form 50,000 buildings damaged during the 1997 Umbria-Marche and the 1998 Pollino earthquakes in Italy. Although originally derived for different building classes, unable to obtain original report. Damage factors presented as beta-distributions for each damage state.
Masi et al. (2002) -) – parameter "r" of Beta pdf	3.046	16.662	32.946	11.262	2.306	0.61	

x

Damage Scale	EMS 98						Comments
Reference/Damage State	DS0	DS1	DS2	DS3	DS4	DS5	
Fah et al. (2001) Central DFs	0%	<5%	20%	55%	90%	100%	**Country:** Switzerland **DF Definition:** Repair cost / Replacement Cost. Non-structural damage is assumed to be included. **Comment:** Values from ATC-13 applied to the EMS 98 damage scale through interpretation by the authors, though no method in particular is mentioned. No consideration of different structure types or occupancy classes in DF estimates.
Milutinovic and Trendafiloski (2003)	0%	1%	10%	35%	75%	100%	**Country:** Italy **DF Definition:** Repair / Replacement cost **Comment:** Part of RISK-UE project. Study carried out by Universita' degli Studi di Genova and reported in Milutinovic and Trendafiloski (2003). DFs mainly based on expert judgement and national "experience" with no stated method.
Kostov et al. (2004)	0%	1%	10%	40%	80%	100%	**Country:** Bulgaria **DF Definition:** Repair / Replacement cost **Comment:** Part of RISK-UE project. Study carried out by the Bulgarian Academy of Sciences. DFs mainly based on expert judgement and national "experience" with no stated method.
Di Pasquale et al. (2005)	0%	1%	10%	35%	75%	100%	**Country:** Italy **DF Definition:** Repair cost / Replacement Cost. Non-structural damage is assumed to be included. **Comment:** Values from judgment based on ATC-13 and the National Seismic Survey (Di Pasquale and Goretti, 2001) applied to the EMS 98 damage. Exact method of derivation is not mentioned. No consideration of different structure types or occupancy classes in DF estimates.

Reference/Damage State	Green-Tag	Yellow-Tag	Red-Tag	Comments
Kappos et al. (2007)	9.8%	25.6%	100%	**Country:** Greece **DF Definition:** Repair cost / Pre-earthquake market value. Non-structural damage is assumed to be included. **Comment:** Based on results of post-earthquake surveys carried out after the 1999 Athens earthquake. A "representative" sample of 150 building blocks, or 983 buildings, corresponding to 10% of the total building population were surveyed (Kappos et al, 2007).

C.1.2 Damage Factor Values for Reinforced Concrete Frames with Masonry Infills

Damage Scale	EMS98						Comments
Reference	D0	D1	D2	D3	D4	D5	
Milutinovic and Trendafiloski (2003)	0%	<15%	15-25%	25-35%	35-45%	>45%	**Country:** Macedonia **DF Definition:** Repair / Replacement cost. Non-structural damage assumed to be included. **Comment:** Part of RISK-UE project. Study carried out by the University Ss. Cyril and Methodius and reported in Milutinovic and Trendafiloski (2003). DFs mainly based on expert judgement and national "experience" with no stated method. Values are significantly different from other studies, especially in the DS5 category.

Goretti and Di Pasquale (2004) – RC – Mean DF value	1.5%	3.4%	14.4%	20.6%	100%	100%	**Country:** Italy **DF Definition:** Repair cost / Replacement Cost. Non-structural damage is assumed to be included. **Comment:** Based on data on 23,000 buildings affected by the 2002 Molise earthquake. Derived for different structure types classified by building material and EMS98 vulnerability class. Some concern over the presence of non-zero values for the DS0 damage state
Goretti and Di Pasquale (2004) – RC – Standard Deviation DF value	2.6%	3.6%	7.2%	8.9%	0%	0%	
Dolce et al. (2006)- RC Vul. Cl. A	0%	0-10%	10-30%	30-60%	60-100%	100%	**Country:** Greece **DF Definition:** Repair cost / Replacement Cost. Non-structural damage is assumed to be included. **Comment:** Based on Greek experience as described by Penelis et al. (2002) and Kappos et al. (2006).
Dolce et al. (2006)- RC Vul. Cl. B	0%	0-1%	1-30%	30-60%	60-100%	100%	
Kappos et al. (2006, 2008) – RC - range DFs	0%	0-1%	1-10%	10-30%	30-60%	60-100%	**Country:** Greece **DF Definition:** Repair cost / Replacement Cost. Non-structural damage is assumed to be included. **Comment:** Based on data collected for 3960 RC buildings affected by the 1978 Thessaloniki earthquake in Greece.
Kappos et al. (2006, 2008) – RC - central DFs	0%	0.5%	5%	20%	45%	80%	
Hill (2011) – Median DF	0%	0.07%	0.40%	0.54%	25.54%	100%	**Country:** Italy **DF Definition:** Repair cost / Replacement Cost. Non-structural damage is included. **Comment:** Based on repair cost survey data collected from 5 civil engineering companies in Italy (not in a post-earthquake scenario). The range of repair quantities (for different types of repair) associated with each damage state, for a single assumed geometry of an RC structure, is calculated based on visual assessment of 14 buildings damaged to differing degrees by the l'Aquila earthquake in Italy.
Hill (2011) – 25 percentile DF	0%	0.03%	0.18%	0.24%	25.24%	100%	
Hill (2011) – 75th percentile DF	0%	0.16%	1.02%	1.33%	26.33%	100%	

Damage Scale	HAZUS99				Comments
Reference/Damage State	**Slight**	**Moderate**	**Extensive**	**Complete**	
Smyth et al. (2004)	1%	10%	100%	100%	**Country:** Turkey **DF Definition:** Repair cost / Replacement Cost. Non-structural damage is assumed to be included. **Comment:** DFs are “assumed” by the authors i.e. based on judgement, with no particular derivation method mentioned.
Crowley et al. (2005)	15%	30%	100%	100%	**Country:** Turkey **DF Definition:** Repair cost / Replacement Cost. Non-structural damage is assumed to be included. **Comment:** DFs are based on judgement, the authors having considered how local Turkish construction and repair/reconstruction policies might alter the HAZUS DFs.
Bal et al. (2008)	16%	33%	105%	104%	**Country:** Turkey **DF Definition:** Repair cost including demolition and carriage (and new build cost) / Replacement Cost (new build). Non-structural damage is assumed to be included. **Comment:** DFs are based on retrofitting cost data obtained for 231 buildings damaged after the 1998 Ceyhan and 1999 Kocaeli earthquakes in Turkey. A replacement cost based on a government publication of “unit construction costs for new buildings” is used. Bal et al. (2008) state that “code and law requirements” in Turkey ensure that only moderately damaged buildings are repaired, all higher damage states warrant full replacement. Cost of carriage and demolition is included in the repair costs..

C.1.3 Damage Factor Values for Unreinforced Masonry Buildings

Damage Scale	EMS98						Comments
Reference	D0	D1	D2	D3	D4	D5	
Goretti and Di Pasquale (2004)							**Country:** Italy **DF Definition:** Repair cost / Replacement Cost. Non-structural damage is assumed to be included. **Comment:** Based on data on 23,000 buildings affected by the 2002 Molise earthquake. Derived for different structure types classified by building material and EMS98 vulnerability class. Some concern over the presence of non-zero values for the DS0 damage state
URM EMS98 vulny class A - Mean	2.9%	10.8%	22.2%	30.6%	87.6%	100%	
Standard Deviation	5.2%	5.0%	5.7%	6.7%	23.4%	0%	
URM EMS98 vulny class B - Mean	0.9%	7.9%	20.3%	29.3%	97.5%	100%	
Standard Deviation	2.6%	4%	4.8%	7.7%	11.2%	0%	
URM EMS98 vulny class C - Mean	0.7%	5.8%	18.7%	26.7%	96.1%	100%	
Standard Deviation	2%	4.2%	4.4%	5.2%	15.5%	0%	
D'Ayala et al. (1997)	0%	5%	20%	50%	80%	100%	**Country:** Portugal **DF Definition:** Repair cost / Replacement Cost. Non-structural damage is assumed to be included. **Comment:** Values from judgment. Applied to predominantly 2-6 storey buildings in Alfama district of Lisbon. Building material is typically poor quality rubble stone or brick masonry. Damage scale used is EMS92 which approximately corresponds to EMS98.
Milutinovic and Trendafiloski (2003)	0%	<20%	20-30%	30-40%	40-50%	>50%	**Country:** Macedonia **DF Definition:** Repair / Replacement cost. Non-structural damage assumed to be included. **Comment:** Part of RISK-UE project. Study carried out by the University Ss. Cyril and Methodius and reported in Milutinovic and Trendafiloski (2003). DFs mainly based on expert judgement and national "experience" with no stated method. Values are

							significantly different from other studies, especially in the DS5 category.
Dolce et al. (2006) and Penelis et al. (2002) - URM	0%	0-5%	5-20%	20-50%	50-95%	95-100%	**Country:** Greece **DF Definition:** Repair cost / Replacement Cost. Non-structural damage is assumed to be included. **Comment:** Based on Greek experience as described by Penelis et al. (2002) and Kappos et al. (2006). The values for URM presented by Dolce et al. (2006) are those reported in Penelis et al. (2002), which are based on 1780 buildings surveyed after the 1978 Thessaloniki earthquake in Greece.
Kappos et al. (2006, 2008) – URM - range DFs	0%	0-4%	4-20%	20-40%	40-70%	70-100%	**Country:** Greece **DF Definition:** Repair cost / Replacement Cost. Non-structural damage is assumed to be included. **Comment:** Based on data collected for 1780 URM buildings affected by the 1978 Thessaloniki earthquake in Greece.
Kappos et al. (2006, 2008) – URM - central DFs	0%	2%	12%	30%	55%	85%	
Hill (2011) – Median DF	0%	0.23%	0.40%	0.40%	26.26%	100%	**Country:** Italy **DF Definition:** Repair cost / Replacement Cost. Non-structural damage is included. **Comment:** Based on repair cost survey data collected from 5 civil engineering companies in Italy (not in a post-earthquake scenario). The range of repair quantities (for different types of repair) associated with single damage states, for a single assumed URM structural geometry, is calculated based on a visual assessment of 18 buildings damaged to differing degrees by the l'Aquila earthquake in Italy.
Hill (2011) – 25 percentile DF	0%	0.11%	0.19%	0.19%	25.58%	100%	
Hill (2011) – 75th percentile DF	0%	0.55%	0.99%	0.99%	28.22%	100%	

C.2 Damage Factor Values Function of Building Occupancy Class (HAZUS-MH MR3)

C.2.1 Structural Damage Factor Values Function of Building Occupancy Class (HAZUS-MH MR3, Table 15.2)

No.	Label	Occupancy Class	Structural Damage State			
			Slight	Moderate	Extensive	Complete
		Residential				
1	RES1	Single Family Dwelling	0.5	2.3	11.7	23.4
2	RES2	Mobile Home	0.4	2.4	7.3	24.4
3--8	RES3	Multi Family Dwelling	0.3	1.4	6.9	13.8
9	RES4	Temporary Lodging	0.2	1.4	6.8	13.6
10	RES5	Institutional Dormitory	0.4	1.9	9.4	18.8
11	RES6	Nursing Home	0.4	1.8	9.2	18.4
		Commercial				
12	COM1	Retail Trade	0.6	2.9	14.7	29.4
13	COM2	Wholesale Trade	0.6	3.2	16.2	32.4
14	COM3	Personal and Repair Services	0.3	1.6	8.1	16.2
15	COM4	Professional/Technical/ Business	0.4	1.9	9.6	19.2
16	COM5	Banks/Financial Institutions	0.3	1.4	6.9	13.8
17	COM6	Hospital	0.2	1.4	7	14
18	COM7	Medical Office/Clinic	0.3	1.4	7.2	14.4
19	COM8	Entertainment & Recreation	0.2	1	5	10
20	COM9	Theaters	0.3	1.2	6.1	12.2
21	COM10	Parking	1.3	6.1	30.4	60.9
		Industrial				
22	IND1	Heavy	0.4	1.6	7.8	15.7
23	IND2	Light	0.4	1.6	7.8	15.7
24	IND3	Food/Drugs/Chemicals	0.4	1.6	7.8	15.7
25	IND4	Metals/Minerals Processing	0.4	1.6	7.8	15.7
26	IND5	High Technology	0.4	1.6	7.8	15.7
27	IND6	Construction	0.4	1.6	7.8	15.7
		Agriculture				
28	AGR1	Agriculture	0.8	4.6	23.1	46.2
		Religion/Non-Profit				
29	REL1	Church/Membership Organization	0.3	2	9.9	19.8
		Government				
30	GOV1	General Services	0.3	1.8	9	17.9
31	GOV2	Emergency Response	0.3	1.5	7.7	15.3
		Education				
32	EDU1	Schools/Libraries	0.4	1.9	9.5	18.9
33	EDU2	Colleges/Universities	0.2	1.1	5.5	11

C.2.2 Acceleration-Sensitive Non-Structural Damage Factor Values Function of Building Occupancy Class (HAZUS-MH MR3, Table 15.3)

No.	Label	Occupancy Class	Acceleration Sensitive Non-structural Damage State			
			Slight	Moderate	Extensive	Complete
		Residential				
1	RES1	Single Family Dwelling	0.5	2.7	8	26.6
2	RES2	Mobile Home	0.8	3.8	11.3	37.8
3--8	RES3	Multi Family Dwelling	0.8	4.3	13.1	43.7
9	RES4	Temporary Lodging	0.9	4.3	13	43.2
10	RES5	Institutional Dormitory	0.8	4.1	12.4	41.2
11	RES6	Nursing Home	0.8	4.1	12.2	40.8
		Commercial				
12	COM1	Retail Trade	0.8	4.4	12.9	43.1
13	COM2	Wholesale Trade	0.8	4.2	12.4	41.1
14	COM3	Personal and Repair Services	1	5	15	50
15	COM4	Professional/Technical/ Business Services	0.9	4.8	14.4	47.9
16	COM5	Banks/Financial Institutions	1	5.2	15.5	51.7
17	COM6	Hospital	1	5.1	15.4	51.3
18	COM7	Medical Office/Clinic	1	5.2	15.3	51.2
19	COM8	Entertainment & Recreation	1.1	5.4	16.3	54.4
20	COM9	Theaters	1	5.3	15.8	52.7
21	COM10	Parking	0.3	2.2	6.5	21.7
		Industrial				
22	IND1	Heavy	1.4	7.2	21.8	72.5
23	IND2	Light	1.4	7.2	21.8	72.5
24	IND3	Food/Drugs/Chemicals	1.4	7.2	21.8	72.5
25	IND4	Metals/Minerals Processing	1.4	7.2	21.8	72.5
26	IND5	High Technology	1.4	7.2	21.8	72.5
27	IND6	Construction	1.4	7.2	21.8	72.5
		Agriculture				
28	AGR1	Agriculture	0.8	4.6	13.8	46.1
		Religion/Non-Profit				
29	REL1	Church/Membership Organization	0.9	4.7	14.3	47.6
		Government				
30	GOV1	General Services	1	4.9	14.8	49.3
31	GOV2	Emergency Response	1	5.1	15.1	50.5
		Education				
32	EDU1	Schools/Libraries	0.7	3.2	9.7	32.4
33	EDU2	Colleges/Universities	0.6	2.9	8.7	29

C.2.3 *Drift-Sensitive Non-Structural Damage Factor Values Function of Building Occupancy Class (HAZUS-MH MR3, Table 15.4)*

No.	Label	Occupancy Class	Drift Sensitive Non-structural Damage State			
			Slight	Moderate	Extensive	Complete
		Residential				
1	RES1	Single Family Dwelling	1	5	25	50
2	RES2	Mobile Home	0.8	3.8	18.9	37.8
3--8	RES3	Multi Family Dwelling	0.9	4.3	21.3	42.5
9	RES4	Temporary Lodging	0.9	4.3	21.6	43.2
10	RES5	Institutional Dormitory	0.8	4	20	40
11	RES6	Nursing Home	0.8	4.1	20.4	40.8
		Commercial				
12	COM1	Retail Trade	0.6	2.7	13.8	27.5
13	COM2	Wholesale Trade	0.6	2.6	13.2	26.5
14	COM3	Personal and Repair Services	0.7	3.4	16.9	33.8
15	COM4	Professional/Technical/ Business	0.7	3.3	16.4	32.9
16	COM5	Banks/Financial Institutions	0.7	3.4	17.2	34.5
17	COM6	Hospital	0.8	3.5	17.4	34.7
18	COM7	Medical Office/Clinic	0.7	3.4	17.2	34.4
19	COM8	Entertainment & Recreation	0.7	3.6	17.8	35.6
20	COM9	Theaters	0.7	3.5	17.6	35.1
21	COM10	Parking	0.4	1.7	8.7	17.4
		Industrial				
22	IND1	Heavy	0.2	1.2	5.9	11.8
23	IND2	Light	0.2	1.2	5.9	11.8
24	IND3	Food/Drugs/Chemicals	0.2	1.2	5.9	11.8
25	IND4	Metals/Minerals Processing	0.2	1.2	5.9	11.8
26	IND5	High Technology	0.2	1.2	5.9	11.8
27	IND6	Construction	0.2	1.2	5.9	11.8
		Agriculture				
28	AGR1	Agriculture	0	0.8	3.8	7.7
		Religion/Non-Profit				
29	REL1	Church/Membership Organization	0.8	3.3	16.3	32.6
		Government				
30	GOV1	General Services	0.7	3.3	16.4	32.8
31	GOV2	Emergency Response	0.7	3.4	17.1	34.2
		Education				
32	EDU1	Schools/Libraries	0.9	4.9	24.3	48.7
33	EDU2	Colleges/Universities	1.2	6	30	60

APPENDIX D Illustrative Examples

Authors: A. Meslem, D. D'Ayala, V. Novelli

D.1 Mid-Rise RC Building Designed According to Earlier Seismic Codes

The method selected for this illustrative example is one of the Non-linear Static-based approaches recommended in this Guidelines document: i.e. Procedure 3.1. The building class selected as example of application constitutes one of the largest portions of existing residential building stock in earthquake-prone countries. For the seismic vulnerability analysis, the considered structure is a typical four-storey RC building, built according to the first generation of seismic codes, and located in a high-seismicity region of Turkey (see Figure D.1 and Table D.1).

The building class was defined based on structural characteristics-related parameters that are associated to mechanical properties, geometric configuration, and structural details, and which are in general affected by the quality of workmanship; i.e. compressive strength of concrete, yield strength of reinforcement, strength and stiffness of infill walls (in terms of thickness of walls), storey height, and transverse reinforcement spacing.

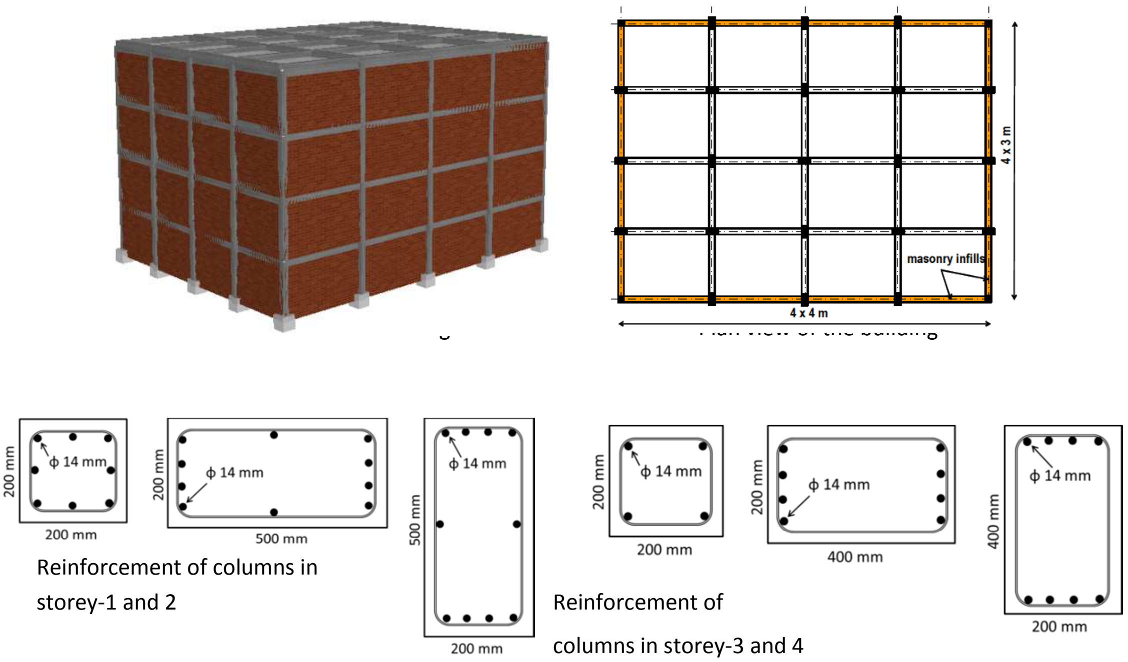

Figure D.1. Typical four-storey low-ductile RC building located in a high-seismically region of Turkey building

D.1.1 Define Building Index

In evaluating the central quality with lower and upper bounds, the choice of range of expected values for each parameter has been based on the results of structural characteristics assessment (see Figure D.2) available from different literature sources such as direct studies (Ay 2006, Bal et al. 2008), post-earthquakes surveys [EERI 2000, EEFIT 2003, Ellul 2006], the requirement from different versions of earlier seismic codes, e.g. TS500 [TSE 1985], and values adopted in previous similar studies on seismic vulnerability [Gulkan et al. 2002, Erol et al. 2004, Kappos 2006]. The value ranges shown in Table D.2 represent the most feasible range of expected values characterizing the low-ductility RC buildings class, typically designed according to earlier seismic codes and, in general, characterized by typical quality of materials, workmanship and detailing.

Table D.1. Classification of 4-storey RC building according to the GEM Basic Building Taxonomy

#	GEM Taxonomy		4-Storey RC Building	
	Attribute	**Attribute Levels**	**Level 1**	**Level 2**
1	Material of the Lateral Load-Resisting System	Material type (Level 1) Material technology (Level 2) Material properties (Level 3)	CR	CIP
2	Lateral Load-Resisting System	Type of lateral load-resisting system (Level 1) System ductility (Level 2)	LFINF	DU
3	Roof	Roof material (Level 1) Roof type (Level 2)	RC	RC1
4	Floor	Floor material (Level 1) Floor type (Level 2)	FC	FC1
5	Height	Number of stories	H:4	
6	Date of Construction	Date of construction		YEP:1975
7	Structural Irregularity	Type of irregularity (Level 1) Irregularity description (Level 2)	IRN IRH IROH	 IROH IROV
8	Occupancy	Building occupancy class - general (Level 1) Building occupancy class - detail (Level 2)	RES	RES2

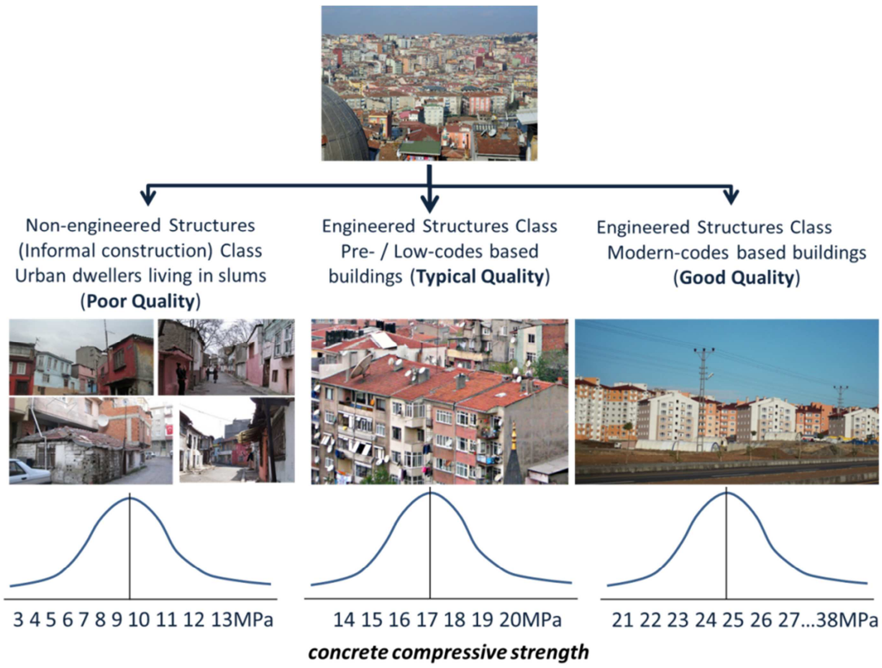

Figure D.2. Illustrative example of selection the range of expected values (central value with lower and upper bounds) for each structural characteristics-related parameter, based on the results of structural characteristics assessment.

Table D.2. Range of expected values for the structural characteristics-related parameters associated to the building class represented by the index building ranges

Parameters	Range of most expected values for Typical Quality Class of Buildings		
	Lower Bound	Central value	Upper Bound
Compressive strength of concrete (fc)	14 MPa	17 MPa	20 MPa
Tensile strength of steel (fy)	200 MPa	260 MPa	320 MPa
Transverse reinforcement spacing (S)	150 mm	200 mm	250 mm
floor-to-floor Story height (h)	2.5 m	2.8 m	3.2 m
Thickness of infill walls (tw)	13 cm	16 cm	19 cm

D.1.2 Derivation of Structural Capacity Curves

Three numerical 3-D models, characterizing central quality, lower bound, and upper bound, were created: Note that, for illustration purposes the analyses were conducted for X-direction only. The response of each frame in terms of capacity curve (resulting from pushover analysis, see ANNEX A) is shown in Figure D.3. Regarding the definition of different damage conditions, four global damage thresholds are considered: Slight Damage, Moderate Damage, Extensive Damage, and Complete Damage (or Collapse), estimated as a progression of local damage through member elements. Note that for illustration purposes

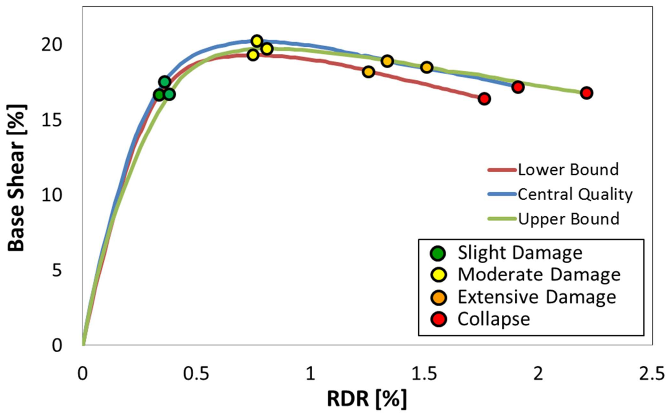

Figure D.3. Resulted pushover curves and definition damage conditions at global level, for Central Quality, Lower Bound and Upper Bound.

the detailed steps of calculations are shown for Central Quality model only. The following input data, parameters and assumption were used in the derivation of idealised capacity curve of equivalent SDoF (see ANNEX A):

The horizontal force pattern for pushover analysis is calculated by multiplying the mode shape and the storey masses:

$$F = M\Phi = \begin{bmatrix} 229.18 & & & \\ & 229.03 & & \\ & & 224.96 & \\ & & & 177.656 \end{bmatrix} \begin{Bmatrix} 0.200 \\ 0.600 \\ 0.800 \\ 1.000 \end{Bmatrix} = \begin{Bmatrix} 45.84 \\ 137.42 \\ 179.97 \\ 177.65 \end{Bmatrix}$$

The mass of the equivalent SDOF system is (see Equation A.1):

$$m^* = \sum m_i \Phi^2 = 229.18 \cdot 0.200 + 229.03 \cdot 0.600 + 224.96 \cdot 0.800 + 177.65 \cdot 1.000 = 540.87\text{tonne}$$

The transformation to an equivalent SDoF model is made by dividing the base shear and top displacement of the MDoF with a transformation factor Γ (see Equation A.3). The result is presented in Figure D.4:

$$\Gamma = \frac{\Phi^T \cdot M \cdot 1}{\Phi^T \cdot M \cdot \Phi} = \frac{\begin{Bmatrix} 0.200 \\ 0.600 \\ 0.800 \\ 1.000 \end{Bmatrix}^T \begin{bmatrix} 229.18 & & & \\ & 229.03 & & \\ & & 224.96 & \\ & & & 177.65 \end{bmatrix} \begin{Bmatrix} 1 \\ 1 \\ 1 \\ 1 \end{Bmatrix}}{\begin{Bmatrix} 0.200 \\ 0.600 \\ 0.800 \\ 1.000 \end{Bmatrix}^T \begin{bmatrix} 229.18 & & & \\ & 229.03 & & \\ & & 224.96 & \\ & & & 177.65 \end{bmatrix} \begin{Bmatrix} 0.200 \\ 0.600 \\ 0.800 \\ 1.000 \end{Bmatrix}} = 1.3088$$

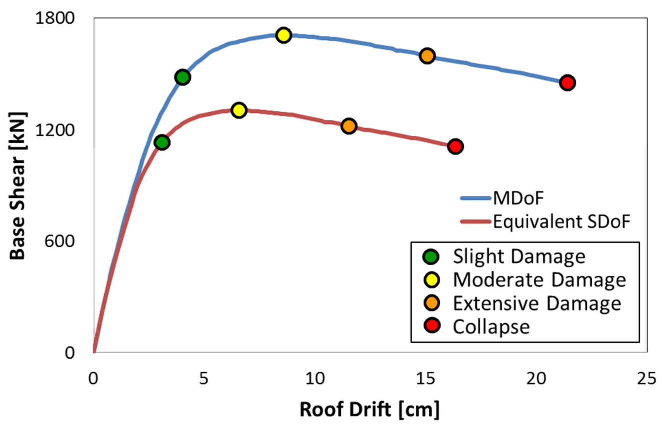

Figure D.4. Transformation of MDoF pushover curve to an equivalent SDoF. Case: Central Quality.

The displacement at yield is determined by applying the equal energy rule for the interval from 0 to D_u, which coincides with the maximum capacity load (see Equation A.7):

$$D_y = 2\left(D_u - \frac{E_{area}}{F_y}\right) = 2\left(16.35 - \frac{18392.13}{1227.85}\right) = 2.74cm$$

The idealized force-displacement relationship is presented in Figure D.5.

The elastic period of idealized system is (see Equation A.4):

$$T^* = 2\pi \cdot \sqrt{\frac{m^* \cdot D_y}{F_y}} = 2\pi\sqrt{\frac{540.87 \cdot 2.74}{1227.85}} = 0.69\sec$$

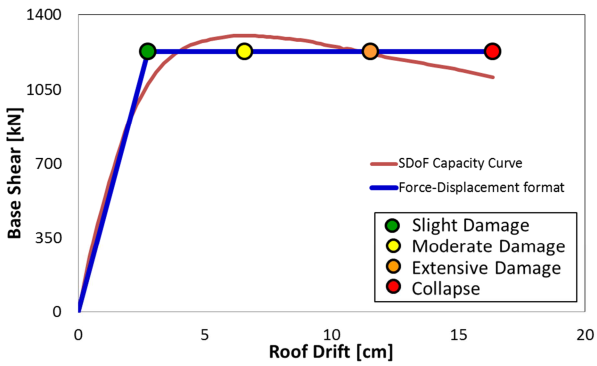

Figure D.5. Equivalent SDoF Pushover curve and the idealized force-displacement relationship. Case: Central Quality.

The idealized capacity curve is transformed from force-displacement to A-D format by dividing the forces in the force-displacement (F- D) idealized diagram by the equivalent mass m*.

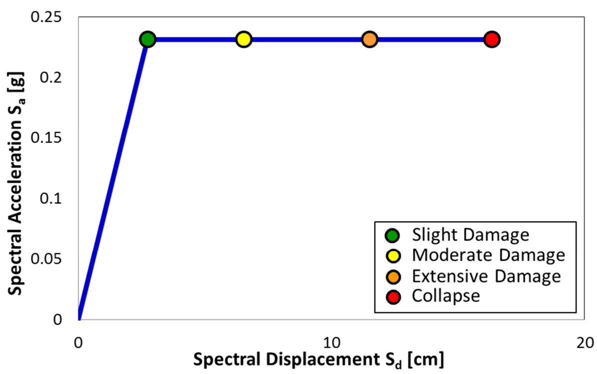

Figure D.6. Equivalent SDoF idealized capacity curve in Acceleration-Displacement format. Case: Central Quality.

D.1.3 Calculation of Performance Points for a Suite of Ground Motion Records

The performance points (see Equation 7.33) were implemented using a suite of ground motion records (see Table D.3, Figure D.7, and Figure D.8). In order to determine the structure's performance under increasing ground motion intensity, the analysis was repeated for the same ground motion record scaled up until all the limit state are reached.

Table D.3. Suite of ground motion records used in the calculation of performance points (seismic demand)

Earthquake Name	Date	Mw	Fault Mechanism	Epicentral Distance [km]	PGA_X [m/s^2]	PGA_Y [m/s^2]
South Iceland	2000_June_17	6.5	strike-slip	5.25	3.1438	3.3895
Dinar	1995_October_01	6.4	normal	0.47	3.2125	2.7292
Loma Prieta	1989_October_18	6.9	oblique	27.59	3.179	5.0258
Northridge	1994_January_17	6.7	reverse	11.02	3.3738	3.021
Darfield	2010_September_03	7.1	strike-slip	9.06	4.9607	4.7367
Hector Mine	1999_October_16	7.1	strike-slip	28.61	3.3026	2.6044
Olfus	2008_May_29	6.3	strike-slip	7.97	5.001	2.103

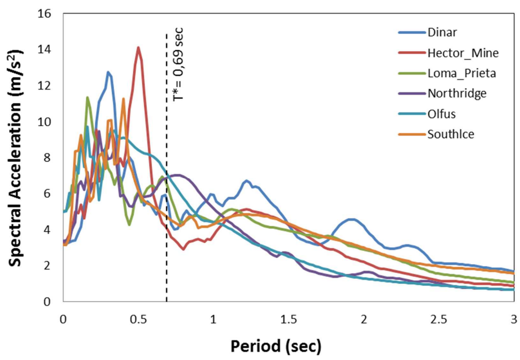

Figure D.7. Ground motion records used in the calculation of performance points (seismic demand).

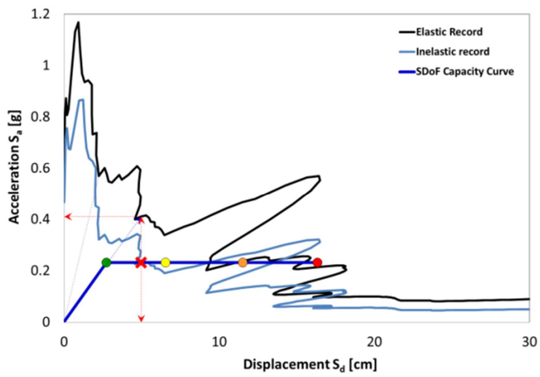

Figure D.8. Illustrative example of determination of seismic performance point (demand) for a selected ground motion record.

The resulting cloud of performance points (see Figure D.9) is then used to determine the EDP for each damage state threshold and the dispersion, and then create a fragility curve by fitting a statistical model.

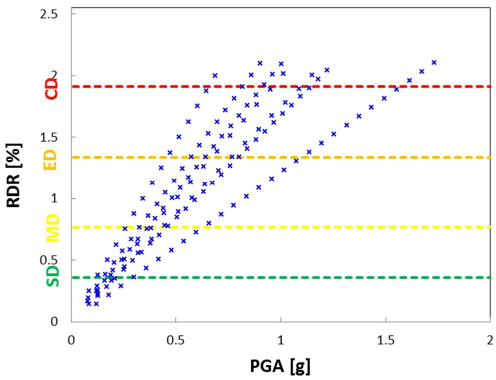

Figure D.9. Clouds of structural-response results. Case of central Quality

D.1.4 Determination of EDPs Damage State Thresholds

The calculation of EDPs of damage state thresholds and their corresponding dispersions is conducted using Least Squares formulation (Figure D.10), described in Section 7.3.1.1. The results are presented below.

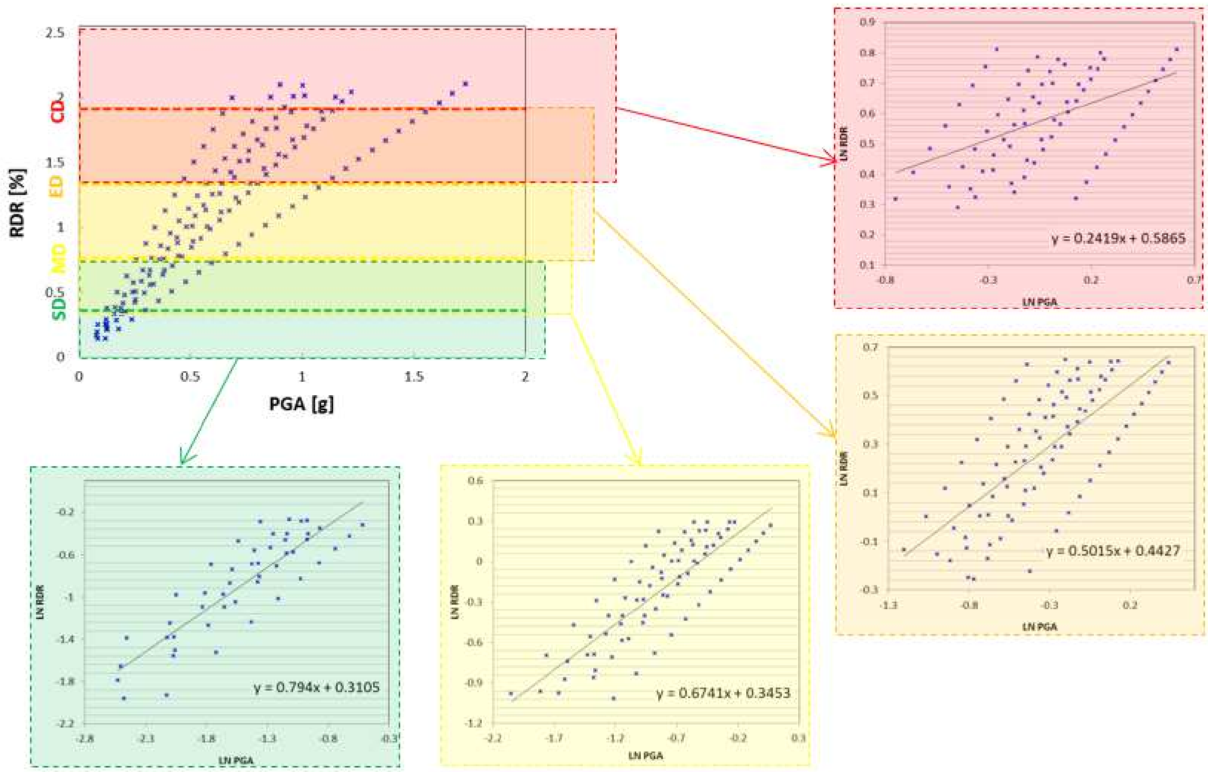

Figure D.10. Calculation of Median capacities and dispersions using Least Squares formulation. Case: central quality

The resulting median capacities and their corresponding record-to-record dispersions are shown in Table D.4, and Figure D.11 shows the fitted fragility curves for Central Quality, Lower Bound, and Upper Bound.

Table D.4. Resulting median capacities and their corresponding dispersions associated to the record-to-record variability

	Slight Damage		Moderate Damage		Extensive Damage		Complete Damage	
	Median PGA [g]	β_D	Median PGA [g]	β_D	Median PGA [g]	β_D	Median PGA [g]	β_D
Lower Bound	0.159	0.270	0.369	0.274	0.636	0.322	1.141	0.475
Central Quality	0.186	0.303	0.403	0.316	0.739	0.373	1.287	0.532
Upper Bound	0.213	0.304	0.425	0.341	0.871	0.380	1.566	0.535

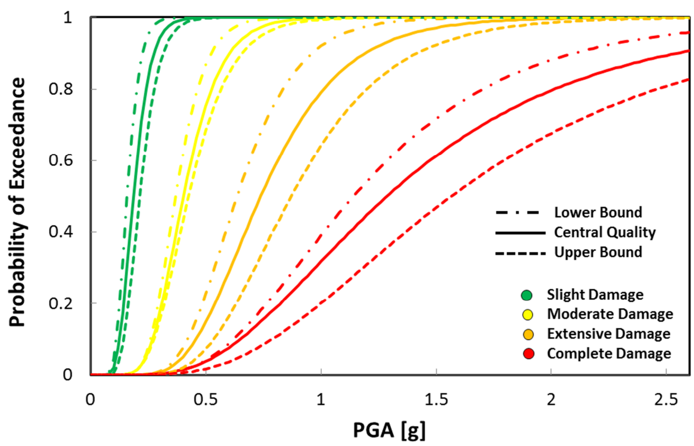

Figure D.11. Generated fragility curves for Central Quality, Lower Bound, and Upper Bound

D.1.5 Building-based repair cost for a specific level of intensity measurement

Recall that, for a reliable estimation of total repair cost it is quite important that the analysts provide their local estimates of repair and reconstruction costs in order to reach a better level of accuracy for the derived vulnerability curves. If such data is available, the analysts can calculate the total repair cost, given damage threshold, $E(C \mid ds_i)$, using Equation 8.8 (see Section 8.1.2).

For illustration purposes, and in the absence of local data, we use default damage factor values provided in ANNEX C (estimated for the entire building) to estimate repair cost given ds_i .

Table D.5. Damage Factors values for reinforced concrete frames with masonry infills

Reference	Damage State				Comment
	Slight	Moderate	Extensive	Complete	
Bal et al. (2008)	16%	33%	105%	104%	**Country:** Turkey **DF Definition:** Repair cost including demolition and carriage (and new build cost) / Replacement Cost (new build). Non-structural damage is assumed to be included. **Comment:** DFs are based on retrofitting cost data obtained for 231 buildings damaged after the 1998 Ceyhan and 1999 Kocaeli earthquakes in Turkey. A replacement cost based on a government publication of “unit construction costs for new buildings” is used. Bal et al. (2008) state that “code and law requirements” in Turkey ensure that only moderately damaged buildings are repaired, all higher damage states warrant full replacement. Cost of carriage and demolition is included in the repair costs.

If we consider that the selected building class is subjected to PGA= 1g, then the resulting repair cost (in terms of Damage factor) is estimated as follows:

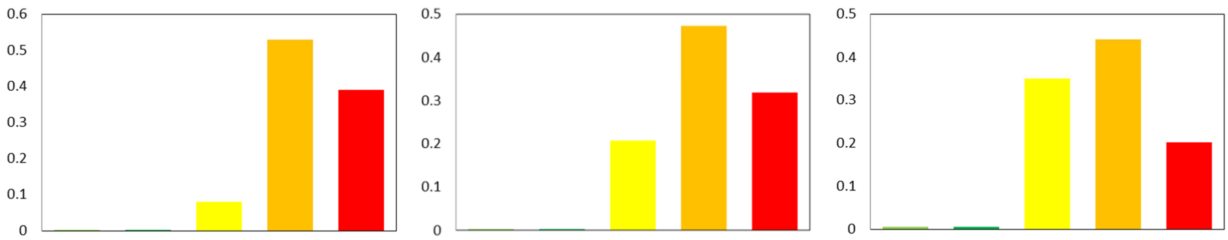

Lower Bound Quality Central Quality Upper Bound Quality

Figure D.12. Calculation of damage probabilities from the fragility curves for PGA = 1g.

For Lower Bound quality:

$$E_1(C \mid PGA = 1g) = 0 + (16\% \times 0) + (33\% \times 0.08) + (105\% \times 0.53) + (104\% \times 0.39) = 98.84\%$$

For Central Quality

$$E_2(C \mid PGA = 1g) = 0 + (16\% \times 0) + (33\% \times 0.21) + (105\% \times 0.47) + (104\% \times 0.32) = 89.58\%$$

For Upper Bound Quality

$$E_3(C \mid PGA = 1g) = 0 + (16\% \times 0) + (33\% \times 0.35) + (105\% \times 0.44) + (104\% \times 0.20) = 78.84\%$$

The mean vulnerability function (in terms of Damage Factor) for the considered three index buildings can be calculated through the following Equation:

$$E(C \mid PGA = 1g) = \frac{1}{3}\sum_{j=1}^{3} E_j(C \mid PGA = 1g) = 89.10\%$$

D.2 Low to Mid-Rise Unreinforced Masonry Buildings in Historic Town Centre

The method selected for this illustrative example is Non-Linear Static analysis based on Simplified Mechanism Models (SMM-NLS) which allows the calculation of the EDPs thresholds for masonry construction typologies (unreinforced masonry and adobe structures). The calculation of the EDPs thresholds can be done using smoothed elastic response spectrum only. This example is developed using Procedure 4.1: Failure Mechanism Identification and Vulnerability Evaluation (FaMIVE) (Section 7.4.1). The building sample used in this application constitutes several UM building subclasses which typically form the building stock of historic town centres in the Mediterranean countries. For the seismic vulnerability analysis, a centre in the Umbria region of Italy is chosen, located in the highest seismicity zoning for Italy (see Figure D.13 and Table D.6).

The building class was defined based on structural characteristics-related parameters that are associated to mechanical properties, geometric configuration, and structural details, and which are in general affected by the quality of workmanship.

Figure D.13. Typical two-storey masonry building in Nocera Umbra, Italy

D.2.1 *Define Building Index*

The building index is not defined in terms of its mechanical and geometric characteristics a priori, but the analysis is run for a large number of buildings representative of the building stock of the site under study and, a posteriori, according to their performance and failure mechanisms they are combined in subclasses and median capacity curves are extracted. Table D.6 presents the Level 1 and Level 2 GEM Taxonomy classes applicable to the whole building stock of Nocera Umbra.

Table D.6. Classification of URM building stock in Nocera Umbra, Italy, according to the GEM Basic Building Taxonomy

#	GEM Taxonomy		4-Storey RC Building	
	Attribute	Attribute Levels	Level 1	Level 2
1	Material of the Lateral Load-Resisting System	Material type (Level 1) Material technology (Level 2) Material properties (Level 3)	MUR	STRUB,STDRE, CLBRS
2	Lateral Load-Resisting System	Type of lateral load-resisting system (Level 1) System ductility (Level 2)	LWAL	D99
3	Roof	Roof material (Level 1) Roof type (Level 2)	RC, RWO, RM	RC2, RWO2,
4	Floor	Floor material (Level 1) Floor type (Level 2)	FC,FW,FM	FC2,FW2, FM1,FM2
5	Height	Number of stories	H:1,5	
6	Date of Construction	Date of construction	YN:1500,1900	
7	Structural Irregularity	Type of irregularity (Level 1) Irregularity description (Level 2)	IRH,IRV	REC,IRHO,CRW,POP,CHV
8	Occupancy	Building occupancy class - general (Level 1) Building occupancy class - detail (Level 2)	RES,COM	RES1,RES2,COM1,COM3

The distribution of the selected buildings used to compute the capacity curves, derive the fragility functions for the historic centre of Nocera and compute the performance point for each building and its probability of damage, are shown in Figure D.14.

Figure D.14. Map of historic centre

D.2.2 Derivation of Structural Capacity Curves

Capacity curves are computed using a limit state mechanisms approach. One collapse load factor is computed for each façade of the building according to the constraints between facades and horizontal structures, and between facades and adjacent buildings. The analyst can choose to consider a capacity curve for each façade or to choose for each building the most vulnerable façade in computing the performance point and the fragility functions. To compute the collapse load factor reference should be made to D'Ayala and Speranza [2003], D'Ayala and Casapulla [2006], Novelli and D'Ayala [2014].

The capacity curves are computed starting from the collapse load factor as shown in D'Ayala [2005] and summarized in Section 7.4.1 Equations 7.46 to 7.52.

The procedure's approach allows a direct assessment of the influence of different parameters on the capacity curves, whether these are geometrical, mechanical, or structural. By way of example Figure D.15a shows a comparison of median capacity curves obtained by sampling the results according to the mode of failure, while Figure D.15b shows median capacity curves obtained by sampling different structural typologies, as classified by the WHE-PAGER project [Jaiswal et al. 2011].

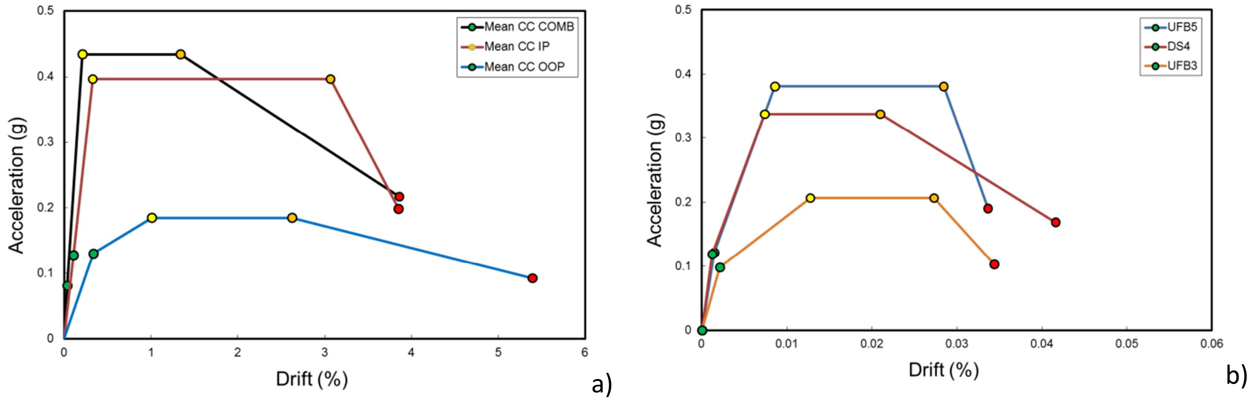

Figure D.15. Median pushover curves for a) different failure modes class, b) different structural typology classification.

D.2.3 Determination of EDPs Damage State Thresholds and Fragility Curves

The vertices on the multilinear curves in Figure D.15 also represent the mean damage thresholds for a given class of buildings, whether identified by their mechanism of failure or by their structural typology. To these mean values, for each group, are associated standards deviations as shown in Table D.7. Fragility functions are derived assuming that the damage threshold values are lognormally distributed using the median values and standard deviation included in Table D.7. These produce the fragility curves shown in Figure D.16.

Table D.7. Median displacement thresholds and their corresponding dispersions due to capacity curves variability in the sample

	Slight Damage		Moderate Damage		Extensive Damage		Complete Damage	
	Median Sd [cm]	β_D	Median Sd [cm]	β_D	Median Sd [cm]	β_D	Median Sd [cm]	β_D
OUT of PLANE	0.30	0.97	0.88	0.97	10.5	0.60	30	0.36
IN PLANE	0.68	0.89	2.04	0.89	10.5	0.65	34.75	0.49
COMBINED	0.04	077	0.12	0.77	10.41667	0.51	31.25	0.42

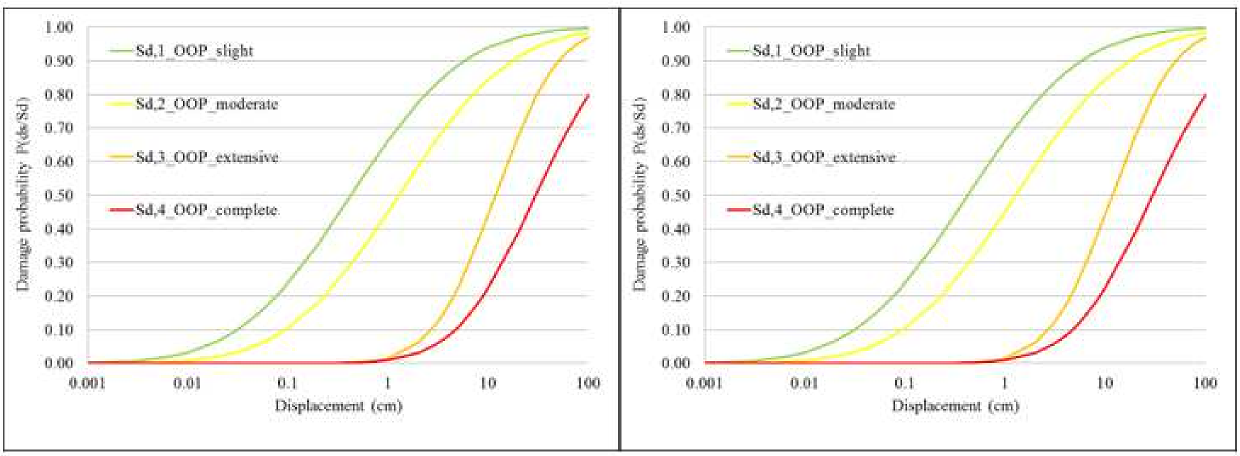

Figure D.16. Fragility functions for a) out-of-plane failure modes, b) in-plane failure mode

D.2.4 Calculation of Performance Points

The identification of the performance point is conducted for each building using its representative capacity curve. Although both elastic smoothed response spectra and natural response spectra can be used, in this application only the smoothed response spectrum is used. Specifically the smoothed elastic spectrum used is constructed using the EC8 shape, assuming the value of PGA recorded in Nocera Umbra on 26 September 1997, mainshock of the Umbria-Marche 1997 sequence, and soil B has been assumed throughout the site. This means that the computed probability of damage for each building does not include the variability associated with considering various scenarios, or by considering record-to-record variability. Two different approaches can be used to determine the performance point: the first assumes the equal displacement rule of EC8, the second the equivalent energy rule. Corresponding performance points are shown in Figure D.17 for a building failing for out-of-plane mechanism and for a building failing with an in-plane mechanism. It should be noted that the equal energy rules requires greater ductility demands and hence identifies performance points corresponding to higher levels of damage.

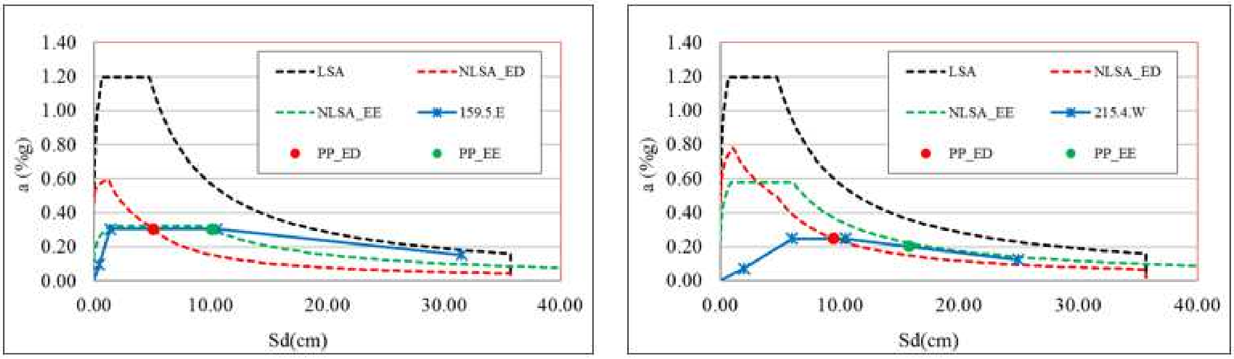

a) b)

Figure D.17. Performance points for a) building failing in out-of-plane mode and b) in plane mode computed by reducing the non-linear spectrum using the equal displacement rule and the equal energy rule.

From the two examples it can be seen that for the equal displacement approach the performance points are in both cases in the range of extensive damage, while for the equal energy approach case (b) is in complete damage state.

The fragility curves can be used to compute the probability that the buildings in the given sample will be in any of the damage state given a lateral deflection. This will also depend on the type of failure mode, as shown in Figure D.18.

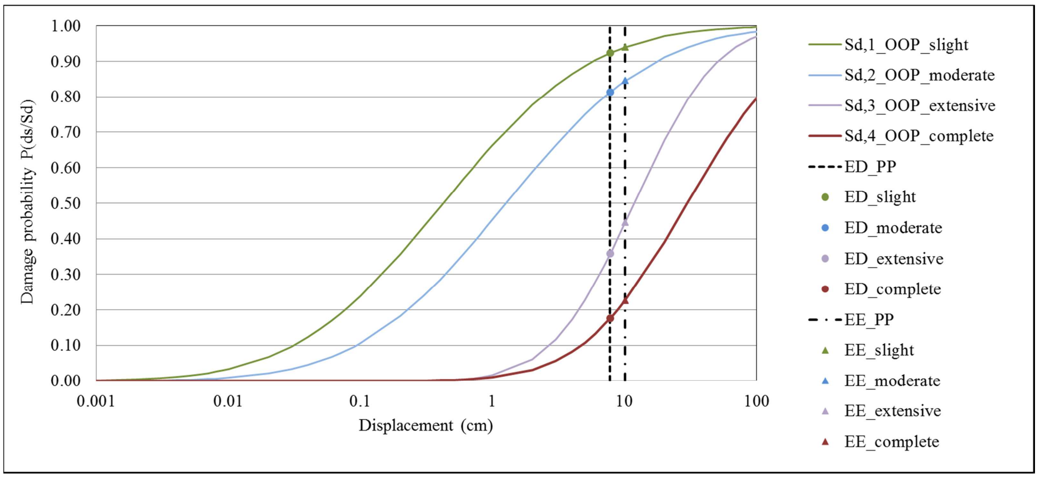

Figure D.18. Probability of exceedance of damage states, given a lateral displacement

The procedure outlined in Section D1.5 can be followed from this point to establish the economic losses.

THE GLOBAL EARTHQUAKE MODEL

The mission of the Global Earthquake Model (GEM) collaborative effort is to increase earthquake resilience worldwide.

To deliver on its mission and increase public understanding and awareness of seismic risk, the GEM Foundation, a non-profit public-private partnership, drives the GEM effort by involving and engaging with a very diverse community to:

- Share data, models, and knowledge through the OpenQuake platform
- Apply GEM tools and software to inform decision-making for risk mitigation and management
- Expand the science and understanding of earthquakes.

GEM Foundation

Via Ferrata 1
27100 Pavia, Italy
Phone: +39 0382 5169865
Fax: +39 0382 529131
info@globalquakemodel.org
www.globalquakemodel.org

AUGUST 2015

GEM
GLOBAL EARTHQUAKE MODEL
working together to assess risk